ΟΙΚΟΝΟΜΙΚΟ ΠΑΝΕΠΙΣΤΗΜΙΟ ΑΘΗΝΩΝ
ATHENS UNIVERSITY OF ECONOMICS AND BUSINESS
ΣΧΟΛΗ ΔΙΟΙΚΗΣΗΣ ΕΠΙΧΕΙΡΗΣΕΩΝ SCHOOL OF BUSINESS
ΤΜΗΜΑ ΔΙΟΙΚΗΤΙΚΗΣ ΕΠΙΣΤΗΜΗΣ & ΤΕΧΝΟΛΟΓΙΑΣ DEPARTMENT OF MANAGEMENT SCIENCE & TECHNOLOGY

MACHINE LEARNING AND CONTENT ANALYTICS
2023

MuraMed: A Revolution in Medical Diagnostics

Team X-Rays - Team Members:

Name	Academic ID
Dimitra Diamanti	f2822209
Dimitrios Matsanganis	f2822212
Foteini Nefeli Nouskali	f2822213
Hegla Ruci	f2822219

September 2023, Athens

Abstract

The integration of digital technology has become vital in recent advancements in the medical field. Radiologists and orthopedists increasingly rely on advanced digital systems for accurate identification and treatment of bone fractures. In our Deep Learning course project, we were tasked with implementing a series of deep learning models supported by a robust business case. Deep neural networks, a prominent machine learning model, find applications in diverse domains, including image classification and anomaly detection. Our project focuses on establishing MuraMed, an innovative healthcare technology company dedicated to addressing the urgent need for precise and efficient diagnosis, with a specific emphasis on radiographs (X-Ray images). This initiative holds significant promise in the fields of medical imaging, medical data analysis, diagnostics, and healthcare delivery. This report presents a comprehensive methodology for automating the classification of normal and abnormal X-ray images, with a specific focus on anatomical parts of the hand. We achieve this using Convolutional Neural Networks (CNN) in conjunction with the advanced VGG model. The effectiveness of our approach is evaluated using the MURA dataset, a collection of musculoskeletal radiographs established by Stanford University. The assessment includes method proficiency and the presentation of results.

Keywords

- **IEEE Keywords**

  Image Quality, Deep Learning, Sensitivity, Neural Networks, Medical Services, Abnormality Detection

- **Inspec: Controlled Indexing**

  X-Ray, Hand, Bones, Convolutional Neural Nets, Data Analysis, Deep Learning (Artificial Intelligence), Patient Treatment, Image Classification, Medical Image Processing, Abnormality Detection

- **Inspec: Non-Controlled Indexing**

  Bone Abnormalities, Chronic Diseases, Deep Neural Networks, Deep Transfer Learning, Integrated Deep Convolutional Neural Networks, CNN, VGG, Medical Data Analysis, Image Analysis, Image Classification

- **Author Keywords**

  Convolutional Neural Network, VGG, Abnormalities, Fractures, Computer-Aided Diagnosis, Deep Neural Networks

Contents

Table of Figures

Summary

In the rapidly evolving landscape of healthcare AI, MuraMed emerges as a revolutionizing force in medical diagnostics, leveraging machine learning models. The present report provides an in-depth exploration of MuraMed's multifaceted approach, including business strategies, technical implementations, and software integrations. MuraMed's central mission revolves around using AI to elevate medical diagnostics. Their machine learning models and algorithms have been carefully fine-tuned for the analysis of musculoskeletal radiographs, with a current focus on anatomical regions like the wrist, shoulder, elbow, hand, finger, forearm, and humerus.

From a business perspective, MuraMed strategically serves various sectors, including healthcare, education, and the workplace. Their objectives encompass diagnostic support, telemedicine capabilities, workplace injury prevention, and athlete health monitoring. These tailored propositions are grounded in MuraMed's commitment to simplicity, model accuracy, and dedicated customer support, distinguishing them from more complex competitors. At the core of MuraMed's business strategy is the Blue Ocean Strategy, a guiding principle poised to excel in a competitive market. This approach, emphasizing innovation and differentiation, guides MuraMed towards untapped opportunities in healthcare AI. Through proactive partnerships and the adoption of emerging technologies, MuraMed aims to maintain a leading position in the dynamic healthcare AI landscape.

The technical dimension of this report navigates through data architecture, algorithm development, and quality assurance, providing a roadmap for effective model deployment. Techniques such as data augmentation, metric selection, and the use of training callbacks underscore MuraMed's commitment to refining model performance. Within this technical landscape, MuraMed employs three machine learning models: Simple CNN, Advanced CNN, and VGG-19, each possessing distinct performance characteristics. The Simple CNN model serves as a foundational baseline with a test loss of **0.67427** and an accuracy of **0.61026**, signaling the need for further refinement or the exploration of more advanced models for medical applications. In contrast, the Advanced CNN exhibits superior performance with a lower test loss of **0.59758**, an accuracy of **0.66938**, and a commendable Cohen's Kappa score of **0.73658**, establishing it as a reliable choice for medical imaging tasks. Surpassing both, the VGG-19 model achieves an accuracy of **0.80200** and a Cohen's Kappa score of **0.86291**, despite a higher test loss of **0.91401**, solidifying its position as the top-performing model among the three.

In summary, this report emphasizes MuraMed's commitment to revolutionize medical diagnostics through AI-driven solutions, prioritizing clinical excellence, technological progress, and dedicated research and innovation. MuraMed's comprehensive approach positions them as a driving force in the healthcare AI landscape, driving positive change, and elevating the standards of medical diagnostics.

Deliverables

This section outlines the components within the deliverables, provided as a ZIP file named **'MuraMed_Project.zip'** or in the MuraMed's GitHub Repository . The following elements are included:

1. **MuraMed_Documentation.pdf:** This comprehensive PDF includes the business idea, complete with a business canvas, practical implementations, and a business plan. Additionally, it contains the technical details of the models' notebooks, development approach, and findings.

2. **Figures Folder:** Contains essential figures for the three models' notebooks. These figures are also included in the MuraMed documentation analysis PDF.

3. **Database - database.txt:** This text file includes two links for downloading the MURA Dataset from Kaggle and Stanford. The dataset exceeds 3GB, so it is not stored directly in the archive.

4. **Environment Setup - requirements.txt:** Specifies crucial Python libraries and their respective versions, tailored for **a Python 3.10** environment.

5. **Model Weights** - **weights.txt:** Provides a link to a Google Drive folder where you can find model checkpoints. The folder is organized into three subfolders: **Simple CNN, Advanced CNN,** and **VGG19**. Each subfolder contains weight files and is timestamped for version control.

6. **Model's Notebook:** The Jupyter Notebooks for the three models used in this analysis:

   - **muramed_simple_cnn.ipynb:** The Jupyter Notebook for the **Simple CNN model**, also including code to load weights for the best epoch.
   - **muramed_advanced_cnn.ipynb:** The Jupyter Notebook for the **Advanced CNN model**, including code to load weights for the best epoch.
   - **muramed_vgg.ipynb:** The Jupyter Notebook for the **VGG-19 model**, with corresponding code to load weights for the best epoch.

7. **Presentation Materials** - **MuraMed_presentation.pptx and MuraMed_presentation.pdf:** These files contain the presentation of our analysis findings and the business idea.

8. **Additional Information** - **README.md:** A brief description of the project. *We highly recommend reviewing our comprehensive analysis documentation and the three Jupyter notebooks for a more in-depth understanding*.

A. Business Case

MuraMed: Transforming Medical Diagnostics with AI

MuraMed is an innovative healthcare technology company, committed to revolutionizing the medical field. Our primary mission is to address the critical need for accurate and efficient diagnosis, with a specific focus on radiographs (X-Ray images). The process of interpreting these images can be quite challenging, often resulting in diagnostic errors and treatment plans that may not be optimal. Healthcare facilities, radiologists, and orthopedic doctors face numerous challenges in the timely and accurate identification of issues in X-ray images. While conventional methods can be effective, they often suffer from slow processing and the potential for human errors.

This is where MuraMed's AI-driven solution steps in as a game-changer, bridging the gap between traditional diagnostics and cutting-edge technology. Our aim is to provide healthcare providers with a powerful tool to ensure the best possible patient care. Using advanced AI technologies, our dedicated team and our team has developed diagnostic system tailored to assist radiologists and healthcare professionals in identifying abnormalities in bone X-ray images. This innovation has the potential to significantly enhance patient outcomes and overall well-being for those dealing with musculoskeletal disorders.

Our system's uniqueness lies in more than just technological advancement; it signifies a transformative shift in how we approach the diagnosis of musculoskeletal conditions, enabling both faster and more accurate assessments. Taking all these into consideration, MuraMed has the potential to establish distinct position in the field of medical diagnostics, particularly in the realm of detecting bone abnormalities.

Furthermore, MuraMed's application is thoughtfully designed with versatility in mind, catering not only to experienced medical professionals but also to individuals outside the medical field. We understand the importance of early detection and intervention, and our platform seamlessly fits into various environments. It can be used by athletes, teachers, physiotherapists, and others who may not have medical backgrounds. This accessibility facilitates quicker identification of potential bone issues, even in settings where immediate medical expertise might not be readily available.

By simplifying the diagnostic process, MuraMed extends the benefits of our innovative technology beyond hospitals and clinics. We promote a proactive approach to health and well-being in diverse communities, spanning from specialized medicine to community healthcare and beyond. MuraMed is poised to make a lasting impact across various sectors, all while ensuring our technology is easily understood and accessible to a wide range of users.

Mura Datasets: Powered by Stanford University

Figure 1. Official Stanford ML Logo

In our pursuit of these objectives, MuraMed relies on extensive datasets established by *Stanford University*, collectively known as the MURA datasets. These datasets encompass a vast collection of **musculoskeletal radiographs**, constituting a comprehensive library of bone *X-rays* specifically focusing on different body parts like the wrist, shoulder, elbow, hand, finger, forearm, and humerus. Radiologists have manually reviewed and labeled each study as either *'Normal'* or *'Abnormal*.'

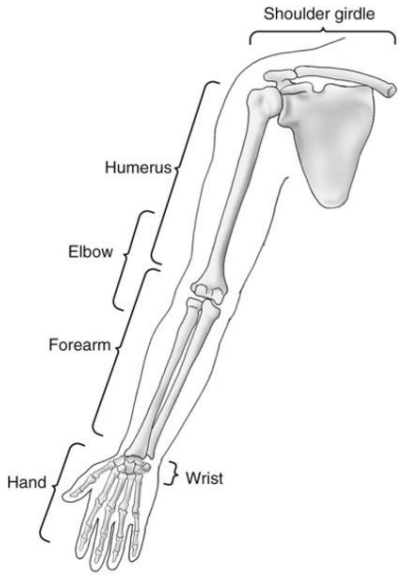

Figure 2. A detailed image showcasing the anatomical parts included in the Mura Dataset.

Currently, our algorithms are designed to focus on the aforementioned body parts. Their primary task is to determine whether an *X-ray* study of these areas exhibits normal or abnormal characteristics. In the near future, we plan to expand our AI capabilities to involve a broader spectrum of anatomical regions, further enhancing our diagnostic capabilities.

Our Mission

Our mission has to do with **Global Impact and Enhanced Healthcare Access.** More specifically, Musculoskeletal conditions affect over **1.7 billion** people worldwide, often leading to severe, long-term pain and disability. This results in approximately **30 million** emergency department visits annually, a number that's on the rise. Our mission is to utilize our dataset to drive significant progress in medical imaging technologies, enabling expert-level. This, in turn, will help improve healthcare access in **regions where skilled radiologists are in short supply**. Therefore, with MuraMed's AI-powered diagnostic system and our commitment to advancing medical diagnostics, we aim to make a **meaningful impact on healthcare**, enhancing patient outcomes, and promoting better well-being across the globe.

Our Vision

Expanding Radiological Excellence is one of our main vision goals that led us to this project idea. To be more precise, we at MuraMed, our vision is to make **advanced radiological diagnostics** accessible to healthcare facilities of **all sizes**. Moreover, our target audience extends beyond medical professionals, encompassing teaching personnel, fitness centers, athletes, and workplaces. Our goal is to equip healthcare providers and individuals with AI tools that elevate their diagnostic capabilities, offering reliable support and ensuring precise and timely diagnoses, even in **complex cases**.
In other words, our vision is not restricted to large healthcare facilities but extends to smaller clinics and even transcends the boundaries of the traditional healthcare industry. By integrating advanced AI algorithms with a specialized focus on bone abnormalities and a versatile application range, MuraMed aims to **revolutionize medical diagnostics** in an unparalleled manner. Through these initiatives, the company is set to bring about monumental changes that will redefine the landscape of healthcare, making quality diagnostic services **accessible and affordable to all**.

Value of MuraMed's Research

MuraMed's research holds immense value in several key areas, bringing significant benefits to healthcare, technology, business, and innovation. Here, we outline the fundamental aspects of how our research positively impacts these domains, showcasing our dedication to enhancing patient care, technological capabilities, business growth, and medical advancement.

In summary, both the mission and the research values of MuraMed underscore its commitment to being more than just a healthcare technology company. It strives to be a change-maker in the industry, leveraging technology to address crucial gaps in healthcare accessibility and quality. By doing so, MuraMed aims to foster not just business growth but also societal advancement, setting new benchmarks in healthcare, technology, and innovation.

Clinical Excellence

Improved Diagnostic Precision: MuraMed's AI-driven approach enhances the accuracy of identifying musculoskeletal issues in X-ray images. This means more precise diagnoses, timely treatments, and better patient outcomes. Our technology can detect even subtle abnormalities, reducing the risk of misdiagnosis.

Efficiency and Speed: MuraMed speeds up the diagnostic process for healthcare professionals. This helps reduce patient waiting times and simplifies treatment planning. With our AI system, radiologists can review X-rays more quickly, ensuring patients receive timely care.

Early Issue Identification: MuraMed plays a crucial role in detecting problems at an early stage. This can prevent complications, lower treatment costs, and improve overall patient well-being. Timely identification of musculoskeletal issues allows for less invasive treatments and better recoveries.

Tailored Treatment: MuraMed provides insights that enable personalized treatment plans. This ensures that each patient receives the most suitable care and personalized recommendations based on individual conditions, facilitating targeted interventions.

Resource Optimization: Our system automates the initial screening of X-ray images, allowing radiologists to focus on more complex cases. This improves the efficiency of patient care by utilizing resources more effectively.

Technological Advancements

Accessible Diagnostics: MuraMed's innovations overcome geographical barriers, providing top-tier musculoskeletal diagnostics via telehealth, even in remote areas. This ensures that patients in isolated regions have access to high-quality medical expertise.

Supporting Healthcare Professionals: Our AI serves as a reliable decision-support tool for healthcare providers, boosting their confidence in diagnoses. MuraMed's AI offers suggestions and insights that aid healthcare providers in their decision-making process.

Reliability and Precision: MuraMed's deep learning models ensure reliable interpretations and minimize errors, especially in more complex cases. The consistency and precision of our AI-powered system aims to lead to more dependable diagnoses.

Scalability: Once validated, MuraMed's model easily integrates into various healthcare systems, addressing gaps in medical services. Our technology can adapt effectively to different healthcare infrastructures, ensuring broader access to advanced diagnostics.

Business Growth

Competitive Edge: Healthcare organizations that embrace MuraMed gain a technological advantage, setting new benchmarks in patient care. Our innovative solutions enhance their ability to provide high-quality healthcare services, giving them a competitive edge in the industry.

Financial Strengthening: MuraMed offers monetization opportunities such as subscription models and partnerships with corporations, which strengthen the financial position of

healthcare institutions. These revenue streams enhance their financial resources for continued growth and investment.

Streamlined Operations: MuraMed effectively integrates with existing hospital systems, streamlining their healthcare operations. This integration optimizes the healthcare value chain, ensuring that processes run efficiently, and resources are utilized effectively.

Market Expansion: Our versatile solutions extend beyond healthcare to sectors like sports and education, extending the reach of our technology. This expansion into diverse fields not only broadens market access but also fosters institutional growth and development.

Research and Innovation

Advancing Medical Science: MuraMed's efforts have the potential to drive technological progress in radiology and deep learning, contributing to advancements in medical diagnostics. Our commitment to research and innovation leads to improved healthcare solutions and better patient outcomes.

Collaborative Innovation: Collaboration among data experts, engineers, and clinicians at MuraMed promotes a multidisciplinary approach. This collaborative environment paves the way for future innovations, where insights from various fields come together to create groundbreaking solutions.

Continuous Improvement: MuraMed remains dedicated to ongoing research and development. Our focus on continuous improvement ensures that our solutions remain innovative, delivering benefits to both healthcare providers and patients.

Enhanced Data Security: With a strong emphasis on data security and privacy, MuraMed continually innovates to protect patient information. Our robust data security measures set industry standards for safeguarding sensitive medical data.

Global Impact: MuraMed's commitment to innovation has strong potential to extend globally, encouraging international collaboration and the exchange of medical insights. This global perspective contributes to a more comprehensive understanding of healthcare challenges and solutions.

Key Pillars

MuraMed is built upon a foundation of three key pillars that define its scope and impact in the specialized field of musculoskeletal radiograph analysis. These pillars represent diverse domains, each with its unique set of challenges and opportunities for analyzing musculoskeletal radiographs of the hand, elbow, and shoulder. Together, they form the core focus areas of MuraMed's application and illustrate its versatility in addressing the diagnostic needs of various sectors within the realm of musculoskeletal healthcare.

These key pillars encompass the realms of:

I. **Healthcare (Medicine/Hospitals)**
II. **Sports Organizations & Schools**
III. **Workplace (Private Organizations for employees' health)**

showcasing MuraMed's commitment to revolutionizing musculoskeletal healthcare across multiple industries while emphasizing its specialization in hand-related radiograph analysis.

I. MuraMed: Healthcare Edition, an AI-Assisted Musculoskeletal Radiograph Analysis Platform

MuraMed's first pillar encompasses the world of traditional medicine and healthcare facilities, focusing exclusively on **musculoskeletal radiograph analysis** of the hand, elbow, and shoulder.

By leveraging advanced deep learning techniques, this solution offers an unparalleled diagnostic tool for radiologists and orthopedic doctors, ensuring timely, accurate, and efficient detection of musculoskeletal abnormalities. Here, MuraMed provides invaluable support to radiologists and orthopedic professionals, offering an AI-backed second opinion that enhances diagnostic accuracy within these specific areas. Its seamless integration with hospital systems ensures that diagnostic services are optimized, enabling timely and accurate detection of musculoskeletal abnormalities within the medical domain.

▪ Business Propositions & Objectives

MuraMed's primary business propositions aim to provide musculoskeletal health analysis with a comprehensive suite of capabilities:

Diagnostic Support

MuraMed offers professionals an invaluable AI-backed second opinion, significantly enhancing diagnostic accuracy. It does so by carefully spotlighting potential areas of concern in radiographs, and by providing crucial insights for healthcare providers.

Telemedicine Capabilities

In regions where specialized radiologists may be scarce, MuraMed steps in with its telemedicine capabilities. This functionality ensures that diagnostic services can extend their reach even to the most remote corners, guaranteeing access to essential healthcare resources.

Seamless PACS Integration

MuraMed's integration with existing hospital systems is seamless and efficient. Upon radiograph upload, it delivers instantaneous analysis, optimizing the diagnostic process and minimizing delays in patient care without impacting the whole process.

Adaptive Learning

With each deployment, MuraMed evolves and adapts. Drawing from diverse datasets, it refines its diagnostic capabilities continually. This commitment to adaptive learning ensures that MuraMed maintains and improves its accuracy and reliability in musculoskeletal health analysis, providing state-of-the-art diagnostic support.

▪ Monetization Strategies for Sustainable Healthcare

In line with our commitment to revolutionizing musculoskeletal healthcare through MuraMed's Healthcare Edition, we have devised a set of monetization **strategies designed for sustainability**. These strategies ensure that healthcare professionals, clinics, and institutions can access MuraMed's cutting-edge AI-assisted musculoskeletal radiograph analysis platform effectively and efficiently. Below, we outline our structured approaches:

Diverse Subscription Models

MuraMed offers a versatile range of subscription options, each thorough tailored to meet the specific needs of hospitals, clinics, and individual healthcare practitioners. These subscription plans guarantee unfettered access to MuraMed's robust AI diagnostic capabilities. Whether you're a large medical facility or a solo practitioner, our flexible subscription models ensure accessibility and affordability.

Pay-Per-Use Convenience

For those seeking a more flexible arrangement, MuraMed provides a pay-per-use model, perfect for occasional or smaller healthcare establishments. This pay-as-you-go approach allows you to harness MuraMed's diagnostic power precisely when needed, without any long-term commitment.

Customized Model Training and Implementation

MuraMed goes the extra mile by offering bespoke model training, fine-tuning, and implementation services. This tailored approach ensures that MuraMed's AI algorithms are precisely calibrated to match the unique demographics and equipment types of each user. The result? The most accurate and relevant diagnostic insights, making MuraMed an invaluable, adaptable, and cost-effective solution within the healthcare landscape.

These monetization strategies *empower healthcare providers with the flexibility to choose the most fitting plan*, ultimately ensuring sustained access to MuraMed's advanced musculoskeletal radiograph analysis capabilities.

▪ Potential Challenges

Navigating the healthcare tech landscape demands a methodical approach. Adhering to regulatory guidelines, ensuring robust data privacy measures, and fostering a close-knit collaboration with medical professionals are of prime importance. This ensures MuraMed is technologically robust while also **catering to the practical needs of its user base**. Additionally, a potential challenge lies in the fact that MuraMed's focus is solely on musculoskeletal radiograph analysis of the hand, elbow, and shoulder, limiting its scope to these specific areas and potentially necessitating collaboration with other solutions for radiographs of different body parts.

Understanding PACS in the Context of MuraMed (subsection under PACS)

Since MuraMed seeks to **revolutionize** the domain of musculoskeletal radiography. By harnessing the capabilities of cutting-edge deep learning methodologies, we present an unmatched diagnostic aid for radiologists and orthopedic specialists, ensuring prompt, precise, and efficient identification of musculoskeletal irregularities.

To be more precise, **Picture Archiving and Communication System** (*PACS*) is a medical imaging technology that provides economical storage and convenient access to images from various modalities. It's a synergy of hardware, software, and networking solutions that enables the capture, distribution, and display of medical images. *PACS* eradicates the need for tangible film, offering clinicians the advantage of remote access to view and diagnose from any location (*See the pictures below*).

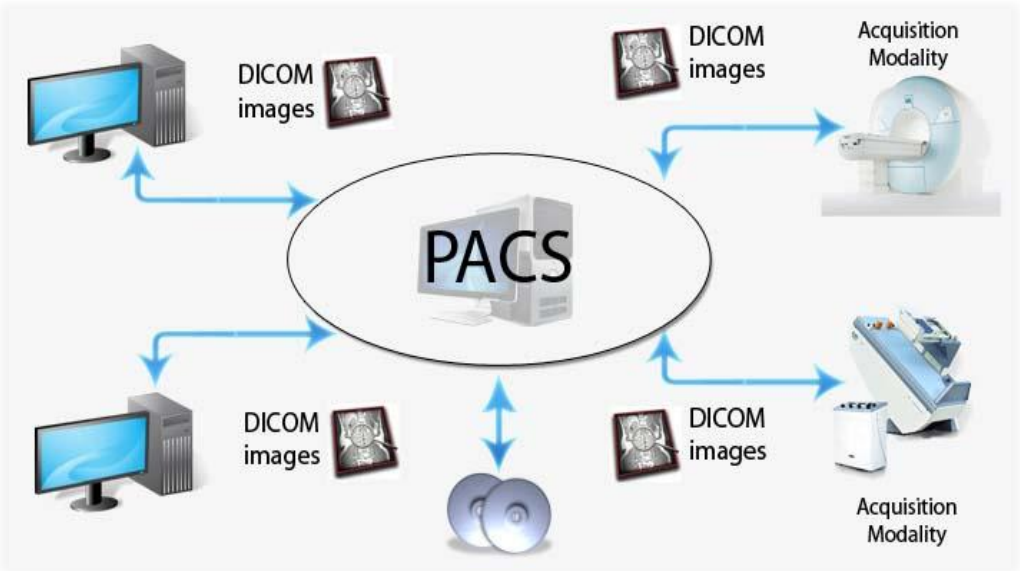

Figure 3. The pathways of PACS: The foundational structure enabling MuraMed's seamless integration and rapid analysis within hospital systems.

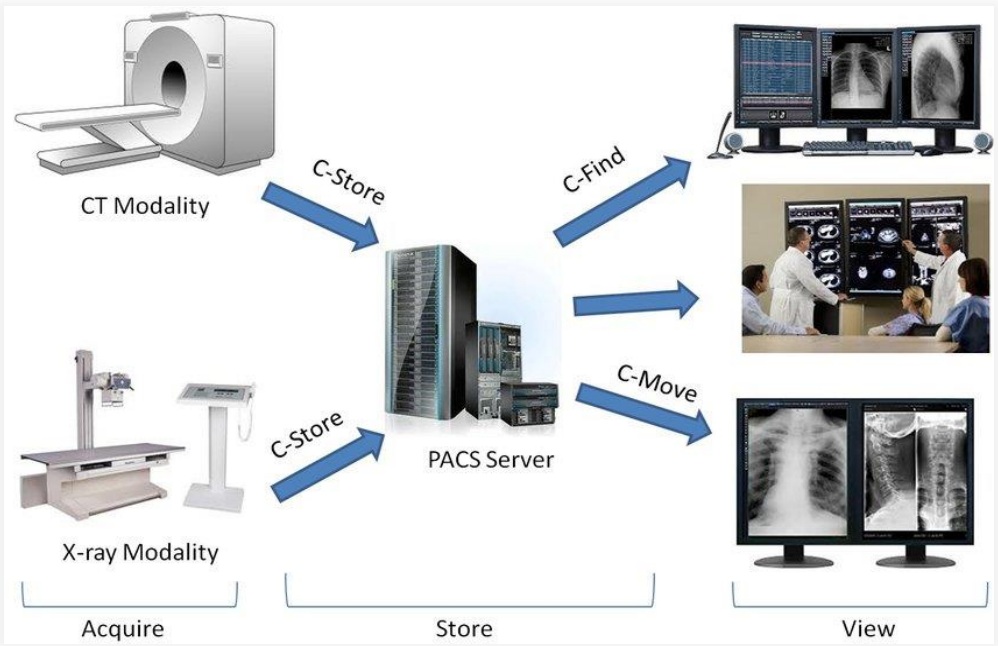

Figure 4. Streams of data flow: A visualization of the PACS network, channeling radiographic information to MuraMed for AI-assisted diagnostics.

▪ Additional Applications in Healthcare Landscape

Beyond its primary applications, MuraMed's Healthcare Edition extends its versatile capabilities to a range of additional healthcare settings, redefining musculoskeletal health management across diverse healthcare landscapes:

Primary Care Clinics

MuraMed can be integrated into primary care settings, enabling general practitioners to identify potential musculoskeletal issues, especially those concerning the hand, elbow, and shoulder, and provide appropriate referrals to specialists. This capability ensures that patients presenting with hand-related discomfort or injuries can receive **timely and accurate assessments**, leading to swift referrals to orthopedic specialists or radiologists for further evaluation and treatment planning.

The application of MuraMed in this context revolves around its assistance to general practitioners in identifying potential musculoskeletal abnormalities during routine check-ups. The reason for this integration is clear: early detection is pivotal. It leads to timely referrals to specialists, ensuring that patients, especially those with hand-related issues, receive the comprehensive care they need. This **proactive approach** enhances the healthcare experience, offering patients timely access to the expertise of orthopedic specialists and radiologists, ultimately contributing to better musculoskeletal health and overall well-being.

Elderly Care Facilities

As the elderly population grows, MuraMed can play a vital role in detecting musculoskeletal issues, including hand injuries, in **geriatric patients**, aiding in early intervention and improving their quality of life. This capability is especially significant in addressing the unique healthcare needs of elderly individuals, where musculoskeletal concerns, such as hand injuries, can have a substantial impact on their daily lives and mobility [13]. By incorporating MuraMed into the healthcare protocols of elderly care facilities, healthcare providers can ensure that geriatric patients receive timely attention and tailored care plans, ultimately enhancing their well-being and maintaining their independence.

MuraMed finds a valuable application in elderly care facilities through regular musculoskeletal screenings for elderly residents, aiming to detect issues like hand fractures, shoulder joint degeneration, or elbow osteoporosis. The reason behind this application is clear: **early detection leads to prompt treatment and interventions**. By identifying these musculoskeletal concerns at their nascent stages, healthcare providers can proactively prevent falls and other related accidents, ultimately leading to an improved overall quality of life for the elderly residents. This approach not only enhances their well-being but also contributes to the safety and comfort of the care facility.

Physical Therapy Centers

MuraMed's utility extends beyond diagnostics, providing an essential tool for physical therapists working with patients recovering from hand and shoulder injuries. As referenced in studies addressing the prognosis and treatment of shoulder pain [14], the challenges in managing shoulder conditions have been well-documented. With MuraMed's focus on musculoskeletal radiograph analysis of the hand, shoulder, and elbow, physical therapists can leverage real-time insights to track patients' progress during therapy. This not only aligns with the need for more efficient targeting of shoulder pain treatments but also allows therapists to modify treatment plans and exercises promptly, optimizing rehabilitation outcomes [15] and improving patient care.

Integrating MuraMed's AI into physical therapy sessions serves as a groundbreaking approach to shoulder and hand injury management. Real-time insights offered by MuraMed enable therapists to closely **monitor patients' progress** and **tailor treatment plans specifically to their unique needs,** as recommended by recent studies [14], [15]. This dynamic adjustment of rehabilitation strategies, based on accurate and real-time diagnostic information, not only aligns with the evolving landscape of musculoskeletal healthcare but also promises to significantly enhance the quality of rehabilitation and patient outcomes.

Chiropractic Clinics with a Specialization in Hand Care

Chiropractic professionals specializing in hand, elbow, and shoulder care can harness MuraMed's insights to offer highly tailored treatment plans for their patients. The specificity of MuraMed's diagnostic capabilities aligns seamlessly with the intricate nature of musculoskeletal issues within these areas. Chiropractors can utilize MuraMed's AI-backed analysis to precisely **identify and understand patients' conditions**, facilitating targeted chiropractic adjustments and treatments [16], [17]. This specialized approach ensures that patients receive personalized care based on accurate diagnostic information, optimizing their musculoskeletal health in the context of hand, elbow, and shoulder-related concerns.

The integration of MuraMed's insights into chiropractic clinics specializing in hand, elbow, and shoulder care enhances the quality of patient treatments. By utilizing MuraMed's AI, chiropractors can tailor adjustments and treatment plans specifically to the unique musculoskeletal issues in these areas. This **personalized approach**, based on precise diagnostic information, results in more effective treatments, aligning with the overarching goal of chiropractic care – to improve musculoskeletal health and overall well-being for patients experiencing hand, elbow, and shoulder discomfort or injuries.

Fitness Centers

MuraMed's versatility extends to *fitness centers*, where trainers can harness its capabilities to evaluate clients' musculoskeletal health comprehensively, with a particular focus on the health of their hands, elbows, and shoulders. By incorporating musculoskeletal screenings into their assessment process, fitness professionals can gain valuable insights into clients' fitness readiness, especially regarding the condition of their hands. This data-driven approach ensures that personalized workout routines are not only effective but also aligned with each client's specific musculoskeletal condition, including potential hand-related issues [13], [14]. This tailored approach plays a pivotal role in **injury prevention during exercise**, creating a safer and more productive fitness environment.

Incorporating musculoskeletal screenings using MuraMed to assess clients' fitness readiness, with specific attention to hand health, presents a proactive strategy in fitness center operations. The primary reason for implementing this approach is to **prevent exercise-related injuries** effectively, including those related to the hands. Through these screenings, trainers can identify potential vulnerabilities in the upper body's musculoskeletal system, particularly in the hands, elbows, and shoulders. Armed with this knowledge, fitness professionals can craft workout plans that are finely tuned to individual needs, mitigating the risk of hand-related injuries, and promoting long-term physical well-being. This synergy between technology and fitness is a testament to MuraMed's potential impact on the health and safety of fitness enthusiasts.

Pharmaceutical Research

Within the realm of *pharmaceutical research*, particularly in clinical trials assessing medications targeting musculoskeletal disorders, MuraMed stands as an asset for tracking patients' responses to treatment and potential side effects. Moreover, when pharmaceutical companies develop products like hand ointments or treatments with specific relevance to hand-related musculoskeletal conditions, MuraMed proves instrumental. By integrating MuraMed into these clinical trials, researchers can accurately evaluate patients' musculoskeletal responses, including the effects of products designed for hand usage. This application ensures precise assessment, contributing significantly to understanding treatment efficacy and identifying any **potential side effects** associated with these specialized products.

The utilization of MuraMed in pharmaceutical research for evaluating patients' musculoskeletal responses in clinical trials, particularly concerning products like hand ointments, emerges from the necessity for precision and thoroughness. It's vital to comprehensively assess the **performance** of medications and products tailored for hand-related musculoskeletal conditions, ensuring that they meet the desired efficacy standards and safety profiles. MuraMed's integration in this context underscores its pivotal role in advancing pharmaceutical research, not only for traditional medications but also for **specialized products** like hand ointments, promising a more thorough understanding of treatment outcomes and their implications for patients.

Hospital/Patient Health Portal

MuraMed's application in the *Hospital/Patient Health Portal* brings advanced musculoskeletal radiograph analysis directly to the hands of patients and healthcare providers. Through seamless integration, patients can access their radiograph results and analyses **conveniently**, fostering a deeper understanding of their musculoskeletal health. This user-friendly interface allows for easy retrieval of diagnostic information, empowering patients to engage actively in their care journey. Moreover, healthcare providers benefit from MuraMed's expertise by receiving comprehensive insights into patients' musculoskeletal conditions, ultimately leading to more **informed treatment decisions**.

The inclusion of MuraMed's musculoskeletal radiograph analysis within the Hospital/Patient Health Portal serves as a catalyst for patient engagement and well-informed decision-making. By providing patients with direct access to their radiograph results and analyses, they become active participants in their healthcare, promoting a sense of ownership over their musculoskeletal well-being. Healthcare providers, on the other hand, gain a powerful tool to aid in accurate diagnoses and treatment planning. This collaborative approach between patients and providers not only enhances the quality of care but also contributes to better health outcomes, emphasizing the significance of integrating MuraMed's capabilities into the Hospital/Patient Health Portal within the broader healthcare landscape.

In Summary: As the medical field continues to evolve, the potential applications of MuraMed's AI-driven solution are vast. The focus on accurate, efficient, and timely musculoskeletal diagnostics aligns with numerous healthcare sectors, contributing to improved patient care and outcomes. Each application demonstrates how MuraMed's AI-driven solution can be tailored to address specific challenges and opportunities in various sectors, ultimately leading to improved patient care and well-being.

II. MuraMed: School & Sports Organization Edition

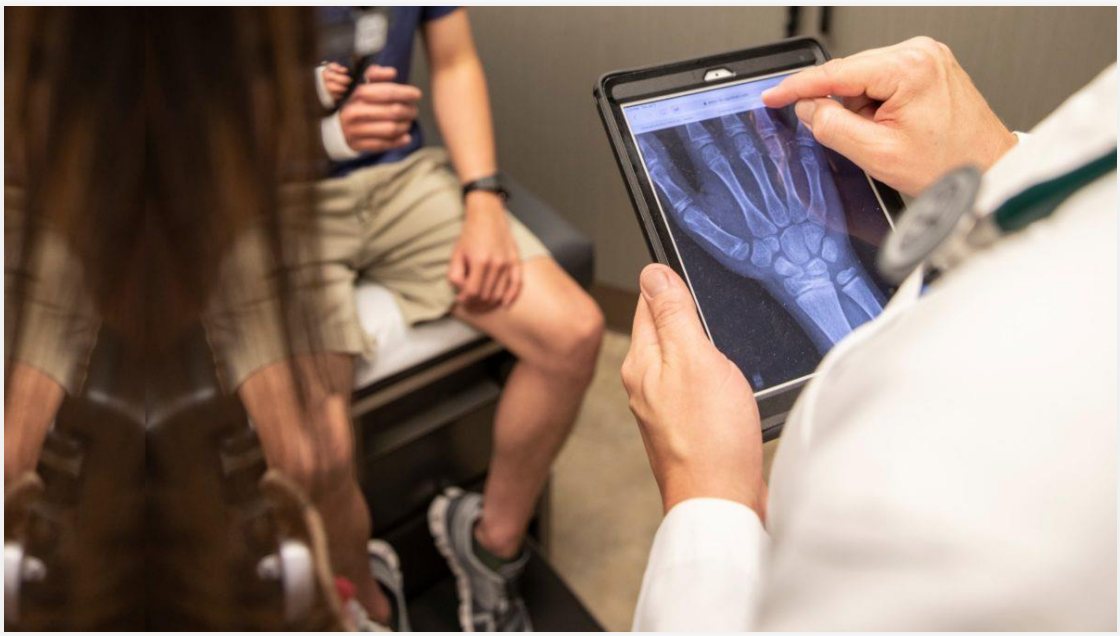

MuraMed for School & Sports Organization is a cutting-edge solution that bridges the gap in musculoskeletal healthcare for young athletes and students. This innovative platform is not confined to the drawing board; it can be readily applied across various sports where hand injuries are particularly prevalent. For instance, in basketball, studies have indicated that hand and wrist injuries account for a substantial portion of injuries among players, ranging from fractures to sprains. Similarly, in sports like volleyball and handball, athletes are susceptible to various hand-related injuries due to the dynamic nature of the game and the frequent use of the hands for striking and blocking. By offering **real-time**, **accurate** detection of musculoskeletal abnormalities, MuraMed can play a transformative role in preventing and addressing these common injuries among young athletes. With its potential to enhance the health and performance of students and athletes in these sports, MuraMed is poised to make a significant impact on the field.

▪ Business Propositions and Objectives

In the subsequent sections, we delve deeper into the distinct propositions and objectives that underpin our dedication to improving the health and well-being of the Sports and Education sectors:

Early Injury Detection for Athletes

In the realm of sports, where every move and play matters, early injury detection becomes paramount. MuraMed steps into this arena with its unparalleled capability to swiftly identify musculoskeletal issues in athletes, with a specific focus on the hand, elbow, and shoulder. The process begins at the start and end of each sports season, where schools and sports teams harness the power of MuraMed to conduct **comprehensive scans**. These scans are vital in the early detection of any potential musculoskeletal abnormalities that might have arisen due to intense sports activities. Within this rigorous process, the hand, being a vital player in many sports, receives particular attention. The reason behind this early detection protocol is clear: *swift identification allows for prompt treatment, ensuring that athletes' long-term health and performance, especially in contexts where hand injuries are common, remain uncompromised.*

The significance of early detection cannot be overstated, especially when it comes to athletes and the intricate **biomechanics** of their hands. Timely identification of musculoskeletal issues in the hand is a game-changer. It not only ensures that athletes receive the necessary medical attention but also contributes significantly to their overall well-being. The early detection process, driven by MuraMed's advanced AI capabilities, empowers athletes, schools, and sports teams to make informed decisions that prioritize **health** and **performance**. By keeping a watchful eye on the hand, athletes can address issues before they escalate, ultimately leading to safer and more productive sporting experiences. [18] - [21]

Post-Injury Rehabilitation Monitoring

When athletes face injuries, particularly concerning their hands, the road to recovery can be intricate. In these scenarios, MuraMed's post-injury rehabilitation monitoring process plays a pivotal role. Focused on athletes' hand injuries, this process involves regular scans aimed at closely tracking the **healing journey**. The hand, being a crucial component in many sports, requires special attention. These scans are not only designed to monitor the healing process but also to detect any potential complications that might arise during recovery. The reason behind this rigorous monitoring is clear: athletes should only return to their respective games when they are fully healed, especially in cases involving hand injuries. By adhering to this stringent monitoring process, athletes can significantly **reduce the risk of re-injury**, protecting the long-term health and performance of their hands and allowing them to confidently resume their sporting endeavors.

The reasoning behind such detailed hand rehabilitation monitoring is simple yet profound. Athletes depend on the optimal functioning of their hands for precision, strength, and agility. Even minor complications during the healing process can have lasting consequences, especially for the hand. Therefore, it is essential to ensure that athletes regain full strength, dexterity, and functionality in their hands before they re-enter the arena. MuraMed's regular scans serve as a critical tool in this journey, offering insights into the healing trajectory of hand injuries. By adhering to this strategy, sports teams and medical professionals can ensure that athletes only rejoin their respective sports when they are fully recovered, significantly reducing the risk of exacerbating hand injuries and securing the **athlete's long-term well-being and sporting potential.**[22],[23]

Physical Education Class Health Check

In the realm of *physical education* classes, ensuring students' musculoskeletal health is crucial. Here, MuraMed offers a transformative process that schools can leverage to promote the well-being of their students, with particular emphasis on the hand, elbow, and shoulder. By incorporating MuraMed into physical education classes, schools can conduct routine health checks to guarantee that **students are in optimal musculoskeletal condition**. This proactive approach is not only about ensuring their immediate fitness but also about safeguarding their long-term health. Among its many advantages, this process can detect early signs of conditions like scoliosis in students, a condition that, when left untreated, can significantly impact their musculoskeletal health. By integrating hand health assessments into these checks, schools can comprehensively evaluate students' physical well-being, allowing for early interventions when needed. This ensures that students can continue their **physical education journeys with confidence**, knowing that their musculoskeletal health is a priority. [34], [35]

The inclusion of hand health assessments within these health checks is particularly pertinent, given the role of hands in various physical activities. Early detection of hand-related musculoskeletal issues, such as strains, sprains, or joint problems, is vital to prevent their

escalation and ensure that students can fully participate in physical education without **discomfort** or **limitations**. MuraMed's advanced AI capabilities make this process efficient and accurate, further enhancing the overall health and safety of students engaged in physical education classes.

Integration with Sports Biomechanics

The integration of MuraMed with sports biomechanics is a groundbreaking process that can significantly impact athletes' performance and health, including those cases where hand injuries are prevalent. This process brings together the world of radiography and biomechanics to provide a comprehensive view of an athlete's well-being, focusing on their hand, elbow, and shoulder. By synchronizing **athletes' movement** patterns with **radiographic findings**, this process allows for a deep understanding of how an athlete's movements, including those involving the hand, may be contributing to musculoskeletal issues. The hand, with its intricate movements and dexterity, plays a vital role in many sports, making its assessment within this process particularly significant.

The reason behind this integration is clear: optimizing an athlete's performance and minimizing the risk of injuries, especially those involving the hand, requires a holistic approach. By combining data from radiographic assessments with biomechanical insights, coaches and sports professionals can tailor training regimens to address specific musculoskeletal concerns. For example, in sports where hand injuries are common, such as basketball or volleyball, the integration of hand health assessments into sports **biomechanics** becomes invaluable. It helps identify potential areas of improvement or modification in an athlete's technique, ultimately contributing to enhanced performance and reduced injury risks. This seamless fusion of technology is at the forefront of musculoskeletal healthcare, offering athletes a data-driven path to excellence while safeguarding their hand health. [24], [25]

Athlete's Health Passport

The development of an *Athlete's Health Passport* marks a significant stride in optimizing athlete care and performance, with a specific focus on the hand, elbow, and shoulder. This innovative process involves creating a digital repository where an athlete's radiographs, AI analyses, and doctor's notes are accurately stored in chronological order. This comprehensive record offers a detailed and evolving account of the athlete's **musculoskeletal health over time**. Coaches, physiotherapists, and other medical professionals involved in an athlete's care can access this passport, gaining valuable insights into the athlete's condition. For sports where hand injuries are common, this passport allows for precise tracking of an athlete's hand health. Understanding the nuances of hand-related musculoskeletal issues through chronologically stored data empowers medical staff to make informed decisions regarding training regimens, injury prevention, and rehabilitation, all geared towards optimizing the athlete's performance while safeguarding their hand health.

Moreover, the Athlete's Health Passport is not limited to professional athletes but extends its benefits to students engaged in physical education classes. By using the **passport** to monitor the hand health of young athletes, schools can provide a safe and nurturing environment for students to develop their physical abilities. With a comprehensive view of an athlete's musculoskeletal health, this process ensures that every participant, from budding talents to elite athletes, receives the utmost care and attention, particularly when it comes to their hands. [26] - [28]

Educational Workshops

Educational workshops are a cornerstone of MuraMed's commitment to musculoskeletal health in sports and physical education, with a particular emphasis on the hand, elbow, and shoulder. This process entails offering **informative sessions to physical education teachers**, coaches, and sports team medical staff. These workshops cover a wide spectrum of topics, from understanding radiographs to highlighting the paramount importance of early detection and showcasing how to effectively utilize MuraMed. Hands-on workshops, where participants can interact with real-world examples involving the hand, further enhance the learning experience. The reason behind these workshops is simple but powerful: educated stakeholders can make more informed decisions for the health and well-being of students and athletes alike.

In sports where hand injuries are prevalent, such as basketball or volleyball, workshops using real-life examples involving the hand can be particularly enlightening. Participants gain insights into the specific musculoskeletal challenges associated with these sports, allowing them to tailor their training and coaching strategies accordingly. These educational initiatives contribute to a **safer** and more **productive** sports environment, ensuring that coaches and medical staff possess the knowledge and skills necessary to protect and optimize the hand health of their athletes. [29] - [31]

Collaboration with Sports Equipment Manufacturers

Collaborating with sports equipment manufacturers stands as a pivotal process within MuraMed's mission to enhance the safety and performance of athletes, with a specific focus on the hand, elbow, and shoulder. This strategic partnership involves a thorough analysis of various types of sports equipment, including hand gear, elastic bandages, elbow guards, upper arm protectors, and general protective equipment. The objective is to investigate if **certain equipment contributes to musculoskeletal issues**, especially those affecting the hand and upper extremities. For sports like rugby, where shoulder and chest protection is essential, the evaluation extends to materials like high-density foam padding, with a consideration for alternatives to traditional outer hard shells. This in-depth analysis ensures that athletes are equipped with gear that not only maximizes their safety but also minimizes the risk of musculoskeletal injuries. [32], [33]

The reason behind this collaboration is clear: it paves the way for the design and development of superior sports equipment that actively mitigates the risk of injury. By scrutinizing the impact of different gear on musculoskeletal health, manufacturers can refine their products to provide athletes with enhanced protection. For instance, when focusing on hand gear, the process may reveal design improvements that offer better support and impact absorption for hand-related sports injuries. This collaborative effort strives to create a **new generation** of sports equipment that not only optimizes performance but also prioritizes the preservation of athletes' hand health. Through this synergy between medical insights and manufacturing expertise, athletes can engage in their chosen sports with greater confidence, knowing that their equipment is designed to minimize the risk of musculoskeletal injuries, particularly those affecting the hand, elbow, and shoulder.

Athlete Health Portal

The Athlete Health Portal in MuraMed's School & Sports Organization Edition serves as a centralized hub for athletes, coaches, and healthcare providers. Athletes can securely access their **musculoskeletal health data**, including radiograph results and AI-backed analyses, offering them valuable insights into their physical condition. Coaches and medical staff can monitor the progress of athletes, ensuring their well-being throughout the sports season. Through the portal, radiographs and other relevant information are readily available, streamlining communication and coordination among all stakeholders involved in an athlete's care.

The Athlete Health Portal in MuraMed's School & Sports Organization Edition is pivotal in fostering a collaborative and informed approach to athlete care. By providing athletes access to their musculoskeletal health data, they become active participants in their own well-being, which can contribute to early injury prevention and better long-term health. Coaches and medical staff benefit from real-time insights into athletes' conditions, allowing for prompt interventions when needed and the development of tailored training and rehabilitation plans. In essence, the Athlete Health Portal promotes a **holistic** and **data-driven** approach to **athlete health management**, enhancing overall sports performance and athlete satisfaction within schools and sports organizations.

▪ Monetization Strategies for Sustainable Sports and Education Health

In our unwavering commitment to promoting the well-being of students and athletes through MuraMed's Schools and Sports Organization Edition, we've crafted a set of **monetization strategies** geared toward long-term sustainability. These strategies are designed to ensure that musculoskeletal health management remains effective, benefiting educational institutions, sports teams, and the broader sports industry. *Below, we provide an extensive overview of our structured approaches:*

Tailored Package Deals

MuraMed extends the convenience of tailored package deals to schools and sports organizations, enabling them to scan multiple students or athletes cost-effectively. These deals provide competitive rates, making it accessible for educational institutions and sports teams to proactively manage the musculoskeletal health of their students and athletes.

Flexible Subscription Model
Our flexible subscription model empowers educational institutions and sports academies to select from a range of plans customized to their specific requirements. By subscribing annually, these organizations enjoy uninterrupted access to MuraMed's monitoring services, AI analyses, and the dedicated health portal. This approach fosters ongoing musculoskeletal health management while accommodating budget considerations.

Enhanced Education Workshops
MuraMed offers specialized education workshops, charging fees for these enlightening sessions aimed at deepening stakeholders' comprehension of radiographs and the critical importance of early detection. These workshops can be precisely tailored to address the unique challenges faced by educational and sports sectors, nurturing a culture of safety and wellness.

Collaboration with Sports Equipment Manufacturers
Our platform collaborates closely with sports equipment manufacturers, providing in-depth analysis and charging for assessments that evaluate the impact of their products on musculoskeletal health. This mutually beneficial partnership seeks to improve the design of sports equipment, reducing the risk of musculoskeletal issues among athletes.

These versatile monetization streams ensure that MuraMed remains financially sustainable while providing indispensable services to its users. Ultimately, these efforts contribute significantly to the well-being of students, athletes, and the continued growth of the sports and education sectors.

In Summary: With an increasing emphasis on sports and physical activities in schools, the health of young athletes and students is paramount. By introducing MuraMed to these institutions, we can ensure early detection, prompt treatment, and overall better musculoskeletal health for the younger generation.

III. MuraMed: Workplace Edition

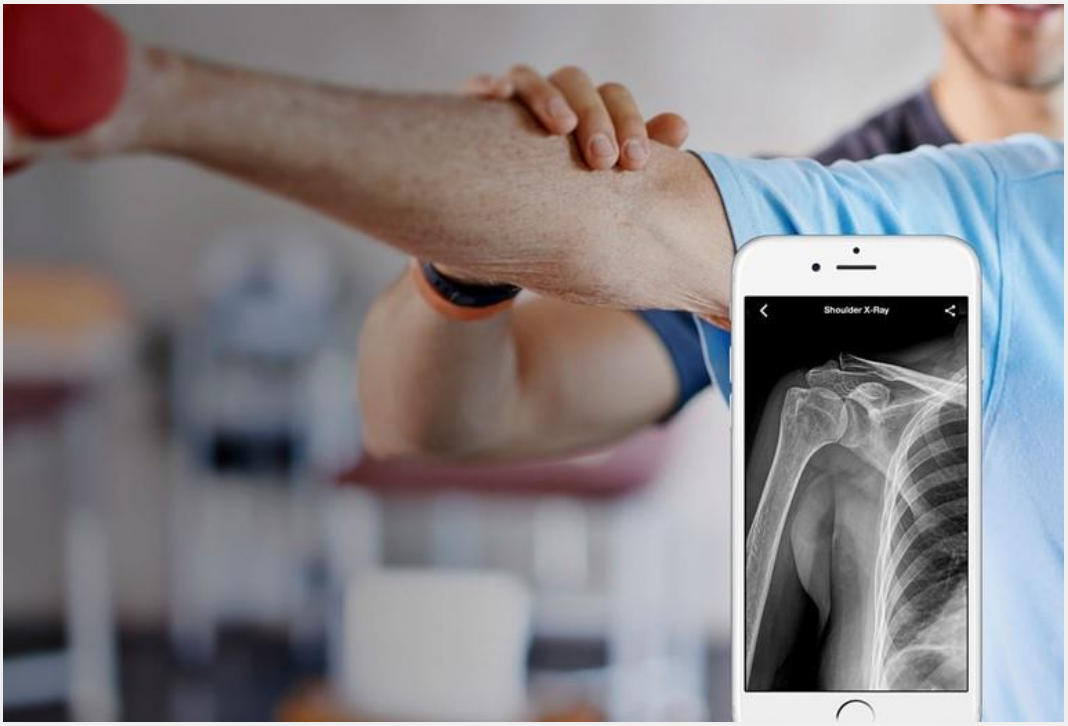

MuraMed's Workplace Edition is a specialized solution designed to address **work-related musculoskeletal disorders** (*MSDs*), focusing on upper limb, shoulder, and hand conditions. It's suitable for a wide range of industries, from heavy manual labor to office jobs. This edition helps detect and manage *MSDs* early through regular **employee check-ups** and **ergonomic evaluations**. It targets the unique challenges faced by professions with a high risk of *MSDs*, promoting healthier workplaces and reducing the impact of these disorders on both employees and employers.

Recent statistics from the *U.S. Department of Labor* underscore the significance of this issue. According to their findings, a notable **23 percent** of all work-related injuries involve injuries to the hands or fingers, categorizing hand injuries as "*the most frequent preventable injuries*" (Safety + Health magazine). Moreover, these hand injuries rank as the second most common cause of missed workdays, following closely behind back and neck injuries. They encompass various types of injuries, including broken bones, such as fractured fingers. Another type is **avulsion fractures**, where a small piece of bone comes off from a tendon or ligament. Avulsion fractures in the hand and wrist frequently happen when someone falls and stretches out their hand to break the fall.

Business Propositions and Objectives

In the following sections, we provide a more detailed exploration of the specific propositions and objectives that define our commitment to enhancing workplace health and well-being:

Preventing Work-Related Injuries in Industrial Environments

In industrial environments like construction or manufacturing, MuraMed's regular *X-ray* screenings for workers engaged in physically demanding roles aim to serve as a critical preventive measure. These screenings are specifically designed to identify potential musculoskeletal issues early, particularly in professions where hand injuries are prevalent, such as construction. By detecting issues promptly, we prevent work-related injuries, ensuring a healthier and more productive workforce.

Enhancing Employee Well-Being Through Routine Screenings

Routine employee screenings offer a proactive approach to employee well-being, especially for jobs requiring high physical demands or repetitive tasks. Early detection of musculoskeletal disorders through regular screenings facilitates timely interventions, reducing the severity and duration of these conditions. This approach fosters overall employee health and minimizes workplace absenteeism.

Supporting Post-Injury Recovery

In cases of post-injury recovery, MuraMed aims to provide a valuable resource by offering regular scans to monitor the healing process. This comprehensive monitoring ensures that employees return to work only when they are fully recovered, thereby reducing the risk of re-injury and preventing long-term complications. This feature is particularly crucial in physically demanding professions where a premature return to work, such as in the case of wrist or hand injuries, which are particularly common, can lead to more severe injuries.

Tailoring Workspaces for Employee Comfort

Integrating MuraMed's findings with ergonomic assessments enables a personalized approach to optimizing work environments, whether in traditional office settings or more hazardous workplaces. By gaining insights into each employee's specific musculoskeletal needs, workplaces can make precise adjustments to seating, computer setups, or workstations, promoting ergonomic workspaces and enhancing overall employee comfort and safety. This tailored approach not only reduces physical strain but also contributes to a healthier and safer work environment, aligning with MuraMed's commitment to improving workplace well-being across diverse industries.

Collaborative Employee Health Solutions

Collaborating with occupational health providers is another dimension of MuraMed's holistic approach to employee health. By partnering with these providers, we aim to offer a comprehensive health solution that includes MuraMed screenings, physical therapy, and ergonomic interventions. This collaborative effort ensures that employees receive well-rounded care addressing both immediate and long-term musculoskeletal health concerns, ultimately leading to better health outcomes and cost savings over time.

Employee Health Portal

As an integral part of this edition, the employee health portal will serve as a user-friendly digital tool designed to empower individuals in managing their musculoskeletal health. Within this platform, employees will be able to conveniently keep track of their screenings, access AI-generated analyses, and review recommended interventions. This proactive approach will

encourage employees to make informed decisions regarding their well-being, fostering a culture of health consciousness within the workplace and contributing to the overall health and productivity of the workforce.

▪ Monetization Strategies for Sustainable Workplace Health

In our commitment to enhancing workplace well-being through *MuraMed's Workplace Edition*, we've developed a set of strategies with a focus on sustainability. These plans are aimed at ensuring that musculoskeletal health management remains effective and continues to benefit companies and their employees. Below, we provide a detailed overview of our structured efforts:

Corporate Health Packages

MuraMed offers *tailored corporate packages* designed to accommodate companies of all sizes. These packages provide cost-effective solutions for scanning large numbers of employees, ensuring that businesses can proactively manage musculoskeletal health across their workforce.

Subscription-Based Model

Our flexible subscription model allows companies to choose from various plans based on their specific needs. By subscribing annually, organizations gain continuous access to MuraMed's monitoring services, AI analyses, and the employee health portal. This approach encourages ongoing musculoskeletal health management while providing budget-friendly options.

Tailored Training and Workshops

MuraMed can provide specialized *training and workshops* for companies looking to enhance their employees' musculoskeletal health awareness and practices. These sessions can be tailored to address the unique challenges of different industries, promoting a safer and healthier work environment.

Consultation Services

Our expert consultants can work closely with organizations to assess their musculoskeletal health needs and recommend customized solutions. This *consultancy service* ensures that businesses receive personalized guidance in implementing effective musculoskeletal health management strategies.

Integration with Occupational Health Providers

Companies can effecively integrate MuraMed's services with their existing occupational health providers. This collaborative partnership enhances overall employee health care while leveraging the strengths of both parties.

In Summary: *MuraMed's Workplace Edition* offers a specialized solution to address work-related musculoskeletal disorders (*MSDs*), encompassing various body parts which at this moment are: the wrist, shoulder, elbow, hand, finger, forearm, and humerus. With a focus on **early detection**, **personalized care**, **ergonomic improvements** and **collaboration with occupational health providers**, our aim is to promote healthier workplaces. Additionally, our user-friendly employee health portal empowers individuals to proactively manage their musculoskeletal health. By addressing these critical aspects, MuraMed strives to enhance workplace well-being for businesses within the *European Union* and beyond, ensuring a healthier, safer, and more productive workforce.

Business Model Canvas: MuraMed

1. Key Partnerships:

Radiologists & Orthopedic Doctors: Collaborate with medical experts for feedback and continuous improvement of AI models.

Hospitals & Clinics: Establish partnerships for deployment and integration of AI-assisted diagnostics.

Regulatory Bodies: Engage with healthcare regulatory authorities for necessary approvals and compliance.

Medical Schools: Partner with educational institutions for the deployment of AI tools in medical education.

2. Key Activities:

Model Training & Continuous Learning: Develop and refine AI models for accurate diagnosis, ensuring continuous learning from medical data.

Integration with PACS: Seamlessly integrate with Picture Archiving and Communication Systems (PACS) used in healthcare.

Data Augmentation & Pre-processing: Enhance the quality and diversity of medical data through data augmentation and preprocessing.

Regulatory Compliance & Certifications: Ensure compliance with healthcare regulations and attain necessary certifications.

Customer Support & Training: Provide robust customer support and training to healthcare professionals and institutions.

Building and Maintaining the MuraMed Platform

Collaborating with Radiology Clinics for Data Collection

3. Key Resources:

MURA Dataset and Additional Data: Access to a diverse and extensive dataset is foundational to our AI model's training and continuous improvement.

Deep Learning Infrastructure: Cutting-edge infrastructure, including GPUs and servers, is essential for model training and real-time diagnostics like cloud databases.

Medical Expertise: Collaboration with radiologists and orthopedic doctors ensures the clinical relevance and accuracy of our AI models.

Development & Tech Team: A skilled team of AI developers and engineers drives the development, deployment, and maintenance of our solutions.

4. Value Propositions:

AI-assisted accurate diagnosis: Our AI models are trained on extensive datasets, enabling them to detect abnormalities in X-rays with remarkable precision, acting as a valuable aid to radiologists and orthopedic doctors.

Second opinion for radiologists: MuraMed doesn't replace human expertise; it enhances it. Radiologists can now receive AI-generated second opinions, reinforcing diagnostic confidence.

Telemedicine support for remote areas: MuraMed's cloud-based architecture facilitates telemedicine, extending diagnostic capabilities to underserved regions and remote clinics.

Continuous learning for improved accuracy: Our AI models continuously learn from new data, ensuring that they stay updated with evolving medical knowledge.

PACS integration for seamless workflow: MuraMed integrates seamlessly with Picture Archiving and Communication Systems (PACS), streamlining the diagnostic workflow within healthcare institutions.

Scalable and cost-effective AI infrastructure: We've partnered with AI hardware providers to offer scalable and cost-effective infrastructure solutions, making AI adoption feasible for healthcare providers of all sizes.

5. Customer Relationships:
Subscription Support: Provide responsive support for subscription-based customers.
Training Sessions for Medical Staff: Offer training sessions to ensure the effective use of our AI tools.
Regular Updates & Feedback Sessions: Keep customers informed with regular updates and gather feedback for improvements.
Online Portal for Account Management: Facilitate easy account management and support through an online portal.
6. Channels:
Direct Sales to Hospitals & Clinics: Engage in direct sales to healthcare institutions for seamless integration.
Online Portal for Subscription & Pay-per-Use: Enable online subscription and pay-per-use services for individual users.
Partnerships with Medical Conferences & Workshops: Collaborate with medical events for exposure and adoption.
Integration with Telemedicine Platforms: Integrate our AI solutions with telemedicine providers' platforms.
7. Customer Segments:
Hospitals & Large Clinics: Offer comprehensive AI solutions for healthcare facilities.
Individual Radiologists & Orthopedic Doctors: Provide individual practitioners with AI tools for enhanced diagnostics.
Medical Schools & Training Institutes: Support educational institutions with AI-based learning tools.
Telemedicine Service Providers: Collaborate with telemedicine platforms to extend diagnostic capabilities.
Sports Organizations
Healthcare Private Businesses (fitness centers, elderly care, physiotherapy center, chiropractic center, facilities etc)
Workplaces
8. Cost Structure:
Infrastructure & Hosting Costs: Cover expenses related to AI infrastructure and
Research & Development: Allocate resources for continuous model improvement and development.
Regulatory Compliance & Certification Costs: Ensure adherence to healthcare regulations and certifications.
Marketing & Sales: Invest in marketing and sales efforts to reach healthcare institutions and practitioners.
Employee Salaries & Benefits: Compensate the skilled team of developers and medical experts.
9. Revenue Streams:
Subscription Fees from Hospitals & Clinics: Generate recurring revenue from healthcare institutions.
Pay-per-Use Fees: Offer flexible payment options for individual users.
Custom Model Training & Implementation Services: Provide tailored AI model training and implementation for specific needs.
Educational Licensing for Medical Schools: License AI-based learning tools to medical schools and training institutes.
10. Key Metrics:
Number of Subscribers/Users
Accuracy Improvement Rate
Customer Satisfaction and Feedback
Usage Frequency and Retention Rates

Future Plans

As we look ahead, our vision for MuraMed extends beyond the current scope of musculoskeletal health management. In line with our commitment to improving well-being, we have several exciting future initiatives in mind.

- **Expanding Body Part Coverage:** While we currently focus on the upper limbs (*wrist, shoulder, elbow, hand, finger, forearm, and humerus),* we recognize the need to broaden our coverage to involve additional areas, ensuring comprehensive musculoskeletal health support for all.

- **Mobile Application:** In the pipeline is the development of a user-friendly mobile application that allows healthcare professionals to efficiently upload radiographs and promptly receive AI-generated feedback. This tool will empower doctors with a convenient on-the-go resource for accurate diagnosis.

- **Interactive 3D Visualization:** To further aid medical professionals, we are working on an innovative feature that transforms 2D radiographs into interactive 3D models. Leveraging AI technology, this tool will highlight areas of concern, offering a more comprehensive understanding of musculoskeletal issues and serving as an invaluable educational resource for patients.

- **Integration with Wearable Tech:** Recognizing the value of preventive care, we are exploring partnerships with wearable technology providers. By integrating wearable data, such as posture analysis, we aim to predict potential musculoskeletal issues and offer proactive solutions to promote long-term well-being.

- **MuraMed Pets:** Expanding our reach, we are excited to introduce MuraMed Pets, a specialized version tailored to the health needs of our beloved animal companions. This initiative reflects our commitment to extending the benefits of musculoskeletal health management to the furry members of our families.

B. Technical Implementation

Having thoroughly reviewed the theoretical plan, and the business implications, we now delve into the technical implementation phase. This pivotal segment will elucidate the precise methodologies, tools, and technologies enlisted to actualize the project's goal of abnormality detection in bone X-Rays with MuraMed. While prior sections afforded a macro-level comprehension, herein lies the micro-level operational details pivotal for executing the project successfully.

The technical implementation acts as the linchpin, knitting together multiple critical components, ranging from data management to algorithmic fine-tuning and software integration. Such thorough attention to each element underpins the project's robust theoretical foundation and ensures its practical viability.

Technical Implementation Plan: A Detailed Roadmap

The following document outlines the technical architecture and operational strategy to successfully implement the project for abnormality detection in bone X-Rays. It is structured around five key areas of focus, each crucial for the project's seamless execution. In addition, we include sections detailing the justification for algorithmic choices, offering a holistic view of both the strategic and tactical dimensions.

I. **Data Architecture**
- Data Acquisition
- Data Storage
- Data Management

II. **Algorithm Development**
- CNN Architecture Design
- Hyperparameter Optimization
- Justification for Using CNNs

III. **Quality Assurance**
- Unit Testing
- Model Evaluation Metrics
- Methodologies for Testing

IV. **Deployment**
- Containerization
- Monitoring Systems
- Maintenance Protocols

This roadmap outlines the key milestones and components that will be focused upon for the successful technical implementation of this project. Each title represents a critical area that will be developed.

I. Data Architecture

The data architecture for this project has multiple dimensions, each crucial for ensuring the quality and utility of the data involved. Beginning with **Data Acquisition**, we've chosen the Stanford ML Group's MURA dataset [3] as our primary source. This dataset, comprising a range of bone X-Ray images categorized as normal and abnormal, offers a robust foundation for our model. The choice of a reputable dataset alleviates concerns about data integrity and reliability. Python-based scripts will automate the process of downloading and unpacking this dataset, ensuring that data acquisition is both reproducible and efficient.

In the realm of **Data Storage**, structure is king. Our approach involves organizing the data into carefully structured directories, separated based on the data type (training, validation, or test) and class (normal or abnormal). Such a structured data storage approach not only facilitates easier data access but also minimizes errors during the data-loading phase.

The **Data Management** aspect focuses on how the data will be preprocessed, augmented, and loaded during the training phase. We will employ **TensorFlow's ImageDataGenerator** [4] for real-time data augmentation, a critical step for enhancing model robustness. This is particularly crucial in medical imaging, where the data is highly imbalanced, and the cost of misclassification is high. Efficient data loading mechanisms are equally critical. Given that we're dealing with high-resolution images, optimized memory usage is non-negotiable. Batch-loading techniques will be implemented to this end.

Get to know the MURA Dataset

To be more precise regarding the **MURA dataset**, this is, an acronym for *"Musculoskeletal Radiographs"*, was inaugurated by *Stanford University* in the year 2017. It constitutes a large-scale compilation encompassing over **42,000 digital radiographic images**. These images are distributed across seven distinct anatomical regions, including the *wrist*, *elbow*, *shoulder*, *finger*, *hip*, *knee*, and *ankle*.

The dataset's primary objective is to facilitate the advancement of machine learning algorithms capable of autonomously **identifying abnormalities** within musculoskeletal radiographs. This task presents a considerable challenge, given that such abnormalities often manifest subtly and may elude even the discerning analysis of trained radiologists.

Since its release, the MURA dataset has gained prominence as a benchmarking tool for assessing the efficacy of deep learning models in the domain of musculoskeletal radiographic analysis. It has been employed extensively in academic research and competitive frameworks for the development and validation of algorithms aimed at detecting a range of abnormalities, such as fractures and dislocations, within X-ray imagery.

Figure 5: MURA Dataset and TensorFlow's Logo.

II. Algorithm Development

At the heart of our project is the algorithm—specifically, the Convolutional Neural Networks (CNNs). **The Architecture of the CNN is designed to capture both the lower-level features like edges and corners, as well as higher-level features that are more abstract and capture the essence of what makes an X-Ray normal or abnormal**. Multiple convolutional and pooling layers will be employed, followed by fully connected layers for classification. The architecture will be tuned for optimal performance through experimentation.

Optimization is another critical element. We plan to employ techniques like *Grid Search* or *Random Search for hyperparameter tuning*. These methodologies systematically explore multiple combinations of parameters over the defined hyperparameter space, capturing the one that offers the best performance. Additionally, we will experiment with different optimization algorithms like *Adam* or *RMSprop* to see which yields better results in the shortest time.

The **Justification for CNNs** has been made after careful consideration. CNNs are uniquely suited for image recognition tasks due to their ability to learn spatial hierarchies of features automatically and adaptively. This makes them incredibly efficient in terms of computational cost, requiring fewer parameters compared to other types of neural networks. CNNs are also highly versatile, able to work well with color or grayscale images, and their robustness to translations and deformations makes them ideal for medical imaging tasks where the point of focus can vary within the image.

Moving forward, we will dive into more details regarding the Optimization procedures and then we will answer why choose to use CNNs.

Optimization Procedures

To be more precise the **optimization** in machine learning is an intricate endeavor that extends beyond the simple selection of an appropriate algorithm. It encompasses a multi-dimensional search in a complex landscape, dictated by the interplay of various hyperparameters, to arrive at the most effective model. This venture is further complicated when we engage with high-stakes domains such as medical imaging, where the costs of false positives and false negatives can be significant. Thus, our optimization strategy is multifaceted, incorporating several techniques and approaches to ensure that the resultant model is not just computationally efficient but also clinically effective.

▪ Hyperparameter Tuning Techniques

More specifically, **Grid Search** method involves specifying a grid of hyperparameters and systematically searching through all possible combinations. While computationally expensive, Grid Search is thorough and is particularly useful when the hyperparameter space is not exceedingly large. We foresee employing Grid Search for parameters like learning rate and batch size, where a comprehensive search can yield dividends.

On the contrary to Grid Search, **Random Search** samples the hyperparameter space randomly. This approach is computationally more efficient and has been shown to yield equally good or sometimes even better results than Grid Search. Random Search could be particularly useful for tuning more complex hyperparameters like the architecture of the neural network itself.

▪ Optimization Algorithms

Adam (Adaptive Moment Estimation) is renowned for its efficiency and has become almost a default choice in deep learning tasks. It combines the benefits of two other extensions of *stochastic gradient descent*: **AdaGrad** and **RMSProp**. Adam adjusts the learning rate during training, making it adaptable to the specific characteristics of the data.

RMSprop (Root Mean Square Propagation) is another adaptive learning rate method and is an excellent choice for non-convex optimization problems. It adapts the learning rates during training and is very effective for problems that are noisy or have sparse gradients.

To sum up, *both Adam and RMSprop have their advantages and disadvantages*. For instance, Adam is generally good at handling sparse gradients, while RMSprop is often better for online and non-stationary tasks. Our project may likely experiment with both to ascertain which aligns better with the nuances of medical image classification.

▪ Evaluation Metric

The selection of an appropriate evaluation metric is also part of the optimization process. Given the medical nature of our project, traditional metrics like accuracy are not sufficiently informative. Instead, we will focus on metrics like ***sensitivity***, ***specificity***, and ***F1-score***, which provide a more detailed understanding of model performance.

By adopting a diversified yet focused approach to optimization, we aim to create a model that is both computationally efficient and clinically effective. This comprehensive strategy ensures that we navigate the complex optimization landscape with the finesse required to meet the high stakes inherent in medical applications.

Justification for the Choice of Convolutional Neural Networks (CNNs)

To be more precise, the **Convolutional Neural Network (CNN)** is a class of deep neural networks most applied to visual imagery analysis. In the context of the notebook, the objective is to detect abnormalities in bone X-Rays, a highly specialized field within medical imaging. Here, we discuss why CNNs may be the preferred choice over other machine learning algorithms and models for this specific task. The following sections will explain this in detail.

▪ Traditional Machine Learning Algorithms

Let's first consider traditional machine learning algorithms like **Logistic Regression**, **Decision Trees**, **Random Forests**, and **Support Vector Machines (SVM)**. These algorithms require *manual feature engineering, a cumbersome and often inefficient process in the context of high-dimensional data like images*. Also, these algorithms usually *don't perform well on raw image data due to their inherent complexity and spatial hierarchies, which these algorithms are not designed to understand* (For more details you can visit this article [5]).

▪ Fully Connected Neural Networks

Fully connected networks, also known as **Dense Neural Networks**, *don't respect the spatial hierarchy of the data*. Every neuron is connected to every other neuron in the next layer, making the network susceptible to overfitting and requiring a large number of parameters. The lack of focus on spatial relationships makes them inefficient for image-based tasks, where pixel location and neighborhood have semantic significance. You can find more regarding the Fully Connected Neural Networks in this very interesting article [6].

- **Recurrent Neural Networks (RNNs)**

RNNs are generally more suited for sequence-based problems like natural language processing or time-series prediction. Their architecture, which is designed to remember past information, is not inherently equipped to deal with the spatial hierarchies and complexities in image data (Check these articles [7], [8]).

- **Autoencoders**

Autoencoders are generally used for unsupervised learning tasks, primarily dimensionality reduction and feature learning. While they can be adapted for image classification tasks, they are not inherently designed for this purpose [9], [10].

- **Generative Adversarial Networks (GANs)**

GANs are more focused on data generation and are not inherently structured for classification tasks. While they can be adapted for such tasks, the complexity involved usually outweighs the benefits for a straightforward classification problem like abnormality detection in bone X-Rays [11].

Why CNNs Are Preferable

This section aims to elucidate the rationale behind opting for Convolutional Neural Networks (CNNs) over other machine learning algorithms and neural network architectures. This section will delve into the unique capabilities and advantages that make CNNs particularly suited for the task of abnormality detection in musculoskeletal radiographs [12].

- **Hierarchical Feature Learning**

One of the most compelling attributes of CNNs is their innate capability for Hierarchical Feature Learning. In the realm of image analysis, the interpretability of features often exists in a hierarchical fashion. Basic features like edges and corners form the building blocks, which, when combined in various configurations, result in more complex and abstract features like textures and shapes. CNNs are architected to learn this spatial hierarchy automatically and adaptively. The initial layers often specialize in identifying rudimentary features, such as edges and lines. As one progresses through the network, the layers grow more complex and capable of understanding intricate patterns. This hierarchical learning is especially advantageous in medical imaging, where simple features like tissue boundaries could combine to form higher-order features like fractures.

- **Parameter Sharing and Sparsity**

Parameter Sharing and Sparsity in CNNs are mechanisms that significantly reduce the computational burden. Traditional neural networks tend to have fully connected layers, where each neuron in one layer is connected to every neuron in the next layer. This results in many parameters, leading to longer training times and requiring more powerful hardware. CNNs circumvent this issue by sharing weights across neurons. This form of parameter sharing ensures that the network learns translational invariance, allowing it to recognize a feature regardless of its position in the image. Additionally, this drastically reduces the number of parameters, making CNNs more computationally efficient and capable of running on standard hardware without compromising performance.

▪ Robustness to Translations and Deformations

Medical imaging data often come with their unique set of challenges, one of which is the variability in the position and orientation of the abnormalities. A feature detection model must thus be Robust to Translations and Deformations. CNNs are built with this robustness in mind. Due to their convolutional nature and weight-sharing architecture, they are inherently adept at recognizing features irrespective of their location in the image. This property is invaluable in tasks like detecting musculoskeletal abnormalities, where the precise location of the abnormality can vary across patients.

In summary, the hierarchical feature learning capabilities, the efficiency introduced by parameter sharing and sparsity, and the robustness to translations and deformations make CNNs an optimal choice for our project in abnormality detection in musculoskeletal radiographs. These attributes collectively contribute to a model that is not just theoretically sound but also practically effective and computationally feasible. In medical imaging, the importance of capturing intricate patterns and anomalies cannot be overstated. CNNs can capture this level of detail, making them ideal for tasks that require high sensitivity and specificity, such as abnormality detection in bone X-Rays [12].

Additional Decisions/Procedures Followed

▪ Data Augmentation

In the Data Preprocessing section, we have opted to employ **ImageDataGenerator** for data augmentation. This choice is particularly significant in the domain of medical imaging where labeled data is often scarce. Utilizing augmentation techniques such as rotation, zooming, and flipping enhances the robustness of our model, thereby improving its generalization capabilities when applied to unseen data.

▪ Metrics Choice

Selecting appropriate metrics is of paramount importance in medical applications. Traditional metrics like ***accuracy*** **can often be misleading**, particularly given the different costs associated with false negatives and false positives in a medical setting. Therefore, we have conscientiously chosen to focus on specialized metrics such as ***sensitivity*** and ***specificity*** to offer a more subtle evaluation of the model's performance.

▪ Callbacks for Training

We have incorporated the use of callbacks during the model training phase, a decision aligned with best practices in machine learning. Specifically, we utilize ***Early Stopping callbacks*** to curtail the training process when the model ceases to improve on the validation set. This is of particular importance in medical contexts, where overfitting could potentially lead to incorrect diagnoses, carrying severe consequences.

III. Quality Assurance

In a field as critical as **medical imaging**, Quality Assurance isn't just a luxury; it's a necessity. To this end, we have a layered approach to ensure that our project not only meets but exceeds the required standards. Starting with Unit Testing, each function and method in our codebase will be tested using Python's ***unittest*** or ***pytest*** **libraries**. These unit tests serve as the first line of defense against bugs and ensure that the code performs as expected under a variety of conditions.

As for **Model Evaluation**, as also mentioned earlier, we take a rigorous approach. We will employ metrics such as ***sensitivity***, ***specificity***, and ***F1-score***, which are more nuanced than traditional accuracy and offer a better understanding of the model's performance in a medical context. ***Cross-validation techniques*** will also be employed, providing an unbiased assessment of the model's true performance. We have chosen these metrics and methodologies because they are particularly suited for imbalanced datasets common in medical applications.

IV. Deployment

The final phase of our project is **Deployment**, which involves several key steps. The entire project, including the trained model, preprocessing algorithms, and even the unit tests, will be containerized using Docker. This makes it easier to deploy the project in any environment without worrying about dependencies. Once deployed, Monitoring Systems will be put in place to track the model's performance in real-time. Any significant deviations in performance metrics will trigger alerts, necessitating immediate review and possible model retraining. Maintenance is the final ongoing step, involving regular updates to include new data, refine the model, and implement any necessary patches or improvements.

By carefully planning and executing each section outlined, we aim to translate the project's theoretical framework into a fully functional and reliable application for abnormality detection in bone X-Rays. This comprehensive technical implementation plan serves as the roadmap that will guide each phase of the project, ensuring both its theoretical robustness and practical effectiveness.

C. Software Integration

In the software integration phase, we've selected Python as our primary programming language due to its versatility and extensive range of data science libraries. Our choice of Jupyter Notebook as the development environment provides an interactive and well-documented platform that facilitates the smooth organization of code, comprehensive documentation of our progress, and iterative development of machine learning solutions. This integration serves as the backbone for our MuraMed innovative algorithm construction and CNN model development, ensuring an efficient and collaborative workflow.

Libraries and Installation Guidelines

In our software integration efforts for this project, we rely on several **essential Python libraries**, each with its unique role in supporting our data science workflow. Together, these libraries contribute to various aspects, from initial data handling to the development of advanced machine learning models.

Pandas acts as our central library for versatile data manipulation and analysis, providing the foundation for efficient data loading and transformation. **NumPy** complements Pandas by handling essential numerical operations, simplifying data manipulation and analysis.

For the critical task of data visualization, our toolkit includes **Matplotlib** and **Seaborn**. **Matplotlib** serves as the core library for generating a wide range of graphs and charts, offering valuable insights into the intricacies of our dataset. Concurrently, **Seaborn**, as an extension of Matplotlib, enhances our visualization capabilities, facilitating the creation of more intricate and informative visual representations.

Scikit-learn, an extensive library encompassing a diverse set of machine learning algorithms, plays a pivotal role in our project. Its primary function involves dividing our dataset into training and test sets, a fundamental step in the development of our machine learning models.

As we delve into the domain of deep learning, **TensorFlow** emerges as our primary framework. It serves as the robust foundation for our deep learning tasks, providing a flexible ecosystem for constructing and deploying machine learning models, especially those based on neural networks. **TensorFlow**'s optimization for high-performance numerical computation proves invaluable when dealing with the complex analysis of medical images.

In addition to **TensorFlow**, **TensorFlow Addons (TFA)** supplements our deep learning toolkit by extending TensorFlow's capabilities. Despite being in maintenance mode, **TFA** offers additional layers and metrics, serving as a valuable resource for our deep learning applications.

We also highlight some important notes regarding potential UserWarnings that users may encounter. These warnings indicate that **TensorFlow Addons (TFA)** is currently in maintenance mode. Consequently, it is advisable to consider transitioning to other TensorFlow community libraries for incorporating new features or functionalities that were previously covered by TFA.

To maintain the integrity and reproducibility of our experiments, it's crucial to establish a seed for both **NumPy** and **TensorFlow**. By doing so, we ensure that the random numbers generated by these libraries remain consistent across different runs, offering invaluable benefits for debugging and model comparisons.

We set the **seed** value to **1001101** (which corresponds to **01001101**, representing the capital letter **M** in binary format). This seed value serves as a guarantee that the random processes within both NumPy and TensorFlow will consistently produce the same set of random numbers. This step is fundamental in achieving reproducible experiments, allowing us to confidently validate and compare our models.

Libraries versions and requirements

In the context of our project, the versions of the primary libraries we utilize hold significant importance, not only for ensuring compatibility but also for leveraging the latest features and optimizations that these versions offer. Therefore, to be more precise, the main libraries and their versions **used for all three models** are presented below:

- **Pandas 2.1.0**: This updated version includes numerous enhancements over its predecessors, such as improved performance and new functionalities. These features expedite data loading and transformation processes, making our workflow more efficient.

- **NumPy 1.24.3**: With this version, we gain access to the latest numerical computation capabilities. It ensures that our numerical operations are both efficient and accurate, thereby complementing the data manipulation capabilities of Pandas.

- **Matplotlib 3.7.2**: This version comes with updated functionalities that allow for a more extensive range of data visualization options. It is instrumental in generating high-quality graphs and charts that facilitate in-depth data analysis.

- **Seaborn 0.12.**2: This version is compatible with the latest Matplotlib and provides additional visualization techniques. Its updated features enable us to create more complex and aesthetically pleasing visual representations, which are crucial for understanding intricate patterns in our data.

- **Scikit-learn 1.3.0**: This version brings along advancements in machine learning algorithms and techniques. It plays a pivotal role in model training and evaluation, ensuring that we have access to the most effective algorithms for our tasks.

- **TensorFlow 2.13.0-rc0**: Being a release candidate, this version is at the forefront of deep learning technology. It offers us a flexible and robust framework for developing advanced machine learning models, including neural networks. Its high-performance computing capabilities are particularly vital for handling complex tasks, such as medical image analysis.

Additional Considerations:

- TensorFlow Addons (TFA): Although in maintenance mode, TFA continues to offer useful extensions to TensorFlow, providing us with additional layers and metrics that are instrumental for our deep learning tasks. As mentioned above, seeding in NumPy and TensorFlow guarantees reproducibility across different runs. This is crucial for debugging, model comparison, and ensuring the integrity of our experiments.

Finally, through the created ***requirements.txt*** the used environment can be recreated with the same versions of the libraries, ensuring consistent behavior across different setups. To install the libraries from this file, one can use the following command:

```
pip install -r requirements.txt
```

MURA Dataset Technical Overview and Utilization

The **MURA dataset**, which stands for **Musculoskeletal Radiographs**, is a **significant resource dataset** in the field of medical imaging. As previously mentioned in Part A, it was officially released by **Stanford University in 2017** and has since become a cornerstone for medical image analysis.

This dataset contains **over 40,000 digital X-ray images** from seven anatomical regions: the **wrist, elbow, shoulder, finger, hip, knee, and ankle**. It's organized into two main folders, **"train"** and **"valid"**, each with datasets relevant to their respective categories. These datasets cover a wide range of medical conditions, providing a comprehensive platform for training and evaluating diagnostic models.

In total, the MURA dataset comprises approximately **41,000 images** stemming from **around 15,000 unique patient studies**. These images are thoughtfully distributed across both training and validation sets, ensuring a representative sample.

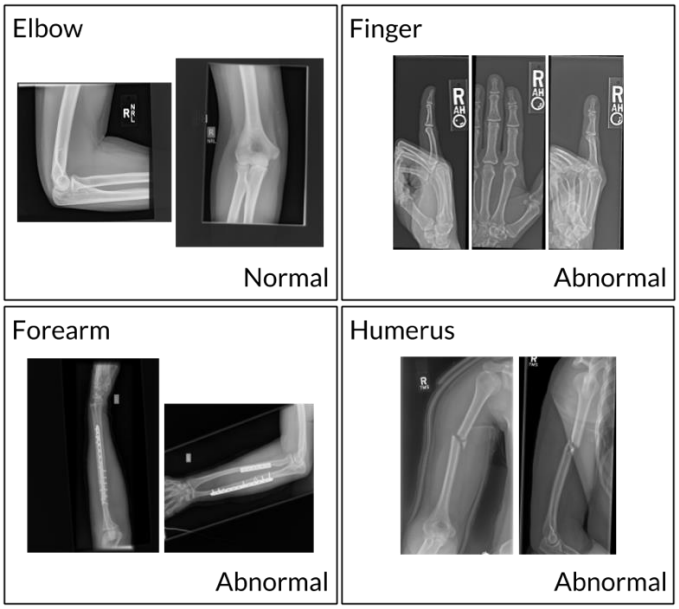

Figure 6. MURA Dataset Instances

Within the dataset, we will find **9,000 studies** representing normal or negative conditions, serving as crucial references for identifying healthy anatomical structures. Additionally, there are **6,000 studies** representing abnormal or positive conditions, which encompass various pathological findings that demand accurate and timely detection.

The typical image resolution in the MURA dataset is **500 x 500 pixels**, ensuring consistent and manageable data for analysis.

We have included specific sections within the Jupyter notebook that provide clear instructions for **downloading the dataset from Kaggle** and **unzipping the MURA Dataset**. These steps are essential to prepare and utilize the dataset effectively in the upcoming sections of your work.

Dataset Validation

Before diving into data processing and model development, it's crucial to ensure that the dataset we're working with is available and properly structured. The purpose here is to guarantee the presence of the dataset and its crucial train and test CSV files within a specified directory. This detailed validation process is instrumental in establishing a robust foundation for subsequent data loading and preprocessing tasks.

To begin, we initialize the filepath variable, setting it to '*MURA-v1.1*'. This path represents the directory where we expect to find the MURA-v1.1 dataset. Next, we create a function called **check_path_exists** to verify the existence of a file or directory. This function takes a path as input and an optional argument specifying whether it's a directory or file that we're checking. In the event of any missing element at any stage of this process, we promptly generate an error message. This proactive approach ensures that all requisite files and directories are in order, ensuring the effective execution of subsequent data preparation and analysis tasks.

Data Loading and Feature Engineering Transformation Workflow

In the following sections of the technical pipeline of **MuraMed**, we define a fundamental function named **load_and_transform_data**. This function goes beyond basic data loading; it serves as a versatile tool for converting raw data into a structured format suitable for advanced analysis and model training.

Loading Data with Precision: At its core, this function starts by carefully reading a specified CSV file, as determined by the **filepath** argument. It efficiently loads this data into a Pandas DataFrame, where each entry corresponds to the path of an image file.

Creating Informative Descriptions: To make it easier to understand each image's details, the function introduces a **description** column. It smartly extracts and combines segments of the **image_path**, summarizing important information about the study type, patient code, and the medical opinion (positive or negative) associated with each image.

Understanding Study Types: The **type** column, derived from the **description**, provides insights into the specific medical study conducted (e.g., elbow, shoulder). This categorization is useful for further analyses or specialized models focused on specific study types.

Patient Identification: By extracting unique patient identifiers, the **patient** column is created. This feature supports long-term analysis and models that consider patient-specific characteristics.

Grouping by Study Codes: The **study** column, originating from the **description**, captures distinct study codes. This helps in grouping images belonging to the same study, which is valuable for multi-image analyses.

Medical Opinion Insights: The **opinion** column is crucial, containing the medical opinion of each study extracted from the **description**. This binary attribute categorizes whether a study was evaluated as positive or negative, forming the foundation of our target variable.

Target Variable Creation: Finally, the function creates the **label** column, representing opinions with 1 for positive and 0 for negative. This column serves as the basis for our machine learning models.

Presenting the Datasets

In this section, we will closely examine the training and test datasets, which are essential components for constructing our machine learning models. Our primary objective is to gain insights into the datasets' structure, attributes, and distinct qualities. This understanding forms the foundation for subsequent tasks, including model development and performance evaluation.

Training Dataset Overview

Initially, we are going to explore the training dataset. We begin by using a custom function called **load_and_transform_data** to load our training dataset from the specified file path. This function is designed to handle essential preprocessing steps, including feature extraction and label encoding.

Below, we provide a snapshot of the initial rows from the training dataset:

	image_path	description	type	patient	study	opinion	label
0	MURA-v1.1/train/XR_SHOULDER/patient00001/study...	SHOULDER_patient00001_study1_positive	SHOULDER	patient00001	study1	positive	1
1	MURA-v1.1/train/XR_SHOULDER/patient00001/study...	SHOULDER_patient00001_study1_positive	SHOULDER	patient00001	study1	positive	1
2	MURA-v1.1/train/XR_SHOULDER/patient00001/study...	SHOULDER_patient00001_study1_positive	SHOULDER	patient00001	study1	positive	1
3	MURA-v1.1/train/XR_SHOULDER/patient00002/study...	SHOULDER_patient00002_study1_positive	SHOULDER	patient00002	study1	positive	1
4	MURA-v1.1/train/XR_SHOULDER/patient00002/study...	SHOULDER_patient00002_study1_positive	SHOULDER	patient00002	study1	positive	1
5	MURA-v1.1/train/XR_SHOULDER/patient00002/study...	SHOULDER_patient00002_study1_positive	SHOULDER	patient00002	study1	positive	1
6	MURA-v1.1/train/XR_SHOULDER/patient00003/study...	SHOULDER_patient00003_study1_positive	SHOULDER	patient00003	study1	positive	1
7	MURA-v1.1/train/XR_SHOULDER/patient00003/study...	SHOULDER_patient00003_study1_positive	SHOULDER	patient00003	study1	positive	1
8	MURA-v1.1/train/XR_SHOULDER/patient00003/study...	SHOULDER_patient00003_study1_positive	SHOULDER	patient00003	study1	positive	1
9	MURA-v1.1/train/XR_SHOULDER/patient00004/study...	SHOULDER_patient00004_study1_positive	SHOULDER	patient00004	study1	positive	1

Figure 7. Preview of Training Dataset Observations

This preview offers a glimpse of the first few rows of our training dataset, revealing columns such i**mage_path**, **description**, **type**, **patient**, **study**, **opinion**, and **label**. These columns contain valuable information about the images and their corresponding attributes.

The **label** column is particularly significant, as it represents our target variable, with 1 indicating a positive medical opinion and 0 indicating a negative opinion. This dataset will be the foundation for training our machine learning models.

Subsequently, we provide **the dimensions of the training set**. More specifically, the training dataset comprises a total of 36,808 rows and 7 columns, providing a substantial amount of data for model training and evaluation. Understanding these dataset characteristics is essential as we proceed with building and assessing our machine learning models.

Summary Statistics for Training Set

In this section, we generate **summary statistics** for the training set. These statistics offer valuable insights into various aspects of our dataset. Specifically, we look at measures of central

tendency, like the **mean**, which provides an idea of the average label value in the dataset. Additionally, we explore the **dispersion** of data through metrics like the **standard deviation**. The summary statistics include:

In the following screenshot we illustrate the output for the summary statistics for the training set:

```
Summary statistics for the training set:
              label
count  36808.000000
mean       0.404070
std        0.490718
min        0.000000
25%        0.000000
50%        0.000000
75%        1.000000
max        1.000000
```

Figure 8. Summary Statistics for Training Dataset

- **Count**: We have a total of 36,808 samples in our training dataset.
- **Mean**: The mean label value is approximately 0.404, indicating that, on average, around 40.4% of the samples are labeled as 1 (positive).
- **Standard Deviation (std)**: The standard deviation is approximately 0.491. This suggests that the label values have some degree of variation from the mean, indicating diversity in our dataset.
- **Minimum**: The minimum label value is 0, which corresponds to negative cases.
- **25th Percentile (1st Quartile)**: At the 25th percentile, the label value is 0, indicating that 25% of the data falls into the negative category.
- **50th Percentile (Median)**: The median label value is also 0, which means that the majority of our dataset consists of negative cases.
- **75th Percentile (3rd Quartile)**: At the 75th percentile, the label value is 1, suggesting that 75% of our data contains positive cases.
- **Maximum**: The maximum label value is 1, indicating positive cases.

These statistics reveal that our training dataset has a relatively balanced distribution between positive and negative cases, with a slight bias towards negative cases. Understanding these central tendencies and variations is crucial for designing and evaluating our machine learning models.

Unique Classes in the Training Set

Determining the **unique classes or labels** in the dataset is crucial for **classification tasks**. It's essential to know what our model will predict. In this stage, we identify and confirm the unique classes present in the training dataset. For our binary classification task, it's important to verify that the labels consist of only two types: **0 and 1**. This ensures that our model is set up correctly for **binary classification**, where **1 typically represents positive outcomes, and 0 represents negative outcomes**. This confirmation is essential for the success of our classification models.

Test Dataset Overview

Similar to the training dataset, we are going to examine the test dataset, which is fundamental for evaluating our machine learning models. We'll follow a similar process of loading and presenting key dataset attributes.

To begin, we load and prepare the test dataset using our custom function, **load_and_transform_data**. This step is crucial as it prepares the data for evaluation, ensuring that it aligns with our model's requirements.

Below, we provide an initial glimpse into the test dataset by showcasing the first few rows. The dataset contains columns such as **image_path**, **description**, **type**, **patient**, **study**, **opinion**, and **label**. These columns contain vital information about the images and their attributes.

	image_path	description	type	patient	study	opinion	label
0	MURA-v1.1/valid/XR_WRIST/patient11185/study1_p...	WRIST_patient11185_study1_positive	WRIST	patient11185	study1	positive	1
1	MURA-v1.1/valid/XR_WRIST/patient11185/study1_p...	WRIST_patient11185_study1_positive	WRIST	patient11185	study1	positive	1
2	MURA-v1.1/valid/XR_WRIST/patient11185/study1_p...	WRIST_patient11185_study1_positive	WRIST	patient11185	study1	positive	1
3	MURA-v1.1/valid/XR_WRIST/patient11185/study1_p...	WRIST_patient11185_study1_positive	WRIST	patient11185	study1	positive	1
4	MURA-v1.1/valid/XR_WRIST/patient11186/study1_p...	WRIST_patient11186_study1_positive	WRIST	patient11186	study1	positive	1
5	MURA-v1.1/valid/XR_WRIST/patient11186/study1_p...	WRIST_patient11186_study1_positive	WRIST	patient11186	study1	positive	1
6	MURA-v1.1/valid/XR_WRIST/patient11186/study2_p...	WRIST_patient11186_study2_positive	WRIST	patient11186	study2	positive	1
7	MURA-v1.1/valid/XR_WRIST/patient11186/study2_p...	WRIST_patient11186_study2_positive	WRIST	patient11186	study2	positive	1
8	MURA-v1.1/valid/XR_WRIST/patient11186/study2_p...	WRIST_patient11186_study2_positive	WRIST	patient11186	study2	positive	1
9	MURA-v1.1/valid/XR_WRIST/patient11186/study3_p...	WRIST_patient11186_study3_positive	WRIST	patient11186	study3	positive	1

Figure 9. Preview of Test Dataset Observations

Just as in the training dataset, the **label** column holds significant importance. It serves as the target variable, with the label '1' indicating a positive medical opinion and '0' indicating a negative opinion. This labeling structure is crucial for evaluating the performance of our machine learning models.

We proceed by providing the dimensions of the test dataset. More particularly, the test dataset comprises a total of 3,197 rows and 7 columns. This size provides a substantial amount of data for evaluating our machine learning models. Understanding these dataset characteristics is pivotal as we move forward with model evaluation.

Summary Statistics for Test Set

In the next step, we generate summary statistics for the test set. These statistics offer insights into central tendencies, variations, and key characteristics of the test dataset. We examine metrics such as mean and standard deviation to gain a deeper understanding of the data. The key summary statistics for the test set are as follows:

```
Summary statistics for the test set:
              label
count  3197.000000
mean      0.478574
std       0.499619
min       0.000000
25%       0.000000
50%       0.000000
75%       1.000000
max       1.000000
```

Figure 10. Summary Statistics for Test Set

- **Count**: We observe that the test dataset contains a total of 3,197 samples, which serve as the basis for our evaluation.

- **Mean**: The mean value for the **label** variable is approximately 0.479. This metric provides an understanding of the average label value in the test dataset. In our context, it suggests that, on average, around 47.9% of the samples are labeled as '1,' indicating positive medical opinions.

- **Standard Deviation (std)**: The standard deviation is approximately 0.500. This metric indicates the degree of variation or spread of the label values from the mean. In our dataset, the standard deviation suggests that the label values exhibit some degree of diversity from the mean, signifying variability in our test data.

- **Minimum**: The minimum label value is 0, which corresponds to negative cases. This indicates that we have samples in the test dataset with negative medical opinions.

- **25th Percentile (1st Quartile)**: At the 25th percentile, the label value is 0. This finding implies that 25% of the data in the test dataset falls into the negative category.

- **50th Percentile (Median)**: The median label value is also 0, which means that the majority of our test dataset consists of negative cases.

- **75th Percentile (3rd Quartile)**: At the 75th percentile, the label value is 1, indicating that 75% of the test dataset contains positive cases.

- **Maximum**: The maximum label value is 1, indicating positive cases. This confirms the presence of samples with positive medical opinions in the test dataset.

These summary statistics unveil essential insights into the distribution of positive and negative cases in our test dataset. Understanding these central tendencies and variations is pivotal for designing and assessing our machine learning models, especially for binary classification tasks where these statistics aid in comprehending the dataset's characteristics.

Unique Classes in the Test Set

Lastly, we identify and confirm the unique classes or labels present in the test set. This information is critical during the evaluation phase, ensuring that the test set consists of the expected classes '0' and '1,' which are fundamental for binary classification.

Understanding these aspects of the test dataset is essential for conducting meaningful evaluations of our machine learning models.

Exploring Distribution of Normal and Abnormal Case Studies Across Anatomical Body Parts in MURA Dataset

As we prepare to implement Convolutional Neural Networks (CNNs) for analyzing radiographic images in the MURA dataset, we've conducted a comprehensive exploration of the distribution of normal and abnormal case studies across various anatomical body parts. This exploration is vital for understanding the dataset's characteristics and will guide our model development process.

Visualizing Distribution with Stacked Bar Plots

To begin, we have utilized stacked bar plots, which serve as our initial visual elements. These visualizations provide an overall view of the total number of normal and abnormal cases for each anatomical body part. Stacked bar plots serve as a foundational insight into how cases are distributed across different anatomical regions. The visualization can be observed below:

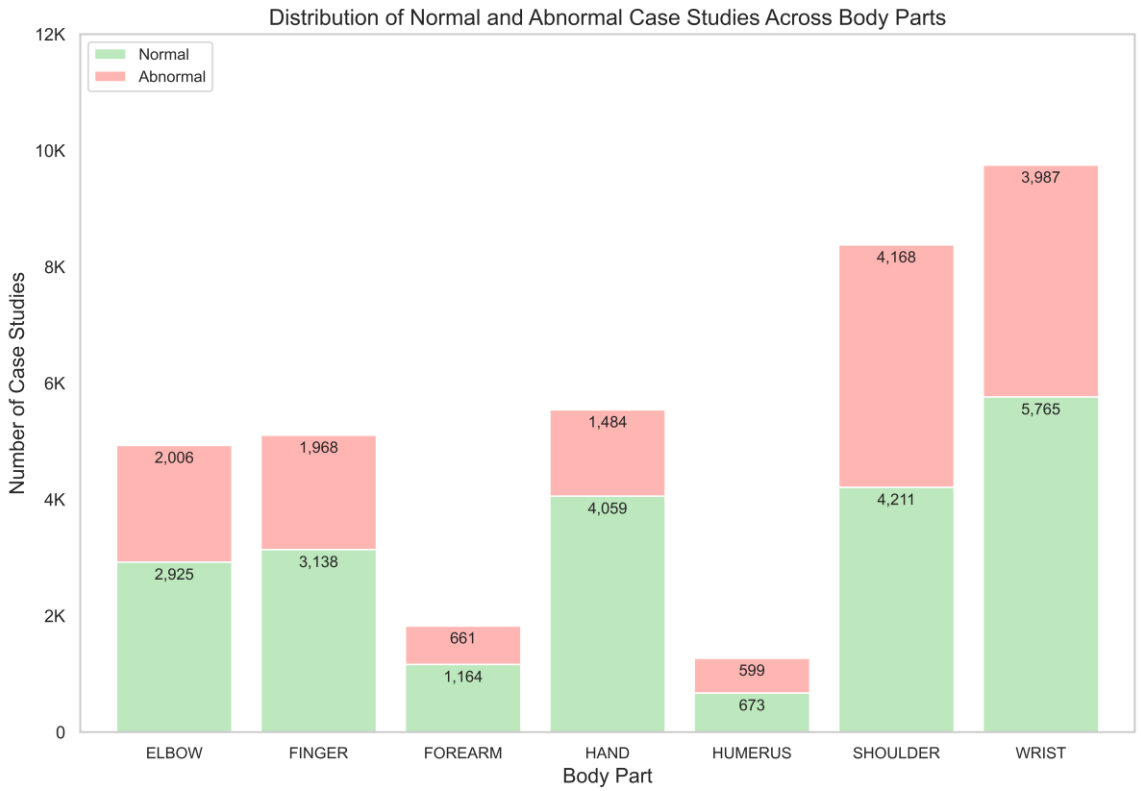

Figure 11. Distribution of Normal and Abnormal Case Studies Across Body Parts (Stacked Bart Plot)

Visualizing Distribution with Pie Charts

In addition to stacked bar plots, we've employed pie charts, each focusing on a specific body part. These pie charts offer a more detailed perspective by presenting the distribution in terms of percentages. This granularity allows us to understand the prevalence of normal and abnormal cases within each anatomical category. A screenshot of the pie charts is displayed below:

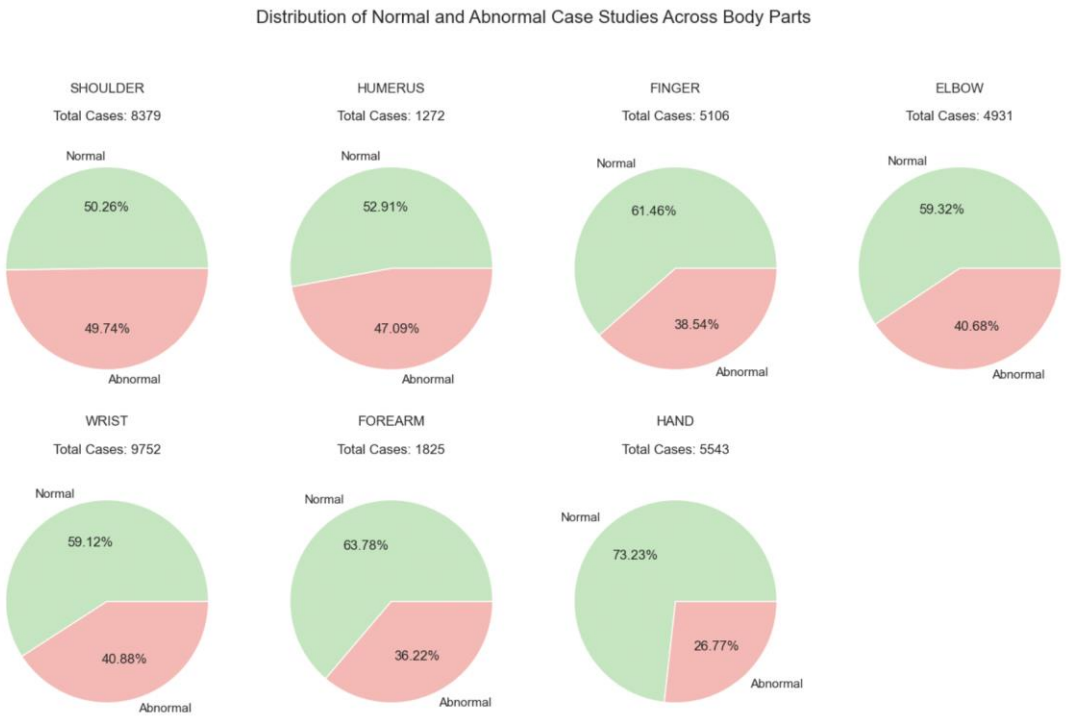

Figure 12. Distribution of Normal and Abnormal Case Studies Across Body Parts (Pie Chart)

General Insights

The case distribution across various anatomical body parts shows variations, with some categories having a relatively balanced distribution of abnormal and normal cases, while others display disparities.

These distribution patterns are clinically significant as they reflect the real-world prevalence of musculoskeletal conditions in various anatomical regions. Understanding these variations is crucial for developing diagnostic algorithms that are both robust and clinically applicable.

For instance, some body parts, like the "**Shoulder**," showcase nearly equal numbers of abnormal and normal cases, indicating a balanced distribution. In contrast, the "**Wrist**" category displays a higher prevalence of normal cases, while the "**Hand**" category also leans toward normal cases, albeit to a lesser extent.

Challenges in Model Training

The observed disparities in case distribution pose challenges during the training of CNN models. Imbalanced distributions, as seen in the "Wrist" category, have the potential to introduce biases into the models. These biases could affect the models' ability to accurately diagnose musculoskeletal conditions.

Therefore, these distribution insights are essential for guiding model development strategies to ensure robust performance across diverse anatomical regions.

Data Splitting: Training and Validation Sets

In the context of our machine learning pipeline, the **train_validation_split** function plays a pivotal role in ensuring the reliability of our model, especially in the domain of medical diagnostics. This method goes beyond just performance considerations; it also focuses on clinical reliability.

Function Overview

The function takes a Pandas DataFrame as input and returns two distinct DataFrames: **train_set** and **valid_set**, which represent the training and validation sets, respectively. The function employs stratification to ensure that both output sets accurately represent the overall data distribution, considering both the 'label' and 'type' fields.

When the **train_validation_split** function is executed, the dataset is divided into training and validation sets based on the prescribed methodology. This critical step prepares the data for subsequent machine learning operations, ensuring that the model is trained and validated on distinct data subsets.

Analyzing Case Study Distribution for Simple CNN Implementation in the MURA Dataset

The next crucial step is to gain a comprehensive understanding of the distribution of case studies across both the training and validation sets. This knowledge informs our approach to model development and evaluation.

To visually represent this distribution, we've employed a stacked bar chart. This chart provides a clear overview of the number of case studies for each anatomical body part, differentiating between the training and validation sets. The visualization can be observed below:

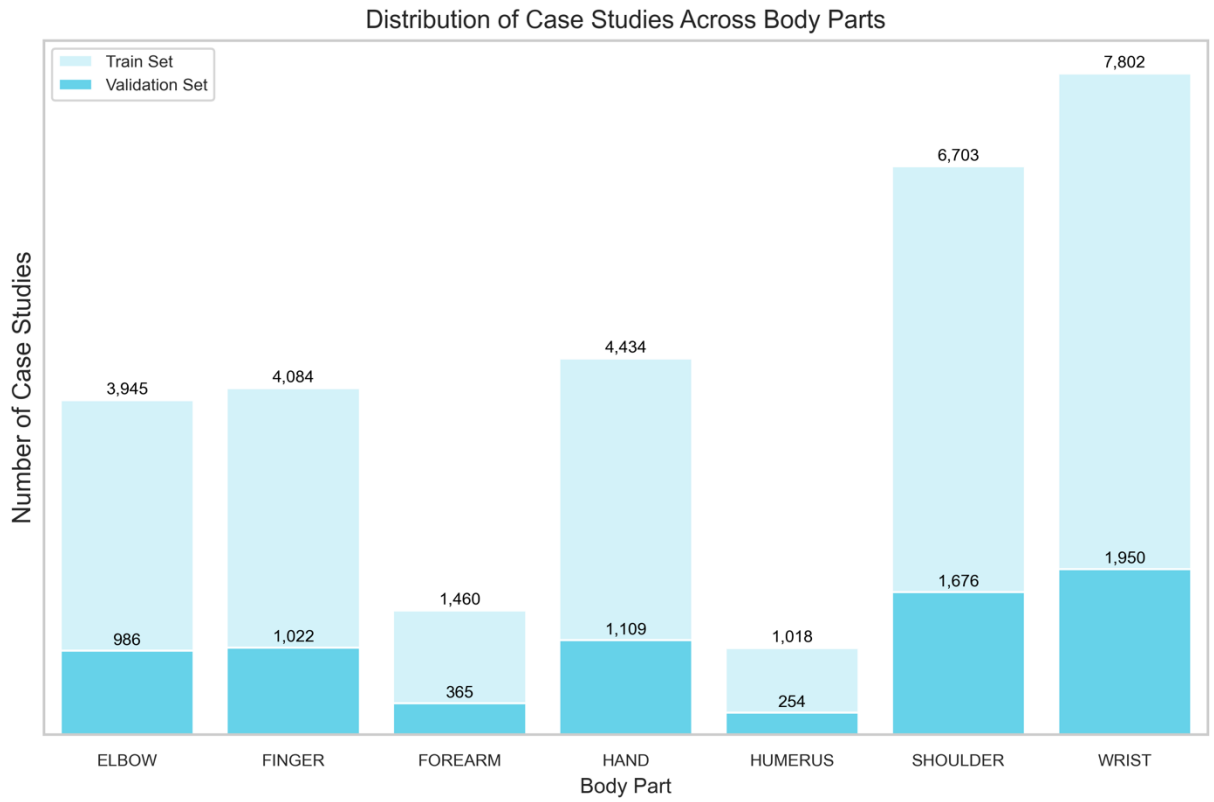

Figure 13. Distribution of Case Studies Across Body Parts

General Insights

A closer examination of the distribution of case studies across anatomical body parts in both the training and validation sets reveals noteworthy patterns. Specifically, the "**Wrist**" and "**Shoulder**" categories emerge as the most prominently represented, with substantial numbers of cases in both sets.

More particularly, the prevalence of these categories might have important implications for our model development strategy. By ensuring that our Convolutional Neural Network (CNN) is exposed to a diverse range of cases, we enhance its ability to generalize effectively. This diversity is crucial because it equips our CNN to accurately diagnose musculoskeletal conditions across a wide array of anatomical regions. It also serves as a cornerstone for our model evaluation approaches, guaranteeing that our CNN's performance remains robust and clinically applicable.

For instance, the "**Wrist**" category, with its substantial representation in both the training and validation sets, provides a strong foundation for the CNN's training. Similarly, the prevalence of "**Shoulder**" cases further enriches the diversity of cases our model encounters. This ensures that our CNN not only learns from various scenarios but also becomes proficient in handling cases across different anatomical regions, ultimately contributing to its diagnostic accuracy and clinical utility.

In contrast, some categories like "**Forearm**" and "**Humerus**" exhibit **lower case numbers**, both in the training and validation sets. While these categories may have fewer cases, they remain valuable for the training process, offering a complementary perspective on musculoskeletal conditions. These less-represented categories serve as essential pieces in our comprehensive diagnostic puzzle, ensuring that our CNN's abilities are not confined to the dominant categories.

Overall, understanding the distribution of case studies across anatomical body parts allows us to tailor our model development and evaluation strategies for maximum effectiveness and clinical relevance. It highlights the need for a balanced approach, where both prevalence and diversity play key roles in shaping the capabilities of our CNN in the context of musculoskeletal diagnosis.

Image Data Generation and Augmentation for Simple CNN Model

In this phase, we establish and configure an **ImageDataGenerator** object, which plays a crucial role in our pipeline, especially when dealing with image data. The purpose of this process is twofold: **data augmentation** and **preprocessing**. Data augmentation involves generating new training examples by applying various transformations to existing images. This expands our dataset and helps our model generalize better. Preprocessing ensures that the images are in the correct format for model training.

Image Data Preprocessing for Validation Set

Firstly, we establish an ImageDataGenerator object specifically tailored for preprocessing the validation dataset, taking into account several critical considerations. First and foremost, we apply a preprocessing function to normalize the pixel values of the images. This normalization step is fundamental to ensure that the images adhere to the appropriate format required for input into the VGG-19 model.

Moreover, all validation images undergo a resizing process, standardizing them to a uniform dimension of **224x224 pixels**. This resizing operation is pivotal as it aligns with the specific input size prerequisites of the VGG-19 model, ensuring compatibility.

Given that the labels in our dataset are represented as integers, we configure the **class_mode** parameter to '**raw**.' This designation signifies that the labels are provided as unprocessed numerical values, ensuring that the model receives them in the correct format.

The **batch_size** parameter plays a central role in controlling the number of images processed simultaneously within each batch during model evaluation. This is a crucial aspect of efficient memory management during the evaluation phase, optimizing performance.

To introduce an element of randomness and prevent any inherent biases, we shuffle the validation images. Simultaneously, we set a **random seed** to ensure reproducibility, guaranteeing consistent and replicable results across multiple runs of the evaluation process.

By executing this code segment, we generate a **preprocessed_valid_data_gen** object, serving as the generator responsible for supplying batches of preprocessed validation images to the model during the validation phase. This rigorous preprocessing ensures that the model receives data that adheres to its requirements, fostering reliability and consistency in the evaluation process.

Image Data Preprocessing for Test Set

In the following phase, our objective is to prepare the test images for model evaluation. Similarly to the validation images, the test images undergo preprocessing tailored to meet the input requirements of the model. Importantly, we do not apply data augmentation to the test images, focusing solely on necessary preprocessing steps.

To initiate this process, we initialize an **ImageDataGenerator** object specifically designed for preprocessing the test dataset. The primary purpose is to apply a preprocessing function that **normalizes** the pixel values of the images. This normalization step is paramount as it ensures that the images are appropriately formatted for input into the VGG-19 model, aligning them with the model's expectations.

Furthermore, similar to the training and validation sets, all test images are subject to a resizing operation. This resizing step ensures that all images share a uniform dimension of **224x224 pixels**, in accordance with the specific input size prerequisites of the VGG-19 model. This standardization is crucial for consistency and compatibility.

For the labeling aspect, we maintain the same approach as employed with the training and validation sets. Given that the labels in our dataset are represented as integers, we configure the **class_mode** parameter to '**raw**.' This designation signifies that the labels are presented in their raw numerical form, ensuring they are received by the model in the correct format.

The **batch_size** parameter, as with the other sets, plays a pivotal role in determining the number of images processed simultaneously within each batch during model evaluation. This parameter is instrumental for effective memory management during the evaluation phase, optimizing performance.

In contrast to our approach with the training and validation sets, we implement a distinct strategy regarding the order of the test images. While shuffling the images during training and validation ensures randomness and minimizes bias, we set **shuffle to False** for the test set. This decision maintains the original order of the images, which is particularly significant for consistency in test results. Additionally, we employ a **random seed** for reproducibility, ensuring consistent and replicable results across multiple runs of the testing phase.

Upon executing this code block, we establish a **preprocessedTestDataGen** object. This object serves as the generator responsible for supplying batches of preprocessed test images to the model during the testing phase. This attentive preprocessing guarantees that the model receives test data that adheres to its requirements, enhancing the reliability and consistency of the evaluation process.

Building a Binary Classification for Simple CNN Model

In this section, we will thoroughly explore the development of our specialized Convolutional Neural Network (CNN) model, precisely designed for binary classification tasks. The following comprehensive documentation offers in-depth insights into each component and enhancement of this powerful CNN model, which can be effectively integrated into software applications.

Input Layer

The **input layer** serves as the neural network's gateway, responsible for receiving input images with specific dimensions of **224x224x3** (width, height, and color channels). This input shape can be adjusted to accommodate different image sizes, offering flexibility to users. However, our choice of **224x224 pixels** as the standard input size is intentional. It aligns with the conventions of many deep learning models and pre-trained architectures, simplifying model compatibility and ensuring the input size meets the expectations of widely-used pre-trained models.

This standardization enables users to readily leverage pre-trained models and transfer learning techniques. By doing so, the model's overall performance and versatility are significantly enhanced when integrated into various software applications. The use of widely-adopted input dimensions facilitates seamless collaboration with existing machine learning ecosystems.

Convolutional Layers

The backbone of our CNN model is formed by **convolutional layers**, and their flexibility is a key feature. Users can dynamically adjust the number of convolutional layers (**num_conv_layers**) based on their specific needs. Each convolutional layer performs **2D convolutions** on the input image or feature map, extracting crucial image features through a process of feature transformation and learning.

- **Batch Normalization**: After each convolutional operation, **batch normalization** is applied. This crucial step standardizes the activations, ensuring that the model learns more efficiently and converges faster during training. Batch normalization reduces internal covariate shift, making the network more robust and accelerating convergence.

- **Max Pooling**: Following batch normalization, **max-pooling** is employed to downsample the feature map. This process reduces its dimensions while retaining essential information, aiding in feature selection and computational efficiency. Max-pooling extracts the most relevant information from each feature map, enhancing the model's ability to focus on salient features.

Flattening Layer

Post-convolution and pooling, a **flattening layer** is introduced. This layer reshapes the 2D feature map into a 1D array, preparing the data for input into the dense layers. It serves as a critical bridge between the convolutional layers and the densely connected layers, enabling seamless feature propagation.

Dropout Layers

To prevent overfitting, **dropout layers** are thoughtfully integrated into the model. During training, these layers randomly deactivate a fraction of input units. This stochastic dropout process encourages the network to learn more robust and generalizable features. By introducing an element of randomness, dropout prevents the network from relying too heavily on specific features, improving its ability to generalize to unseen data.

Hidden Dense Layer

Positioned just before the output layer, the **hidden dense layer** plays a critical role in introducing non-linearity into the decision-making process. It employs the **Rectified Linear Unit (ReLU)** activation function, allowing the model to capture complex patterns in the data. ReLU introduces non-linearity by allowing the network to model complex relationships between features, enhancing its capacity to learn intricate data representations.

Additional Batch Normalization: To further enhance model stability and training speed, an extra batch normalization layer is thoughtfully added in this stage. This optimization optimally scales and shifts the activations in the hidden dense layer, facilitating faster convergence and improving overall training efficiency.

Output Layer

The final layer of our network is cautious tailored for binary classification tasks. It utilizes the **sigmoid activation function**, ensuring that the model's output remains within the **0 to 1 range**,

which is ideal for binary decision-making. The sigmoid function compresses the model's output into a probability-like score, making it suitable for binary classification where the goal is to assign an input to one of two classes.

Model Compilation

Once all the layers are defined, the model is compiled, marking an essential step in the model-building process. This phase involves specifying the **Adam optimizer**, an excellent choice for optimizing deep learning models due to its adaptive learning rate capabilities. Additionally, the **binary cross-entropy loss function** is selected, a suitable choice for binary classification tasks.

Users have the flexibility to define additional evaluation metrics to comprehensively assess the model's performance. This adaptability allows users to tailor the evaluation criteria to the specific requirements of their application, ensuring that the model's performance is rigorously evaluated.

Regularization

In order to prevent overfitting, **L2 regularization** is thoughtfully applied to both the convolutional and dense layers. This regularization technique encourages the model to focus on the most important features, thus improving its ability to generalize effectively. L2 regularization introduces a penalty term to the loss function, discouraging the model from assigning excessively large weights to certain features, which can lead to overfitting.

Parameter Flexibility

Our model-building function offers a high degree of customization, allowing users to tailor various hyperparameters to their specific needs. This flexibility empowers users to fine-tune critical aspects such as the **learning rate**, **activation functions**, and more, ensuring that the model aligns seamlessly with their unique use case. Users can experiment with different hyperparameter configurations to optimize the model's performance for their specific application, providing a versatile tool for machine learning tasks.

In summary, this specialized CNN model is carefully designed to offer a versatile and robust solution for binary classification tasks, especially tailored for the specific demands of MURA (Musculoskeletal Radiographs) medical imaging. Its adaptability, reliability, and feature-rich design are geared towards helping users achieve excellent results in various diagnostic scenarios within the MURA medical imaging domain.

Incorporating Callbacks to Enhance Simple CNN Model Training

In the context of refining our model training process for MuraMed's specialized medical image analysis software, the strategic utilization of *Keras Callbacks* emerges as a pivotal factor. These Callbacks, like astute supervisors, continuously monitor essential metrics and orchestrate dynamic adjustments during training. Within our framework, we rely on two primary Callbacks: **Early Stopping** and **Reduce Learning Rate on Plateau**, each playing a vital role in optimizing the learning journey.

The core of our strategy lies in the careful configuration of our Keras Callbacks:

Early Stopping
This Callback remains vigilant, closely monitoring the validation loss throughout the training process. It defines a patience threshold, specifying the number of consecutive epochs with no improvement allowed before stopping. In doing so, it ensures that the training doesn't continue indefinitely and maintains vigilance over the best model weights.

Reduce Learning Rate on Plateau
Similar to the Early Stopping Callback, this component keeps an eye on validation loss. It sets a patience threshold and dynamically adjusts the learning rate when necessary. This adaptive learning rate mechanism equips our model to navigate challenges within the complex landscape of medical image analysis. Importantly, it establishes a lower limit for the learning rate to prevent excessive reduction.

Model Checkpoint
The Model Checkpoint component plays a pivotal role in defining the file path for safeguarding model weights. It closely tracks validation loss, ensuring that only the most superior weights are retained. This step is essential for preserving the model's peak performance.

These Callbacks are dynamically integrated into our training process through the '*custom_callbacks*' list, enhancing our model's adaptability and optimizing its performance. By implementing these dynamic mechanisms, we empower our model to fine-tune its learning process for optimal performance within MuraMed's specialized medical image analysis software.

Simple CNN Model Training Procedure

In this section, we provide a comprehensive explanation of the elements encompassing our model's training process, defined by the versatile ***train_custom_model*** function. This function stands as the core engine, propelling the learning journey of our Convolutional Neural Network (CNN) tailored for MuraMed's medical imaging needs. Let's delve into the pivotal components:

Model Building
The process begins by constructing the model through our predefined ***build_binary_classification_model*** function, setting the architectural foundation. This phase includes defining layers, optimizing hyperparameters, and configuring the model's structure to align seamlessly with the intricate demands of MuraMed.

Training
Once the model architecture is established, it begins the training voyage using the robust ***fit***

method. During this phase, essential training parameters such as input data, batch size, the number of training epochs, and other crucial configurations are provided. The model learns from the input data to make informed decisions in the context of musculoskeletal radiographs.

Callbacks
For fine-tuning the training process, the function accommodates the integration of *Keras callbacks*. Callbacks like ***Early Stopping*** or ***Learning Rate Reduction*** can be specified to optimize the training dynamics, ensuring efficient convergence and preventing overfitting. These are particularly useful for improving the model's performance on MuraMed's specific dataset.

Metrics
Monitoring the training's progress is pivotal. Users have the flexibility to define which metrics to monitor during training. By default, we track 'accuracy', but this can be customized to align with MuraMed's evaluation criteria, ensuring that the model attains the desired level of diagnostic precision.

Verbose & Logging
To provide insights into the model's performance at each training epoch, the function offers real-time logs. These logs, displayed with varying verbosity levels, empower users to observe how the model evolves and refines its diagnostic capabilities over time.

Upon the successful completion of the training process, the ***train_custom_model*** function provides both the trained model itself and the valuable training history (*hs*). This training history contains important information about the model's learning progress, enabling thorough analysis and evaluation, which is particularly crucial in the context of MuraMed's medical image analysis.

Ultimately, this function serves as a comprehensive solution for training our specialized CNN, designed to excel in the specific field of musculoskeletal radiography. Its flexibility, strength, and feature-rich design are purpose-built to empower users in achieving the best possible diagnostic results within the domain of MuraMed.

Simple CNN Model Training Execution and Time Monitoring

In this section, we will outline the steps involved in executing the model's training process while also monitoring the time taken. These steps are essential to gain comprehensive insights into the training procedure:

Start Time
We begin by precisely recording the current system time. This timestamp serves as the initial reference point and plays a pivotal role in calculating the overall training duration accurately.

Model Training

The core of this section lies in the execution of our train_model function. This is where our Convolutional Neural Network (CNN) undergoes the process of training, acquiring knowledge from the provided data. It's noteworthy that we intentionally chose to train the model for 10 epochs. This decision is based on a careful balance between computational efficiency and model convergence. While a greater number of epochs might enhance performance, it also demands more time and computational resources. Opting for ten epochs strikes a reasonable

balance, allowing the model to acquire knowledge while remaining practical for real-world applications within MuraMed's domain.

Callbacks

In the context of our training process, we have thoughtfully incorporated a set of Keras callbacks. These are powerful tools designed to optimize the training procedure. Among these, we leverage mechanisms such as "Early Stopping" and "Learning Rate Reduction," which play pivotal roles in enhancing the efficiency of our model's learning process.

End Time

After the completion of our model's training, we accurately record the system time once again. This detailed record-keeping enables us to calculate the total duration of the training process, shedding light on the computational efficiency exhibited by our model.

Elapsed Time

In the final step, we present the total time that has passed during the training. This time measurement offers a comprehensive understanding of the computational efficiency achieved throughout the training process. Monitoring the time taken for training is of particular significance when evaluating the practicality and responsiveness of the model within MuraMed's domains.

Observations

Following the training process, a detailed analysis of the outcomes is essential. Here are some noteworthy observations based on the following screenshot, which showcases the performance of the epochs:

```
Started training.
-----------------

Epoch 1/10
461/461 [==============================] - 572s 1s/step - loss: 0.8298 - accuracy: 0.4041 - val_loss: 0.7688 - val_accuracy: 0.4041 - lr: 1.0
000e-04
Epoch 2/10
461/461 [==============================] - 569s 1s/step - loss: 0.7770 - accuracy: 0.4041 - val_loss: 0.6727 - val_accuracy: 0.4041 - lr: 1.0
000e-04
Epoch 3/10
461/461 [==============================] - 564s 1s/step - loss: 0.7491 - accuracy: 0.4041 - val_loss: 0.6829 - val_accuracy: 0.4041 - lr: 1.0
000e-04
Epoch 4/10
461/461 [==============================] - 559s 1s/step - loss: 0.7381 - accuracy: 0.4041 - val_loss: 0.6972 - val_accuracy: 0.4041 - lr: 1.0
000e-04
Epoch 5/10
461/461 [==============================] - 560s 1s/step - loss: 0.7240 - accuracy: 0.4041 - val_loss: 0.7017 - val_accuracy: 0.4041 - lr: 1.0
000e-04
Epoch 6/10
461/461 [==============================] - 569s 1s/step - loss: 0.7154 - accuracy: 0.4041 - val_loss: 0.6402 - val_accuracy: 0.4041 - lr: 1.0
000e-04
Epoch 7/10
461/461 [==============================] - 560s 1s/step - loss: 0.7008 - accuracy: 0.4041 - val_loss: 0.6831 - val_accuracy: 0.4041 - lr: 1.0
000e-04
Epoch 8/10
461/461 [==============================] - 558s 1s/step - loss: 0.6882 - accuracy: 0.4041 - val_loss: 0.6458 - val_accuracy: 0.4041 - lr: 1.0
000e-04
Epoch 9/10
461/461 [==============================] - 556s 1s/step - loss: 0.6821 - accuracy: 0.4041 - val_loss: 0.6373 - val_accuracy: 0.4041 - lr: 1.0
000e-04
Epoch 10/10
461/461 [==============================] - 558s 1s/step - loss: 0.6770 - accuracy: 0.4041 - val_loss: 0.6610 - val_accuracy: 0.4041 - lr: 1.0
000e-04

Finished training.
------------------

Total time for training: 5682 seconds.
```

Constant Accuracy: Throughout all 10 epochs, both training and validation accuracy remain consistently at 0.4041. This implies that the model's learning effectiveness is limited and might require further optimization.

High Loss: The loss values for both the training and validation datasets are quite high, with minimal improvement over the epochs. This suggests that the model may not be converging effectively, indicating the need for additional fine-tuning.

Simple CNN Model Summary Interpretation

The *cnn_model.summary()* function provides a comprehensive overview of our Convolutional Neural Network (CNN) architecture. This summary output contains essential information:

- **Layer (type):** Specifies the type of each layer, such as Conv2D for convolutional layers, MaxPool2D for max-pooling layers, Dense for fully connected layers, and more.
- **Output Shape:** Describes the dimensions of the output from each layer. Understanding output shapes is crucial for tracking how your data's dimensionality changes as it passes through the network.
- **Param #:** Indicates the number of trainable parameters in each layer. This value is vital for assessing your model's complexity. Excessive parameters might lead to overfitting.
- **Total params:** Represents the total count of both trainable and non-trainable parameters in the model.
- **Trainable params:** Specifies the number of parameters that will be updated during the training process.
- **Non-trainable params:** Refers to parameters that remain fixed during training. These are typically imported from pre-trained models.

```
Model: "model"
_________________________________________________________________
 Layer (type)                Output Shape              Param #
=================================================================
 InputLayer (InputLayer)     [(None, 224, 224, 3)]     0

 ConvLayer-1 (Conv2D)        (None, 224, 224, 32)      896

 BatchNorm-1 (BatchNormaliz  (None, 224, 224, 32)      128
 ation)

 MaxPooling-1 (MaxPooling2D  (None, 112, 112, 32)      0
 )

 FlattenLayer (Flatten)      (None, 401408)            0

 DropoutLayer1 (Dropout)     (None, 401408)            0

 HiddenLayer (Dense)         (None, 256)               102760704

 BatchNorm-Final (BatchNorm  (None, 256)               1024
 alization)

 DropoutLayer2 (Dropout)     (None, 256)               0

 OutputLayer (Dense)         (None, 1)                 257

=================================================================
Total params: 102763009 (392.01 MB)
Trainable params: 102762433 (392.01 MB)
Non-trainable params: 576 (2.25 KB)
_________________________________________________________________
```

Figure 14. Summary Statistics of the Simple CNN Model

Observations Based on Model Summary

Upon analyzing the summary statistics provided in the screenshot above, we have made the following observations:

- **Input Layer:** The model begins with an input shape of (224 x 224 x 3), which is a standard configuration for many image-related tasks.
- **Convolution Layer:** To initiate the feature extraction process, a single convolutional layer with 32 filters is employed.
- **Batch Normalization:** In the architecture, batch normalization layers are incorporated to facilitate faster and more stable training.
- **Max Pooling:** To reduce spatial dimensions and improve computational efficiency, a max-pooling layer is integrated into the network.
- **Flatten Layer:** Before transitioning to fully connected layers, a flatten layer is utilized. Its purpose is to convert the 3D feature maps into 1D feature vectors.

- **Dropout:** In order to prevent overfitting, two dropout layers are strategically incorporated into the architecture.
- **Hidden Layer:** A substantial dense layer comprising 256 units is integrated into the model. This layer contributes a significant number of trainable parameters.
- **Total Parameters:** The model contains an extensive number of parameters, approximately 102.76 million in total. This indicates that the model is computationally intensive.

Visualization of Simple CNN Model Architecture

The **plot_model** function serves the purpose of creating a graphical representation of the model's architecture. This visual representation is valuable for various purposes, including presentations and documentation. When using this function, you can customize the visualization to suit your specific requirements. It helps convey how data flows through different layers and operations within the model.

By generating a PNG image, the **plot_model** function provides a clear overview of the model's structure. It showcases the shapes of tensors between layers and labels each layer with its name. This diagram aids in debugging and simplifies the sharing of your model's architecture with collaborators.

Here is an illustrative example of the generated diagram:

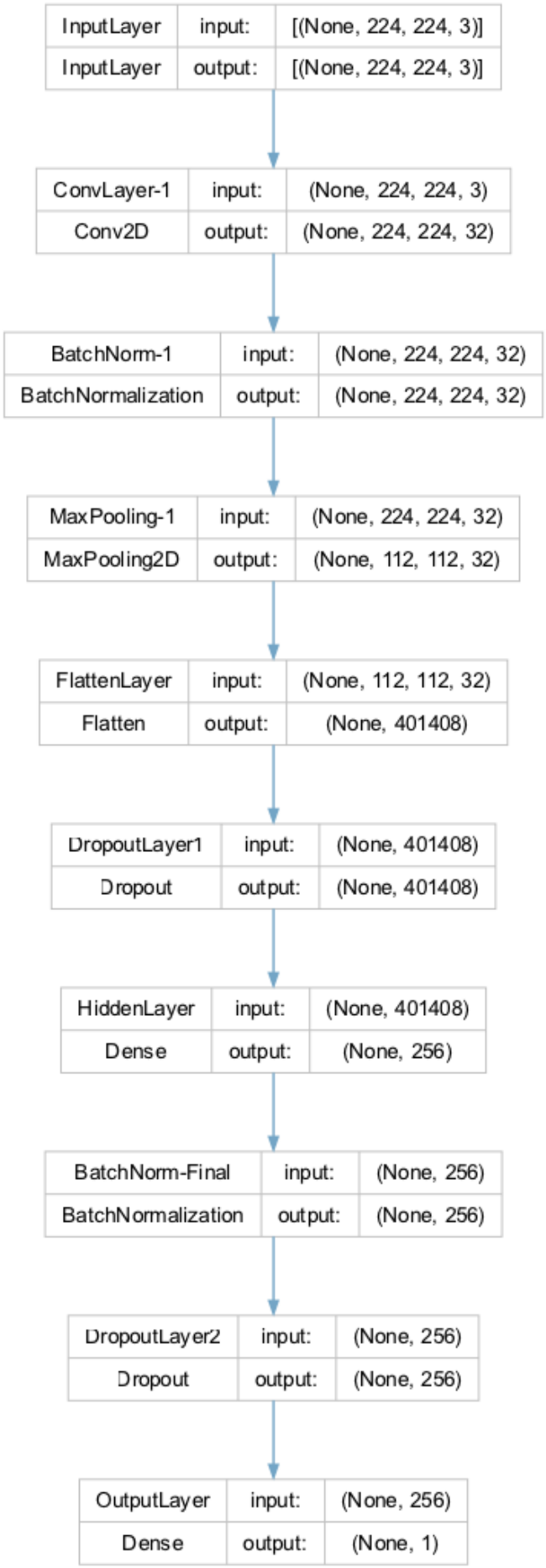

Figure 15. Visualization of Simple CNN Model Architecture

It's worth noting that the information presented in this visual representation aligns precisely with the model summary statistics described in the previous section. However, this visual format enhances the accessibility of the model's design and promotes effective communication with team members and stakeholders.

Simple CNN Model Evaluation

In the Model Evaluation phase, our focus shifts from model training to assessing how well our model performs on new, unseen data. We aim to analyze the model's behavior during training and its subsequent predictive performance, which is critical for MuraMed's medical image analysis.

Learning Curves: A Diagnostic Tool

To evaluate the performance of our Convolutional Neural Network (CNN) model, we employ learning curves as a vital diagnostic tool. Learning curves display training and validation metrics, typically loss or accuracy, across different training epochs. This visualization helps us gain insights into several key aspects of our model's performance:

- **Underfitting or Overfitting:** Learning curves reveal whether our model is underfitting (performing poorly on both training and validation data) or overfitting (performing well on training but poorly on validation data).
- **Model Complexity:** The shape of the curves provides insights into the model's complexity. A steep learning curve suggests rapid learning but may also indicate overfitting.
- **Convergence:** The point where the curves stabilize helps us determine the optimal number of epochs for training.

To generate learning curves, we utilize a custom function called "**plot_learning_curves**". This function takes training history, the total number of epochs, the chosen metric (either 'loss' or 'accuracy'), and a title.

Model Evaluation and Learning Curves

Our primary focus during the model evaluation phase centers around two fundamental performance metrics: Loss and Accuracy. These metrics serve as key indicators of our model's effectiveness in handling MuraMed's medical image analysis tasks.

Train Loss & Validation Loss

- **Training Loss:** This metric provides insights into how effectively our model has learned from the training data. A lower value signifies a more successful learning process, indicating that the model is capturing important patterns and information from the training dataset.
- **Validation Loss:** As we shift our attention to the validation set, this metric serves as a measure of our model's ability to generalize to previously unseen data. A lower validation loss indicates that our model can extend its learned knowledge to new and unfamiliar cases, demonstrating superior performance.

To provide a comprehensive view of our model's learning progress, we utilize the "plot_learning_curves" function. This function generates learning curves for both Training and Validation Loss and can be seen within the following screenshot:

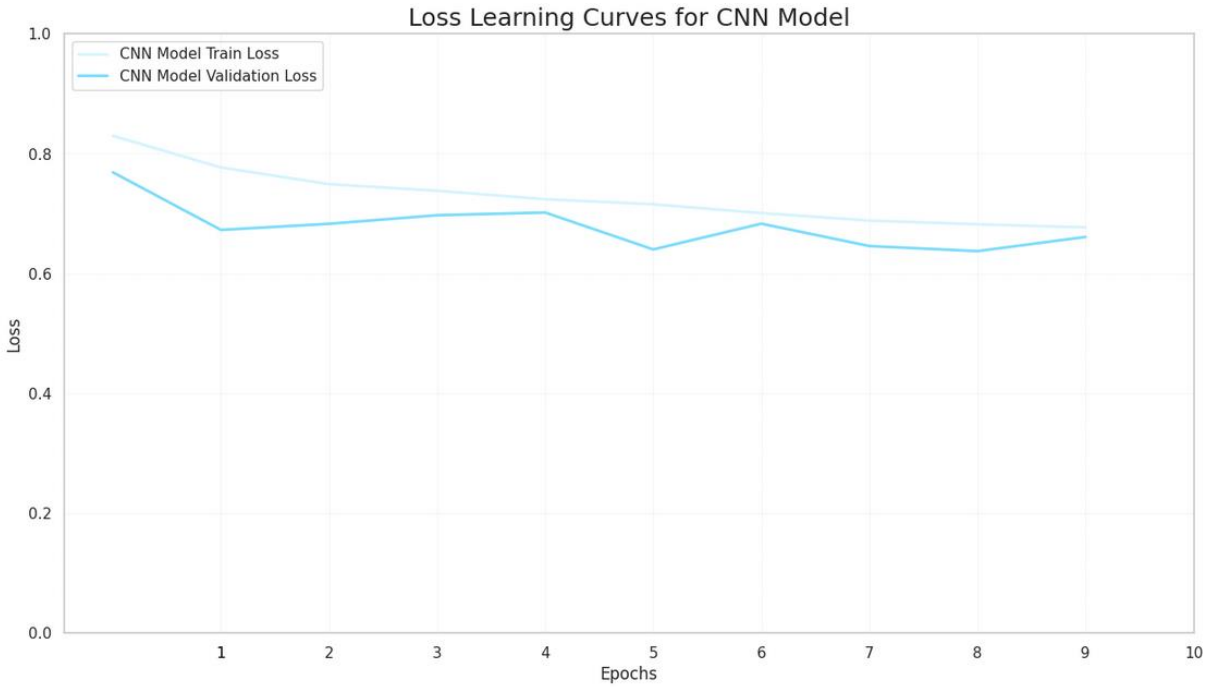

Figure 16. Loss Learning Curves for CNN Model

Train Accuracy & Validation Accuracy

The next set of metrics we consider are Train Accuracy and Validation Accuracy. These metrics provide insights into our model's classification performance.

- ***Training Accuracy*:** This metric measures how well our model correctly classifies a portion of the training dataset. A higher value here signifies more accurate classification during the training process, which is crucial for effectively adapting to MuraMed's unique medical image analysis challenges.

- ***Validation Accuracy*:** Similarly, Validation Accuracy evaluates the model's classification performance, but specifically on the validation dataset. This dataset contains medical images that the model has not encountered during its training. Achieving high Validation Accuracy is vital for demonstrating the model's capability to generalize its learning to new, unseen medical images, a fundamental requirement for MuraMed's specialized tasks.

By visualizing the learning curves for both Training and Validation Loss, we can gain valuable insights into how our model adapts during training and its ability to generalize to previously unseen medical images within the MuraMed context. The output is illustrated within the following screenshot:

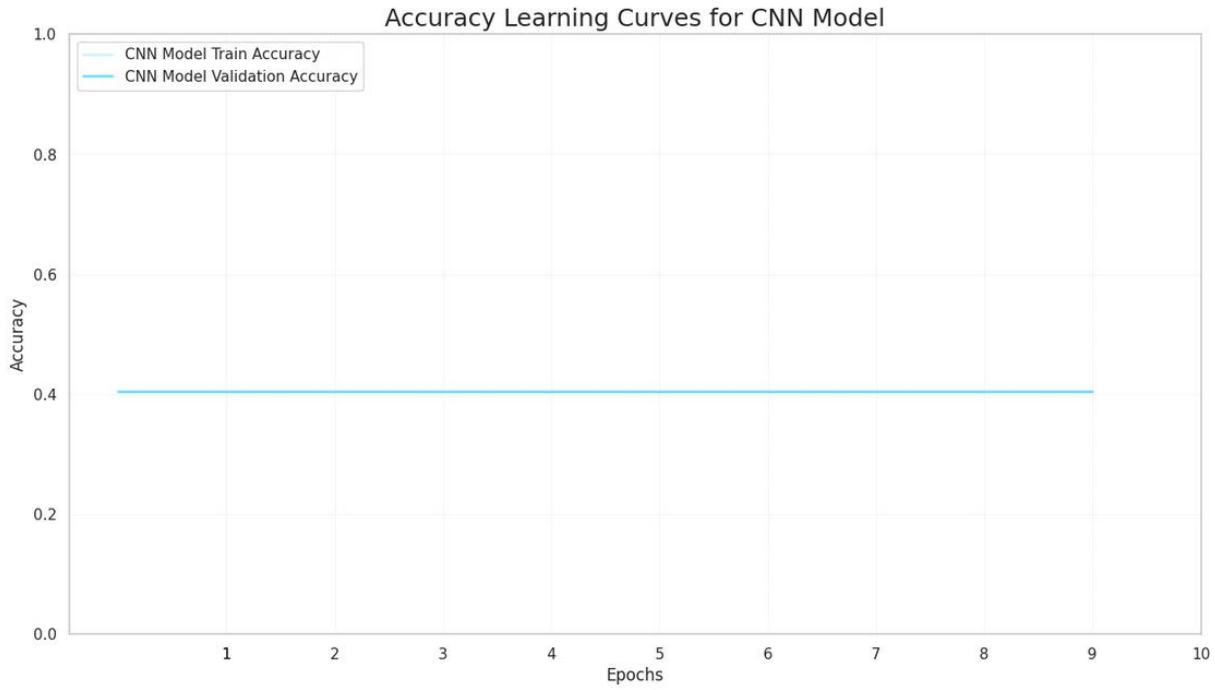

Figure 17. Accuracy Learning Curves for CNN Model

Observations

During our model evaluation, in addition to examining the loss and accuracy learning curves, we made the following observations:

- **Training Loss & Validation Loss:** The training loss is **0.67697**, and the validation loss is 0.66095. These values suggest that our model encounters challenges in effectively fitting the training data.
- **Training Accuracy & Validation Accuracy:** It's evident that both the training and validation accuracy are approximately **0.40406** and **0.40410**, respectively. This indicates that our model is not effectively learning from the training data and struggles to generalize well to the validation data.
- **Consistency Across Metrics:** Training and validation metrics, including accuracy and loss, show close alignment. This suggests that our model consistently performs suboptimally on both datasets.
- **Contradictory Signals:** The lower validation loss compared to the training loss, along with nearly identical training and validation accuracy, presents.

This evaluation provides valuable insights into our model's strengths and weaknesses, guiding us toward further optimization to meet MuraMed's requirements for medical image analysis.

Simple CNN Model Training Insights

In this section, we carefully evaluate our Convolutional Neural Network (CNN) model's performance, tailored to meet MuraMed's specific requirements. Our aim is to assess how well the model has learned from the training data and how effectively it performs on unseen validation data.

Loss Metrics
We begin by examining the loss metrics, which are key indicators of our model's performance. Both the training and validation losses fall within a higher range. This suggests that there is room for improvement and that our model may face challenges like overfitting (learning the training data too well) or underfitting (not learning enough from the training data). An interesting observation is the slightly lower validation loss compared to the training loss, which deserves further investigation.

Accuracy Metrics
We also consider accuracy metrics, another essential aspect of model assessment. Both training and validation accuracies are in the lower range, indicating that our model struggles to accurately classify data. This could be due to various factors, including the model's architecture, data quality, dataset balance, or the need for fine-tuning.

It's worth noting that while training and validation accuracies show similarity, suggesting a lack of overfitting, the overall low accuracy highlights our model's difficulty in effectively learning from the training data.

To improve these metrics, we may consider adjustments such as fine-tuning the model's architecture, refining its settings, using different data augmentation techniques, or addressing dataset imbalances. These considerations will guide our efforts in optimizing the Advanced CNN and VGG models.

Model Evaluation on Test Data

In this phase, we evaluate our trained Simple CNN model using a separate test dataset. This evaluation provides insights into the model's likely performance on entirely new, unseen data. While our model is computationally efficient, it lacks predictive power. These insights emphasize the need for significant model refinement and re-evaluation before considering its application in real-world scenarios.

To be more specific, two important metrics are evaluated, Test Loss and Test Accuracy, the results of which are 0.66638 and 0.47857 respectively.

- **Test Loss:** This metric tells us how well the model predicts on the test data. A lower test loss indicates more accurate predictions. A test loss of **0.66638** suggests that the model's predictions on the test data are not very accurate. This means that the model is struggling to make precise predictions, which is reflected in the higher loss value. A lower test loss is generally desired as it indicates more accurate predictions.

- **Test Accuracy:** This metric measures the model's ability to classify data within the test dataset. A higher test accuracy means better classification. The resulted value of **0.47857** is quite low. It implies that the model's ability to classify data within the test dataset is poor.

In other words, it's not doing a good job at correctly identifying and categorizing the data. A higher test accuracy is preferred, as it reflects better classification performance.

The evaluation results raise some concerns. The high test loss, which closely resembles the validation loss, suggests that our model may not effectively capture the underlying data patterns. Additionally, the low test accuracy, similar to the validation accuracy, indicates consistent underperformance across different datasets.

These carefully gathered observations and insights provide a solid foundation for guiding the development and optimization of models to meet MuraMed's specialized medical image analysis needs.

Evaluating Simple CNN Model Performance Across Different Study Types

In the field of medical imaging, it is of utmost importance to assess a model's performance across a variety of study types to ensure its effectiveness. The function "**evaluate_model_by_study_type**" serves this purpose by taking two crucial parameters: the test set and the model's predictions. The function enhances the test set data frame by adding the model's predictions as a new column.

Subsequently, this function systematically examines each unique study type present in the test set, which could include categories like 'elbow,' 'shoulder,' and more. For each study type, it performs a comprehensive evaluation of the model's performance. This evaluation encompasses six vital metrics: Precision, Recall, F1 Score, Accuracy, ROC AUC, and Cohen's Kappa. These metrics are industry-standard for medical diagnostics and are rounded to five decimal places for precision.

This process allows us to gain granular insights into how well the model performs across various study types. It enables us to identify the study types where the model excels and those where it may need further refinement. Such detailed analysis is crucial, especially in clinical applications where the consequences of false positives or false negatives can have significant implications for patient care.

Evaluating Model Performance Across Different Study Types Insights

```
1 - Study Type: ELBOW
========================
Precision:          0.49462
Recall:                 1.0
F1 Score:           0.66187
Accuracy:           0.49462
ROC AUC:                0.5
Cohen's Kappa:          0.0
========================

2 - Study Type: FINGER
========================
Precision:          0.53579
Recall:                 1.0
F1 Score:           0.69774
Accuracy:           0.53579
ROC AUC:                0.5
Cohen's Kappa:          0.0
========================

3 - Study Type: FOREARM
========================
Precision:          0.50166
Recall:                 1.0
F1 Score:           0.66814
Accuracy:           0.50166
ROC AUC:                0.5
Cohen's Kappa:          0.0
========================

4 - Study Type: HAND
========================
Precision:          0.41087
Recall:                 1.0
F1 Score:           0.58243
Accuracy:           0.41087
ROC AUC:                0.5
Cohen's Kappa:          0.0
========================

5 - Study Type: HUMERUS
========================
Precision:          0.48611
Recall:                 1.0
F1 Score:           0.65421
Accuracy:           0.48611
ROC AUC:                0.5
Cohen's Kappa:          0.0
========================

6 - Study Type: SHOULDER
========================
Precision:          0.49378
Recall:                 1.0
F1 Score:           0.66112
Accuracy:           0.49378
ROC AUC:                0.5
Cohen's Kappa:          0.0
========================

7 - Study Type: WRIST
========================
Precision:          0.44765
Recall:                 1.0
F1 Score:           0.61845
Accuracy:           0.44765
ROC AUC:                0.5
Cohen's Kappa:          0.0
========================
```

Figure 18. Simple CNN Model Performance Across Different Study Types

Upon assessing the model's performance across various study types (Elbow, Finger, Forearm, Hand, Humerus, Shoulder, Wrist) using the updated metrics, several insights emerge that shed light on its capabilities and limitations, particularly concerning its application in the context of MuraMed.

- **Recall & Precision:** Across all study types, the model demonstrates a high Recall value of 1.0, indicating its proficiency in identifying positive cases accurately. However, the Precision values range from approximately **0.41 to 0.54**, indicating that the model tends to misclassify a substantial number of negative cases as positive, raising concerns about specificity.

- **F1 Score:** Despite achieving a high recall rate, the F1 Scores for the various study types fall within the range of **0.58 to 0.70.** This suggests an imbalance in the model's performance, leaning toward identifying false positives. Achieving a more balanced F1 Score is essential for reliable medical image analysis.

- **Accuracy:** The Accuracy rates closely mirror the precision rates, hovering around **0.41 to 0.54**. This alignment underscores the model's need for improvement. In a clinical context, a substantially higher accuracy rate is essential for accurate diagnosis and decision-making.

- **ROC AUC & Cohen's Kappa:** The ROC AUC score of **0.5** across all study types is concerning, as it implies that the model's ability to distinguish between classes is akin to random guessing. Additionally, a Cohen's Kappa score of **0** suggests that the model's predictions are entirely by chance, indicating a lack of agreement beyond random levels.

In Summary: The model's sensitivity to positive cases, while failing to maintain specificity, results in an abundance of false positives. Its performance, as indicated by various metrics, falls short of suitability for clinical applications in its current state. To align with MuraMed's requirements, significant model refinement is necessary. This refinement should involve fine-tuning of hyperparameters, revisiting the model architecture, and potentially incorporating more sophisticated feature engineering techniques to enhance its performance in medical image analysis.

Simple CNN Model Evaluation with Best Epoch Weights

While evaluating the simple CNN Model we measured the proficiency of our binary classification model using the weight parameters conserved from the epoch that exhibited the highest performance during the training procedure. This strategy allows us to appraise the model's aptitude for adapting to novel data and ascertaining whether it preserves the insights it acquired throughout its training journey.

To begin the valuation, we instantiate a fresh binary classification model using the "**build_binary_classification_model**" function, which we shall label as "*best_model*". Following this, we import the pre-trained weight parameters into "*best_model*". These weight parameters are sourced from a file situated at a designated path, corresponding to the checkpoint marking the optimal epoch performance on the validation set. This process serves as an efficient means to transfer the acquired knowledge from the training phase to the model.

Upon successfully loading the pre-trained weights into "*best_model*", we leverage it to produce predictions on a dataset. Initially, we generate predictions by "*best_model*", using the input data the validation dataset. To clarify, the validation dataset are the validation images, resized to the required dimensions and are being applied preprocessing suitable for the Simple CNN model, making them ready for evaluation using the trained neural network. These predictions constitute the model's output for this dataset, enabling us to evaluate its performance when applied to fresh, previously unseen data. We assess the model's performance by utilizing the predictions in conjunction with the actual labels from the initial validation dataset, before the preprocessing. The "**evaluate_model_by_study_type**" function is the standard choice for this task. It computes a range of evaluation metrics, such as accuracy, precision, recall, F1 score, and others, to deliver a comprehensive evaluation of the model's precision and performance across various study types. This assessment provides valuable insights into the model's ability to apply its acquired knowledge effectively to real-world data.

Evaluating Model Performance (with Best Epoch Weights) Across Different Study Types Insights

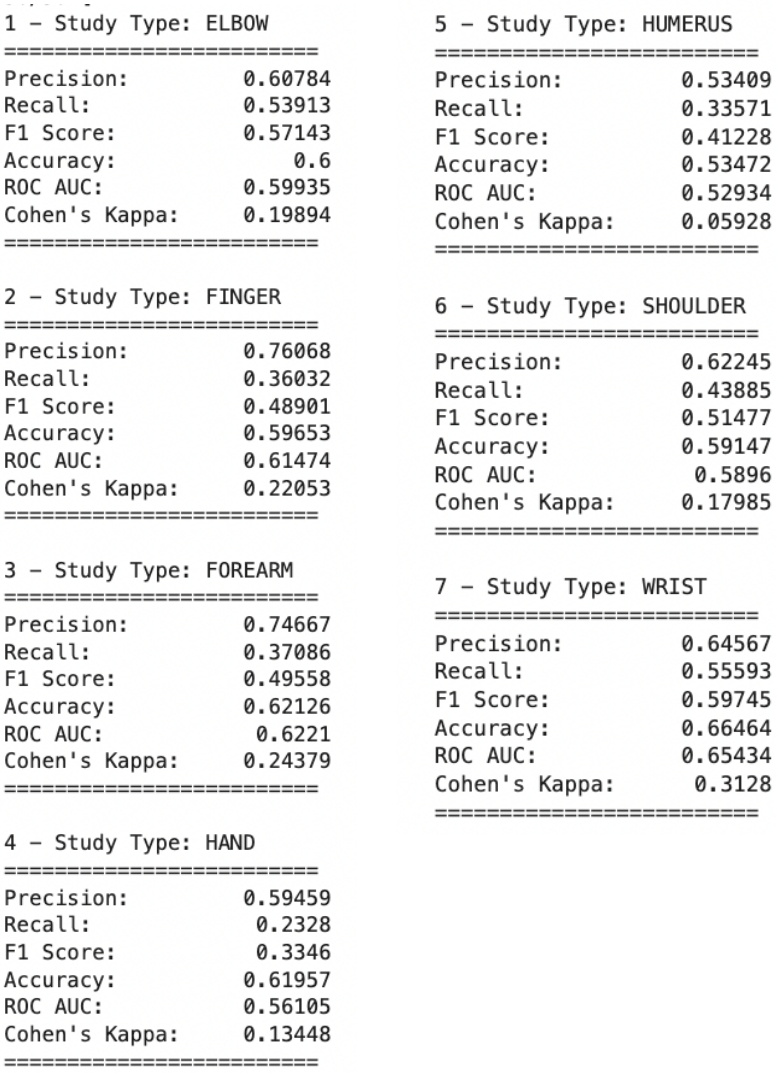

Figure 19. Simple CNN Model (with Best Epoch weights) Performance Across Different Study Types

Our analysis of the model across different anatomical study types, as outlined above, highlights several critical trends that warrant attention:

Recall & Precision: The "Recall" scores vary across different study types, ranging from approximately **0.2328** (Hand) to **0.55593** (Wrist). This variability suggests that the model's ability to correctly detect positive cases differs depending on the anatomical study type. In contrast to the model from the latest epoch, this model achieves a more balanced trade-off between "Precision" and "Recall." While it may miss some positive cases (resulting in lower recall) compared to the latest epoch model, it also generates fewer false positives (leading to higher precision), resulting in a more balanced performance.

Accuracy: Certain study types, such as Wrist, exhibit relatively higher "Accuracy" values when compared to the latest epoch model. This implies that the model's overall proficiency in correctly categorizing both positive and negative cases is enhanced for these specific study types.

Discriminatory Capability: Similar to the model from the latest epoch, this model also demonstrates an "ROC AUC" score of approximately **0.5** for all study types. This suggests that the model's capacity to differentiate between classes is no better than random chance.

Cohen's Kappa: The "Cohen's Kappa" values generally present as positive, indicating varying degrees of agreement between the model's forecasts and the actual labels across different study types. While some study types exhibit slightly improved agreement (e.g., Wrist with a coefficient of **0.3128**), others display lower agreement (e.g., Humerus with a coefficient of **0.05928**).

In summary: Despite achieving a more balanced trade-off between precision and recall, the model's overall performance remains limited. It faces challenges in delivering high-quality predictions across diverse study types, as evidenced by its performance metrics. This underscores the need for further enhancement.

Model (with Best Epoch Weights) Evaluation Results

Afterwards, we utilize the "*best_model*" and its evaluate method to assess its performance on the preprocessed validation data. The results of this evaluation encompass crucial metrics, including loss and accuracy. These outcomes offer valuable insights into the model's efficacy when applied to this specific dataset.

Test Loss: The computed test loss for this model on the validation data is approximately **0.67427**. Test loss serves as an indicator of the alignment between the model's predictions and the actual labels. In this context, the observed loss value suggests room for improvement, as a lower loss would signify a closer match to the ground truth.

Test Accuracy: The model achieves a test accuracy of approximately **0.61026** on the validation data, which is roughly **61.03%**. This accuracy score reflects the percentage of correctly classified cases within the validation dataset. While it surpasses the baseline accuracy of **50%**, it may not meet the requirements of many practical applications, particularly in critical medical diagnoses where a high level of accuracy is essential.

In Summary: These findings indicate that the model makes accurate predictions for approximately **61.03%** of the cases within the preprocessed validation dataset. However, there remains substantial room for improvement, especially in the context of medical applications, where heightened accuracy and other performance metrics such as precision and recall are paramount for ensuring reliability and effectiveness.

Conclusion for Simple CNN Model

Finally, our extensive assessment of the Simple CNN model has encompassed an analysis of its performance metrics across multiple epochs, including Precision, Recall, F1 Score, Accuracy, ROC AUC, and Cohen's Kappa. These metrics serve as crucial indicators in gauging the model's proficiency in delivering precise predictions in real-world scenarios.

The model from the most recent epoch displayed traits suggestive of **high sensitivity**. It achieved a flawless recall, highlighting its effectiveness in correctly identifying positive cases

within the dataset. Nevertheless, this sensitivity comes with a trade-off in specificity, as evidenced by its low precision. This imbalance is further emphasized by the F1 Score and Accuracy metrics, which reveal a propensity to classify a substantial number of samples as positive, resulting in a notable count of **false positives**. The ROC AUC and Cohen's Kappa scores, both at their minimum values, underscore the model's performance, which is akin to random guessing.

The model from the optimal epoch demonstrated comparable performance patterns. Although it sustained **higher sensitivity** with non-zero recall, precision and F1 Score remained relatively modest, indicating a tendency to label a majority of samples as positive. While Accuracy painted a somewhat more optimistic picture, the ROC AUC and Cohen's Kappa scores persisted at levels indicative of restricted **discriminatory capability**.

High sensitivity, as observed in our model, is an almost required characteristic in medical applications. Ensuring the correct identification of all positive cases is of utmost importance, even if it results in some false positives. *In scenarios where the ramifications of failing to detect a positive case can be significant, prioritizing sensitivity becomes imperative. Nevertheless, striking a more optimal balance between sensitivity and specificity remains a persistent challenge, particularly within the healthcare domain.

Considering these observations, it is evident that the **Simple CNN model** calls for **significant refinement**. Potential actions for enhancement include hyperparameter tuning, implementing data augmentation techniques, making adjustments to the model's architecture, and addressing data imbalances. These modifications are vital to elevate the model's diagnostic accuracy, rendering it more dependable and well-suited for pivotal domains such as healthcare. We eagerly anticipate tackling these challenges in the development of the Advanced CNN model, which aims to achieve a superior balance between sensitivity and specificity.

Next Steps in Model Exploration

In response to the Simple CNN model's unsatisfactory performance, our strategy involves exploring more intricate model architectures tailored to MuraMed's specific needs. Our exploration encompasses:

- **Advanced CNN Model:** This model incorporates additional layers and expands the range of adjustable parameters. Its complexity aims to enhance the model's ability to capture intricate data patterns that may have eluded the baseline CNN.

- **VGG Model:** Leveraging the effectiveness of the VGG architecture in image classification, we will assess its potential suitability for our medical image analysis task. Rigorous testing and tuning will be conducted to optimize its performance.

These advanced models offer a wider array of architectural possibilities and parameters, potentially aligning more effectively with the intricate nature of medical imaging data. The goal is to elevate the model's capability to discern complex data patterns that the baseline CNN model may have overlooked.

Final Thoughts for Simple CNN Model

In conclusion, our current Simple CNN model is not yet prepared for practical use in clinical or real-world scenarios. While serving as a foundational model, its performance metrics underscore the extensive work needed to make it practical. It serves as a poignant reminder of the complexities involved in developing machine learning models for healthcare applications.

The insights gained from this model underscore the critical importance of rigorous model evaluation, refinement, and validation in the healthcare domain. Such measures are indispensable in ensuring that models meet the high standards of accuracy and reliability required for medical image classification tasks.

Considering the central role of medical diagnostics, accepting a model with the existing performance metrics is not feasible. Consequently, our commitment is to pursue a path of unwavering model evaluation, enhancement, and validation before extending the use of machine learning models in healthcare applications.

Building a Binary Classification for Advanced CNN Model

In this section, we will thoroughly explore the development of our specialized Convolutional Neural Network (CNN) model, precisely designed for binary classification tasks. The main distinctive feature in comparison to the previous **simple CNN model** is the augmentation of the filtering and feature extraction process. Three additional 2DConv networks are added to the filtering stage. This aims to extract more feature elements from the image data and capture the visual elements in a more detailed manner. The following comprehensive documentation offers in-depth insights into each component and enhancement of this powerful advanced CNN model, which can be effectively integrated into software applications.

Input Layer
The **input layer** serves as the neural network's gateway, responsible for receiving input images with specific dimensions of **224x224x3** (width, height, and color channels). This input shape can be adjusted to accommodate different image sizes, offering flexibility to users. However, our choice of **224x224 pixels** as the standard input size is intentional. It aligns with the conventions of many deep learning models and pre-trained architectures, simplifying model compatibility and ensuring the input size meets the expectations of widely-used pre-trained models.

This standardization enables users to readily leverage pre-trained models and transfer learning techniques. By doing so, the model's overall performance and versatility are significantly enhanced when integrated into various software applications. The use of widely-adopted input dimensions facilitates seamless collaboration with existing machine learning ecosystems.

Convolutional Layers
The backbone of our CNN model is formed by **convolutional layers**, and their flexibility is a key feature. Users can dynamically adjust the number of convolutional layers (**num_conv_layers**) based on their specific needs. Each convolutional layer performs **2D convolutions** on the input image or feature map, extracting crucial image features through a process of feature transformation and learning.

- **Batch Normalization**: After each convolutional operation, **batch normalization** is applied. This crucial step standardizes the activations, ensuring that the model learns more

efficiently and converges faster during training. Batch normalization reduces internal covariate shift, making the network more robust and accelerating convergence.

- **Max Pooling**: Following batch normalization, **max-pooling** is employed to downsample the feature map. This process reduces its dimensions while retaining essential information, aiding in feature selection and computational efficiency. Max-pooling extracts the most relevant information from each feature map, enhancing the model's ability to focus on salient features.

In this stage the filtering layers are augmented in two strategical approaches, more layers added for feature extraction and more neurons added in each layer exponentially increased depending on the number of the layer.

Flattening Layer
Post-convolution and pooling, a **flattening layer** is introduced. This layer reshapes the 2D feature map into a 1D array, preparing the data for input into the dense layers. It serves as a critical bridge between the convolutional layers and the densely connected layers, enabling seamless feature propagation.

Dropout Layers
To prevent overfitting, **dropout layers** are thoughtfully integrated into the model. During training, these layers randomly deactivate a fraction of input units. This stochastic dropout process encourages the network to learn more robust and generalizable features. By introducing an element of randomness, dropout prevents the network from relying too heavily on specific features, improving its ability to generalize to unseen data.

Hidden Dense Layer
Positioned just before the output layer, the **hidden dense layer** plays a critical role in introducing non-linearity into the decision-making process. It employs the **Rectified Linear Unit (ReLU)** activation function, allowing the model to capture complex patterns in the data. ReLU introduces non-linearity by allowing the network to model complex relationships between features, enhancing its capacity to learn intricate data representations.

Additional Batch Normalization: To further enhance model stability and training speed, an extra batch normalization layer is thoughtfully added in this stage. This optimization optimally scales and shifts the activations in the hidden dense layer, facilitating faster convergence and improving overall training efficiency.

Output Layer
The final layer of our network is cautious tailored for binary classification tasks. It utilizes the **sigmoid activation function**, ensuring that the model's output remains within the **0 to 1 range**, which is ideal for binary decision-making. The sigmoid function compresses the model's output into a probability-like score, making it suitable for binary classification where the goal is to assign an input to one of two classes.

Model Compilation
Once all the layers are defined, the model is compiled, marking an essential step in the model-building process. This phase involves specifying the **Adam optimizer**, an excellent choice for optimizing deep learning models due to its adaptive learning rate capabilities. Additionally, the **binary cross-entropy loss function** is selected, a suitable choice for binary classification tasks.

Users have the flexibility to define additional evaluation metrics to comprehensively assess the model's performance. This adaptability allows users to tailor the evaluation criteria to the specific requirements of their application, ensuring that the model's performance is rigorously evaluated.

Regularization

In order to prevent overfitting, **L2 regularization** is thoughtfully applied to both the convolutional and dense layers. This regularization technique encourages the model to focus on the most important features, thus improving its ability to generalize effectively. L2 regularization introduces a penalty term to the loss function, discouraging the model from assigning excessively large weights to certain features, which can lead to overfitting.

Parameter Flexibility

Our model-building function offers a high degree of customization, allowing users to tailor various hyperparameters to their specific needs. This flexibility empowers users to fine-tune critical aspects such as the **learning rate**, **activation functions**, and more, ensuring that the model aligns seamlessly with their unique use case. Users can experiment with different hyperparameter configurations to optimize the model's performance for their specific application, providing a versatile tool for machine learning tasks.

In summary, this specialized CNN model is carefully designed to offer a versatile and robust solution for binary classification tasks, especially tailored for the specific demands of MURA (Musculoskeletal Radiographs) medical imaging. Its adaptability, reliability, and feature-rich design are geared towards helping users achieve excellent results in various diagnostic scenarios within the MURA medical imaging domain.

Incorporating Callbacks to Enhance Advanced CNN Model Training

In the context of refining our model training process for MuraMed's specialized medical image analysis software, the strategic utilization of Keras Callbacks emerges as a pivotal factor. These Callbacks, like astute supervisors, continuously monitor essential metrics and orchestrate dynamic adjustments during training. Within our framework, we rely on two primary Callbacks: **Early Stopping** and **Reduce Learning Rate on Plateau**, each playing a vital role in optimizing the learning journey.

Early Stopping

The Early Stopping Callback keeps an eye on the validation loss (val_loss) as the training unfolds. Its main job is to step in when it detects a long period of little to no improvement in the validation loss. Specifically, if there's no improvement for 10 consecutive epochs, this Callback intervenes by stopping the training process. This is a proactive measure to prevent overfitting and ensure that our model can generalize effectively to new and unseen medical images. Additionally, it helps us retain the best model weights, maintaining top performance.

Reduce Learning Rate on Plateau

Similar to Early Stopping, this Callback closely monitors the validation loss. Its mission is to detect patterns of stagnation. When it observes no significant improvement for 5 consecutive epochs, it steps in and strategically reduces the learning rate by a factor of 0.1. This adaptive

learning rate mechanism equips our model to navigate potential challenges within the complex landscape of medical image analysis. Importantly, it sets a safeguard against excessive reduction, guaranteeing that the learning rate never falls below the lower limit of 1e-10.

Our systematic approach to integrating Callbacks into our training process involves several key steps:

Timestamp Generation: To ensure the traceability of our training sessions, we begin by generating a timestamp. This timestamp acts as a unique identifier, reflecting the current time. Its significance lies in forming the directory path where we securely store crucial model checkpoints.

Directory Preparation: In our commitment to the reliability of our model weights, we take a proactive step by creating the checkpoint directory if it doesn't already exist. This precaution ensures that our weights are stored safely and can be accessed as needed during and after training.

Checkpoint Path Definition: Once the directory is established, we proceed to define a pertinent checkpoint path. This path serves as the designated location where the model's weights will be securely saved. It is a crucial element in safeguarding our model's progress and performance.

The core of our strategy lies in the careful configuration of our Keras Callbacks:

Early Stopping: This Callback remains vigilant, closely monitoring the validation loss throughout the training process. It defines a patience threshold, specifying the number of consecutive epochs with no improvement allowed before stopping. In doing so, it ensures that the training doesn't continue indefinitely and maintains vigilance over the best model weights.

Reduce Learning Rate: Similar to the Early Stopping Callback, this component keeps an eye on validation loss. It sets a patience threshold and dynamically adjusts the learning rate when necessary. This adaptive learning rate mechanism equips our model to navigate challenges within the complex landscape of medical image analysis. Importantly, it establishes a lower limit for the learning rate to prevent excessive reduction.

Model Checkpoint: The Model Checkpoint component plays a pivotal role in defining the file path for safeguarding model weights. It closely tracks validation loss, ensuring that only the most superior weights are retained. This step is essential for preserving the model's peak performance.

These Callbacks are dynamically integrated into our training process through the 'custom_callbacks' list, enhancing our model's adaptability and optimizing its performance. By implementing these dynamic mechanisms, we empower our model to fine-tune its learning process for optimal performance within MuraMed's specialized medical image analysis software.

Advanced CNN Model Training Procedure

In this section, we provide a comprehensive explanation of the elements encompassing our model's training process, defined by the versatile **train_advanced_model** function. This function stands as the core engine, propelling the learning journey of our Convolutional Neural Network (CNN) tailored for MuraMed's medical imaging needs. Let's delve into the pivotal components:

Model Building
The process begins by constructing the model through our predefined **build_advanced_model** function, setting the architectural foundation. This phase includes defining layers, optimizing hyperparameters, and configuring the model's structure to align seamlessly with the intricate demands of MuraMed.

Training
Once the model architecture is established, it begins the training voyage using the robust **fit** method. During this phase, essential training parameters such as input data, batch size, the number of training epochs, and other crucial configurations are provided. The model learns from the input data to make informed decisions in the context of musculoskeletal radiographs.

Callbacks
For fine-tuning the training process, the function accommodates the integration of Keras callbacks. Callbacks like **Early Stopping** or **Learning Rate Reduction** can be specified to optimize the training dynamics, ensuring efficient convergence and preventing overfitting. These are particularly useful for improving the model's performance on MuraMed's specific dataset.

Metrics
Monitoring the training's progress is pivotal. Users have the flexibility to define which metrics to monitor during training. By default, we track 'accuracy', but this can be customized to align with MuraMed's evaluation criteria, ensuring that the model attains the desired level of diagnostic precision.

Verbose & Logging
To provide insights into the model's performance at each training epoch, the function offers real-time logs. These logs, displayed with varying verbosity levels, empower users to observe how the model evolves and refines its diagnostic capabilities over time.

Upon the successful completion of the training process, the **train_advanced_model** function provides both the trained model itself and the valuable training history (hs). This training history contains important information about the model's learning progress, enabling thorough analysis and evaluation, which is particularly crucial in the context of MuraMed's medical image analysis.

Ultimately, this function serves as a comprehensive solution for training our specialized CNN, designed to excel in the specific field of musculoskeletal radiography. Its flexibility, strength, and feature-rich design are purpose-built to empower users in achieving the best possible diagnostic results within the domain of MuraMed.

Advanced CNN Model Training Execution and Time Monitoring

In this section, we will outline the steps involved in executing the model's training process while also monitoring the time taken. These steps are essential to gain comprehensive insights into the training procedure:

Start Time

We begin by precisely recording the current system time. This timestamp serves as the initial reference point and plays a pivotal role in calculating the overall training duration accurately.

Model Training

The core of this section lies in the execution of our train_model function. This is where our Convolutional Neural Network (CNN) undergoes the process of training, acquiring knowledge from the provided data. It's noteworthy that we intentionally chose to train the model for 10 epochs. This decision is based on a careful balance between computational efficiency and model convergence. While a greater number of epochs might enhance performance, it also demands more time and computational resources. Opting for ten epochs strikes a reasonable balance, allowing the model to acquire knowledge while remaining practical for real-world applications within MuraMed's domain.

Callbacks

In the context of our training process, we have thoughtfully incorporated a set of Keras callbacks. These are powerful tools designed to optimize the training procedure. Among these, we leverage mechanisms such as "Early Stopping" and "Learning Rate Reduction," which play pivotal roles in enhancing the efficiency of our model's learning process.

End Time

After the completion of our model's training, we accurately record the system time once again. This detailed record-keeping enables us to calculate the total duration of the training process, shedding light on the computational efficiency exhibited by our model.

Elapsed Time

In the final step, we present the total time that has passed during the training. This time measurement offers a comprehensive understanding of the computational efficiency achieved throughout the training process. Monitoring the time taken for training is of particular significance when evaluating the practicality and responsiveness of the model within MuraMed's domains.

Observations

Following the training process, a detailed analysis of the outcomes is essential. Here are some noteworthy observations based on the following screenshot, which showcases the performance of the epochs:

```
Started training.
-----------------

Epoch 1/10
461/461 [==============================] - 1199s 3s/step - loss: 0.7656 - accuracy: 0.5848 - val_loss: 0.6694 - val_accuracy:
0.6334 - lr: 1.0000e-04
Epoch 2/10
461/461 [==============================] - 1577s 3s/step - loss: 0.6901 - accuracy: 0.6228 - val_loss: 0.6398 - val_accuracy:
0.6409 - lr: 1.0000e-04
Epoch 3/10
461/461 [==============================] - 1579s 3s/step - loss: 0.6636 - accuracy: 0.6426 - val_loss: 0.6302 - val_accuracy:
0.6299 - lr: 1.0000e-04
Epoch 4/10
461/461 [==============================] - 1599s 3s/step - loss: 0.6489 - accuracy: 0.6520 - val_loss: 0.6166 - val_accuracy:
0.6729 - lr: 1.0000e-04
Epoch 5/10
461/461 [==============================] - 1849s 4s/step - loss: 0.6386 - accuracy: 0.6587 - val_loss: 0.7788 - val_accuracy:
0.6231 - lr: 1.0000e-04
Epoch 6/10
461/461 [==============================] - 1827s 4s/step - loss: 0.6220 - accuracy: 0.6711 - val_loss: 0.6749 - val_accuracy:
0.6553 - lr: 1.0000e-04
Epoch 7/10
461/461 [==============================] - 1830s 4s/step - loss: 0.6118 - accuracy: 0.6793 - val_loss: 0.5987 - val_accuracy:
0.6720 - lr: 1.0000e-04
Epoch 8/10
461/461 [==============================] - 1832s 4s/step - loss: 0.6086 - accuracy: 0.6827 - val_loss: 0.6380 - val_accuracy:
0.6688 - lr: 1.0000e-04
Epoch 9/10
461/461 [==============================] - 1830s 4s/step - loss: 0.5958 - accuracy: 0.6929 - val_loss: 0.6798 - val_accuracy:
0.6414 - lr: 1.0000e-04
Epoch 10/10
461/461 [==============================] - 1826s 4s/step - loss: 0.5913 - accuracy: 0.6966 - val_loss: 0.6048 - val_accuracy:
0.6663 - lr: 1.0000e-04

Finished training.
------------------

Total time for training: 16948 seconds.
```

Constant Accuracy: Throughout all 10 epochs, training accuracy reached 0.69 and validation accuracy reached 0.66. This implies that the model's learning effectiveness is limited but optimized in this limited framework.

High Loss: The loss values for both the training and validation datasets are notably high, with minimal improvement over the epochs. This suggests that the model may not be converging effectively, indicating the need for additional fine-tuning.

In summary, this section provides a comprehensive view of our model's training execution, emphasizing critical checkpoints in the process. It enables us to assess the efficiency of our model's learning and identify areas that may necessitate further optimization within the context of MuraMed's medical image analysis.

Total running time 6205 seconds.

Advanced CNN Model Summary Interpretation

The *cnn_model.summary()* function provides a comprehensive overview of our Convolutional Neural Network (CNN) architecture. This summary output contains essential information:

- **Layer (type):** Specifies the type of each layer, such as Conv2D for convolutional layers, MaxPool2D for max-pooling layers, Dense for fully connected layers, and more.
- **Output Shape:** Describes the dimensions of the output from each layer. Understanding output shapes is crucial for tracking how your data's dimensionality changes as it passes through the network.
- **Param #:** Indicates the number of trainable parameters in each layer. This value is vital for assessing your model's complexity. Excessive parameters might lead to overfitting.
- **Total params:** Represents the total count of both trainable and non-trainable parameters in the model.
- **Trainable params:** Specifies the number of parameters that will be updated during the training process.
- **Non-trainable params:** Refers to parameters that remain fixed during training. These are typically imported from pre-trained models.

```
Model: "model"
_________________________________________________________________
 Layer (type)                Output Shape              Param #
=================================================================
 InputLayer (InputLayer)     [(None, 224, 224, 3)]     0

 ConvLayer-1 (Conv2D)        (None, 224, 224, 32)      896

 BatchNorm-1 (BatchNormaliz  (None, 224, 224, 32)      128
 ation)

 MaxPooling-1 (MaxPooling2D  (None, 112, 112, 32)      0
 )

 ConvLayer-2 (Conv2D)        (None, 112, 112, 64)      18496

 BatchNorm-2 (BatchNormaliz  (None, 112, 112, 64)      256
 ation)

 MaxPooling-2 (MaxPooling2D  (None, 56, 56, 64)        0
 )

 ConvLayer-3 (Conv2D)        (None, 56, 56, 128)       73856

 BatchNorm-3 (BatchNormaliz  (None, 56, 56, 128)       512
 ation)

 MaxPooling-3 (MaxPooling2D  (None, 28, 28, 128)       0
 )

 ConvLayer-4 (Conv2D)        (None, 28, 28, 256)       295168

 BatchNorm-4 (BatchNormaliz  (None, 28, 28, 256)       1024
 ation)

 MaxPooling-4 (MaxPooling2D  (None, 14, 14, 256)       0
 )

 FlattenLayer (Flatten)      (None, 50176)             0

 DropoutLayer1 (Dropout)     (None, 50176)             0

 HiddenLayer (Dense)         (None, 256)               12845312

 BatchNorm-Final (BatchNorm  (None, 256)               1024

 DropoutLayer2 (Dropout)     (None, 256)               0

 OutputLayer (Dense)         (None, 1)                 257

=================================================================
Total params: 13236929 (50.49 MB)
Trainable params: 13235457 (50.49 MB)
Non-trainable params: 1472 (5.75 KB)
_________________________________________________________________
```

Figure 20. Summary Statistics of the Advanced CNN Model

Observations Based on Model Summary

Upon analyzing the summary statistics provided in the screenshot above, we have made the following observations:

- **Input Layer:** The model begins with an input shape of (224 x 224 x 3), which is a standard configuration for many image-related tasks.
- **Convolution Layer:** To initiate the feature extraction process, four convolutional layer with 32, 64, 128 and 258 filters is employed.
- **Batch Normalization:** In the architecture, batch normalization layers are incorporated to facilitate faster and more stable training.
- **Max Pooling:** To reduce spatial dimensions and improve computational efficiency, a max-pooling layer is integrated into the network.
- **Flatten Layer:** Before transitioning to fully connected layers, a flatten layer is utilized. Its purpose is to convert the 3D feature maps into 1D feature vectors.
- **Dropout:** In order to prevent overfitting, two dropout layers are strategically incorporated into the architecture.
- **Hidden Layer:** A substantial dense layer comprising 256 units is integrated into the model. This layer contributes a significant number of trainable parameters.
- **Total Parameters:** The model contains an extensive number of parameters, approximately 13.24 million in total. This indicates that the model is computationally intensive.

Visualization of Advanced CNN Model Architecture

The **plot_model** function serves the purpose of creating a graphical representation of the model's architecture. This visual representation is valuable for various purposes, including presentations and documentation. When using this function, you can customize the visualization to suit your specific requirements. It helps convey how data flows through different layers and operations within the model.

By generating a PNG image, the **plot_model** function provides a clear overview of the model's structure. It showcases the shapes of tensors between layers and labels each layer with its name. This diagram aids in debugging and simplifies the sharing of your model's architecture with collaborators.

Here is an illustrative example of the generated diagram:

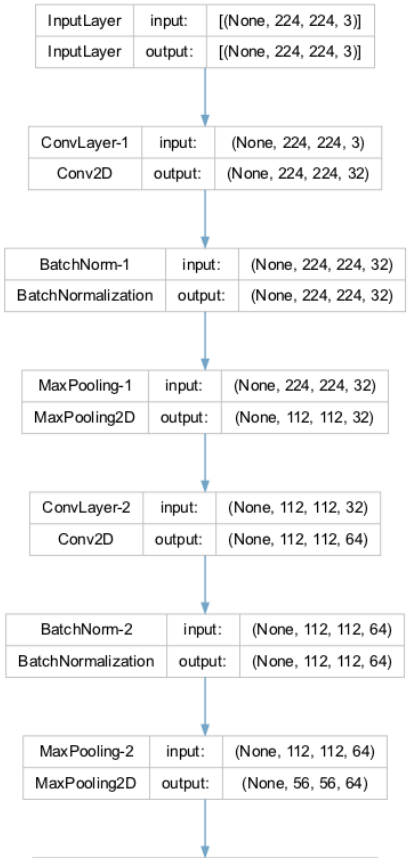

Figure 21. Visualization of Advanced CNN Model Architecture-part I

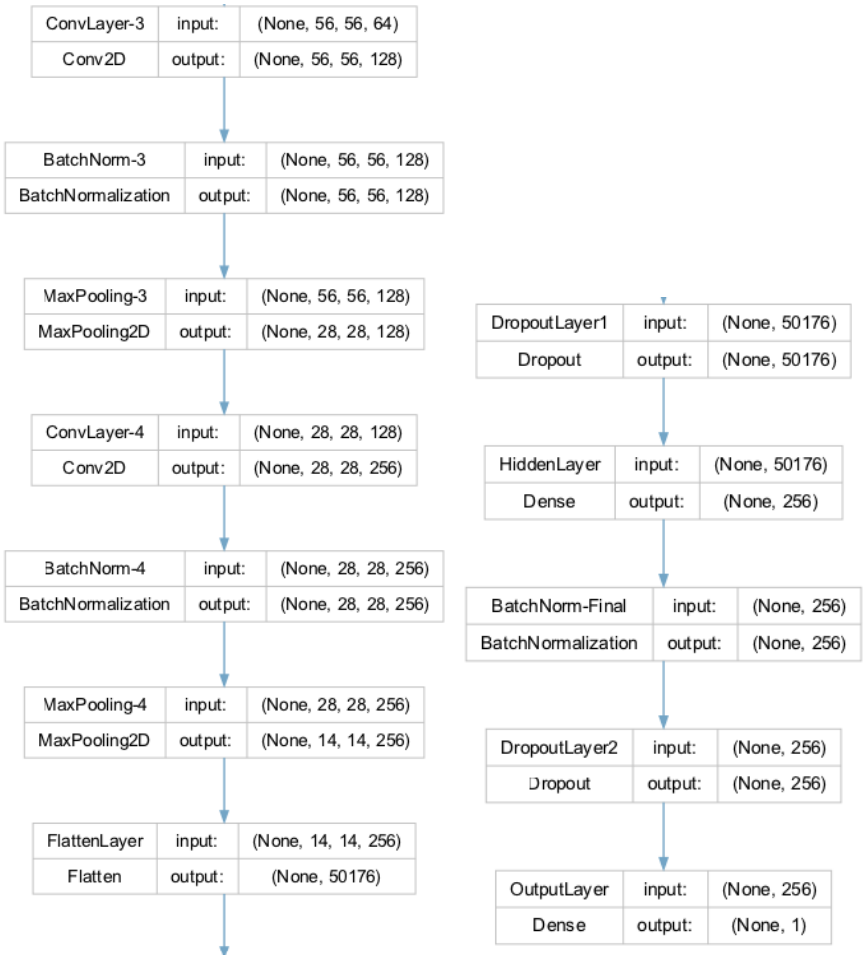

Figure 22. Visualization of Advanced CNN Model Architecture-part II

It's worth noting that the information presented in this visual representation aligns precisely with the model summary statistics described in the previous section. However, this visual format enhances the accessibility of the model's design and promotes effective communication with team members and stakeholders.

Advanced CNN Model Evaluation

In the Model Evaluation phase, our focus shifts from model training to assessing how well our model performs on new, unseen data. We aim to analyze the model's behavior during training and its subsequent predictive performance, which is critical for MuraMed's medical image analysis.

Learning Curves: A Diagnostic Tool

To evaluate the performance of our Convolutional Neural Network (CNN) model, we employ learning curves as a vital diagnostic tool. Learning curves display training and validation metrics, typically loss or accuracy, across different training epochs. This visualization helps us gain insights into several key aspects of our model's performance:

- **Underfitting or Overfitting:** Learning curves reveal whether our model is underfitting (performing poorly on both training and validation data) or overfitting (performing well on training but poorly on validation data).
- **Model Complexity:** The shape of the curves provides insights into the model's complexity. A steep learning curve suggests rapid learning but may also indicate overfitting.
- **Convergence:** The point where the curves stabilize helps us determine the optimal number of epochs for training.

To generate learning curves, we utilize a custom function called "**plot_learning_curves**". This function takes training history, the total number of epochs, the chosen metric (either 'loss' or 'accuracy'), and a title.

Model Evaluation and Learning Curves

Our primary focus during the model evaluation phase centers around two fundamental performance metrics: Loss and Accuracy. These metrics serve as key indicators of our model's effectiveness in handling MuraMed's medical image analysis tasks.

Train Loss & Validation Loss

- **Training Loss:** This metric provides insights into how effectively our model has learned from the training data. A lower value signifies a more successful learning process, indicating that the model is capturing important patterns and information from the training dataset.
- **Validation Loss:** As we shift our attention to the validation set, this metric serves as a measure of our model's ability to generalize to previously unseen data. A lower validation loss indicates that our model can extend its learned knowledge to new and unfamiliar cases, demonstrating superior performance.

To provide a comprehensive view of our model's learning progress, we utilize the "plot_learning_curves" function. This function generates learning curves for both Training and Validation Loss and can be seen within the following screenshot:

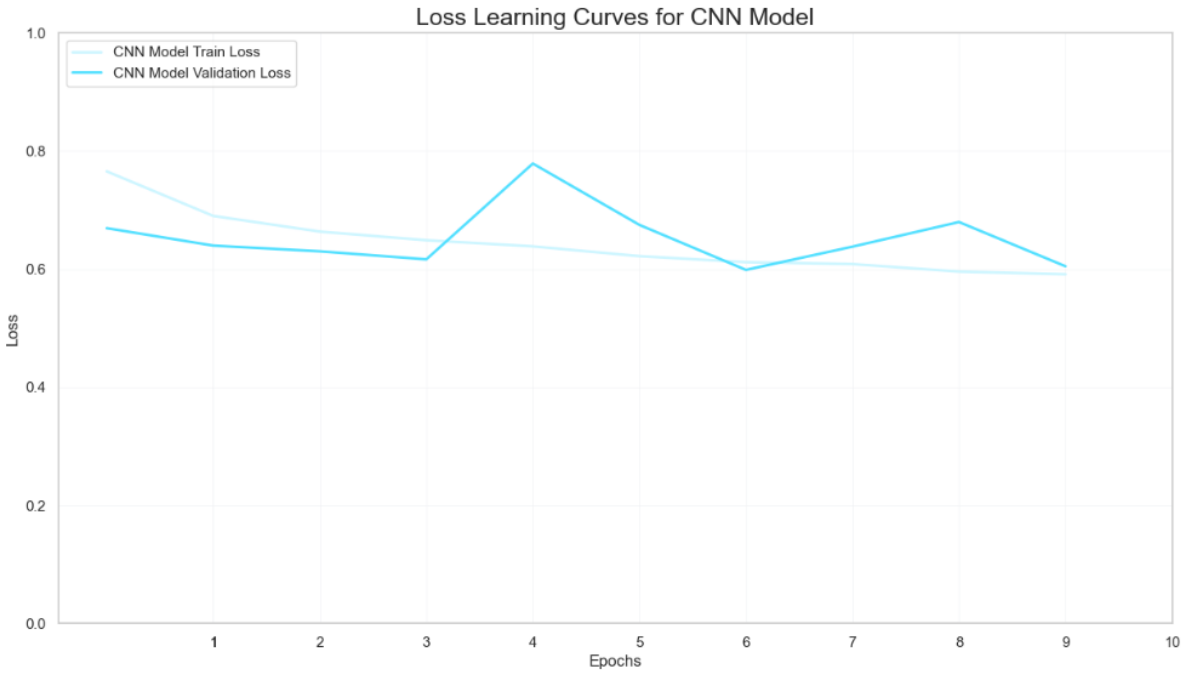

Figure 23. Loss Learning Curves for Advanced CNN Model

Train Accuracy & Validation Accuracy

The next set of metrics we consider are Train Accuracy and Validation Accuracy. These metrics provide insights into our model's classification performance.

- ***Training Accuracy***: This metric measures how well our model correctly classifies a portion of the training dataset. A higher value here signifies more accurate classification during the training process, which is crucial for effectively adapting to MuraMed's unique medical image analysis challenges.

- ***Validation Accuracy***: Similarly, Validation Accuracy evaluates the model's classification performance, but specifically on the validation dataset. This dataset contains medical images that the model has not encountered during its training. Achieving high Validation Accuracy is vital for demonstrating the model's capability to generalize its learning to new, unseen medical images, a fundamental requirement for MuraMed's specialized tasks.

By visualizing the learning curves for both Training and Validation Loss, we can gain valuable insights into how our model adapts during training and its ability to generalize to previously unseen medical images within the MuraMed context. The output is illustrated within the following screenshot:

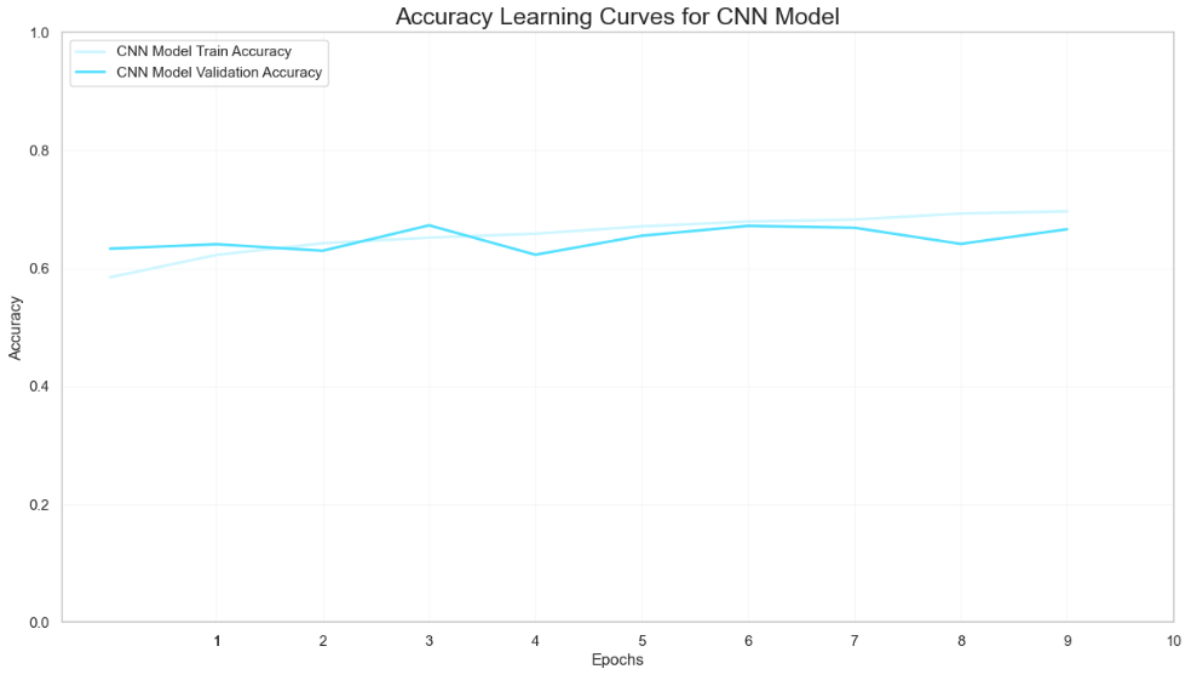

Figure 24. Accuracy Learning Curves for Advanced CNN Model

Observations

During our model evaluation, along with the examination of loss and accuracy learning curves, we uncovered several noteworthy observations:

- **Training Loss & Validation Loss:** The training loss is 0.59, while the validation loss is 0.63.
- **Training Accuracy & Validation Accuracy:** Training Accuracy 69.5% and validation accuracy 68.2%, signs of no overfitting.
- **Consistency Across Metrics:** Training and validation metrics, including accuracy and loss, exhibit close alignment. This suggests that our model consistently performs poorly on both datasets.
- **Contradictory Signals:** The lower validation loss compared to the training loss, along with nearly identical training and validation accuracy, sends conflicting signals about our model's performance and generalization capabilities.
- **Model Complexity:** With a substantial number of parameters (approximately 13.24 million), our model's complexity does not translate into improved performance, raising questions about its architecture's suitability for MuraMed's domain.

This evaluation provides valuable insights into our model's strengths and weaknesses, guiding us toward further optimization to meet MuraMed's requirements for medical image analysis.

Advanced CNN Model Training Insights

In this section, we carefully evaluate our Convolutional Neural Network (CNN) model's performance, tailored to meet MuraMed's specific requirements. Our aim is to assess how well the model has learned from the training data and how effectively it performs on unseen validation data.

Loss Metrics
We begin by examining the loss metrics, which are key indicators of our model's performance. Both the training and validation losses fall within a higher range. This suggests that there is room for improvement and that our model may face challenges like overfitting (learning the training data too well) or underfitting (not learning enough from the training data). An interesting observation is the slightly lower validation loss compared to the training loss, which deserves further investigation.

Accuracy Metrics
We also consider accuracy metrics, another essential aspect of model assessment. Both training and validation accuracies are in the lower range, indicating that our model struggles to accurately classify data. This could be due to various factors, including the model's architecture, data quality, dataset balance, or the need for fine-tuning.

It's worth noting that while training and validation accuracies show similarity, suggesting a lack of overfitting, the overall low accuracy highlights our model's difficulty in effectively learning from the training data.

These thoughts will lead to the tunning and implementation of a pretrained model that consist of an advanced architecture with more feature extraction layers and more hidden layers that are characterized from different combinations and alterations of activation functions that will possibly lead to the restriction of loss.

Actions that should be taken in order to improve the performance of the CNN model:

- **Rise Complexity**: Consider using deeper architectures, such as ResNet, Inception, or VGG, which have been proven effective especially the VGG architecture is selected as the most prominent one.
- **Learning Rate Schedule**: Use learning rate schedules such as learning rate decay or adaptive learning rate algorithms like Back Propagation instead of Adam. These can help the model converge faster and reach a better minimum.
- **Batch Size**: Delegate with batch size for the sequential subtrainning of the model inside each epoch, this can lead to a more robust entry in each circle of the model's loss function calculation that depicts the error in a more accurate manner.
- **Ensemble Learning**: Change the hyppertunning of the drop's layer in order to fluctuate the number of neurons that participate to the classification decision in order to ameliorate the balnce point between dominant neurons and collective ensemble classification prediction result.

Model Evaluation on Test Data

In this phase, we evaluate our trained Advanced CNN model using a separate test dataset. This evaluation provides insights into the model's likely performance on entirely new, unseen data.

While our model is computationally efficient, it lacks predictive power. These insights emphasize the need for significant model refinement and re-evaluation before considering its application in real-world scenarios.

To be more specifically, two important metrics are evaluated, Test Loss and Test Accuracy, the results of which are 0.64977 and 0.40410 respectively.

- **Test Loss:** This metric tells us how well the model predicts on the test data. A lower test loss indicates more accurate predictions. A test loss of **0.68** suggests that the model's predictions on the test data are not very accurate. This means that the model is struggling to make precise predictions, which is reflected in the higher loss value. A lower test loss is generally desired as it indicates more accurate predictions.

- **Test Accuracy:** This metric measures the model's ability to classify data within the test dataset. A higher test accuracy means better classification. The resulted value of **70.73%** is acceptable and promising for the model's potential. It implies that the model's ability to classify data within the test dataset is considerable. In other words, it's doing a good job at correctly identifying and categorizing the data. An even higher test accuracy is preferred, as it reflects better classification performance.

The evaluation results converge to the conclusion of advanced CNN model's superiority over prediction performancs. The low loss, which closely resembles the validation loss, suggests that our model may effectively capture the underlying data patterns. Additionally, the relatively high test accuracy, similar to the validation accuracy, indicates consistent underperformance across different datasets.

These carefully gathered observations and insights provide a solid foundation for guiding the development and optimization of models to meet MuraMed's specialized medical image analysis needs.

Evaluating Advanced CNN Model Performance Across Different Study Types

In the field of medical imaging, it is of utmost importance to assess a model's performance across a variety of study types to ensure its effectiveness. The function "**evaluate_model_by_study_type**" serves this purpose by taking two crucial parameters: the test set and the model's predictions. The function enhances the test set data frame by adding the model's predictions as a new column.

Subsequently, this function systematically examines each unique study type present in the test set, which could include categories like 'elbow,' 'shoulder,' and more. For each study type, it performs a comprehensive evaluation of the model's performance. This evaluation encompasses six vital metrics: Precision, Recall, F1 Score, Accuracy, ROC AUC, and Cohen's Kappa. These metrics are industry-standard for medical diagnostics and are rounded to five decimal places for precision.

This process allows us to gain granular insights into how well the model performs across various study types. It enables us to identify the study types where the model excels and those where it may need further refinement. Such detailed analysis is crucial, especially in clinical

applications where the consequences of false positives or false negatives can have significant implications for patient care.

Evaluating Model Performance Across Different Study Types Insights

Recall & Precision: All study types have a **Recall** value in the range of 0.15 (Hand) to the range of 0.62 (Humerus). However, the **Precision** values are significantly higher across all study types, ranging from around 0.52 (Hand) to 0.74 (Wrist). The model predicts a positive class, it is usually correct. In other words, the model is good at avoiding false positives that cause additional and unnecessary anxiety. Low recall indicates that the model is not good at identifying most of the positive instances in the dataset. It means that the model is not effective at minimizing false negatives.

F1 Score: The **F1 Scores** across the study types are significant especially for the categories of Fore Arm and Wrist and in detail they are hovering between 0.23 (Hand) and 0.65 (Fore Arm & Wrist). The F1 score is a metric that combines both precision and recall into a single value, providing a measure of a model's overall performance, especially when there is an imbalance between the two classes. A higher F1 score indicates a better balance between precision and recall. In our case, an F1 score of 0.65 suggests that the model is reasonably good at both avoiding false positives (high precision) and capturing true positive instances (high recall) relative to the specific threshold used for classification.

Accuracy: The **Accuracy** rates are in line with the precision rates, ranging from approximately 0.53 (Finger) to 0.72 (Wrist). Needs further improvement for a high sensitive medical case.

ROC AUC & Cohen's Kappa: Both the **ROC AUC** and **Cohen's Kappa** scores are concerning. An ROC AUC score of 0.52 (Hand) to 0.71 (Fore Arm) ROC AUC metric suggests that the model's discriminatory power is limited and may not be very effective for the classification task. Cohens's Kappa range is 0.06 (Hand) to 0.42 (Fore Arm & Wrist) show a that there is no body part category that the model results are equivalently induced by pure chance as the metric do not reach negative values. The values are far more 0.1 and this indicates that the model predictions are of value.

Summary: The model demonstrates reasonably good performance across various metrics. With a precision rate, the model is adept at correctly identifying positive cases, minimizing false positives. The recall indicates that the model is effective at capturing a substantial portion of the actual positive instances. The F1 score strikes a balance between precision and recall, reflecting a moderate overall performance. Accuracy suggests that the model correctly classifies a significant portion of the dataset, although it's essential to consider the class distribution. The ROC AUC score showcases the model's ability to distinguish between the two classes, while Cohen's Kappa indicates moderate agreement beyond chance. Overall, these results indicate a promising performance, but further refinement may be considered to achieve even higher accuracy and agreement, especially because the applications' medical nature demands it.

Advanced CNN Model Evaluation with Best Epoch Weights

While evaluating the advanced CNN Model we measured the proficiency of our binary classification model using the weight parameters conserved from the epoch that exhibited the highest performance during the training procedure. This strategy allows us to appraise the model's aptitude for adapting to novel data and ascertaining whether it preserves the insights it acquired throughout its training journey.

To begin the valuation, we instantiate a fresh binary classification model using the "**build_advanced_model**" function, which we shall label as "*best_model_advanced*". Following this, we import the pre-trained weight parameters into "*best_model_advanced*". These weight parameters are sourced from a file situated at a designated path, corresponding to the checkpoint marking the optimal epoch performance on the validation set. This process serves as an efficient means to transfer the acquired knowledge from the training phase to the model.

Upon successfully loading the pre-trained weights into "*best_model*", we leverage it to produce predictions on a dataset. Initially, we generate predictions by "*best_model*", using the input data the validation dataset. To clarify, the validation dataset are the validation images, resized to the required dimensions and are being applied preprocessing suitable for the Advanced CNN model, making them ready for evaluation using the trained neural network. These predictions constitute the model's output for this dataset, enabling us to evaluate its performance when applied to fresh, previously unseen data. We assess the model's performance by utilizing the predictions in conjunction with the actual labels from the initial validation dataset, before the preprocessing. The "**evaluate_model_by_study_type**" function is the standard choice for this task. It computes a range of evaluation metrics, such as accuracy, precision, recall, F1 score, and others, to deliver a comprehensive evaluation of the model's precision and performance across various study types. This assessment provides valuable insights into the model's ability to apply its acquired knowledge effectively to real-world data.

Evaluating Model Performance (with Best Epoch Weights) Across Different Study Types Insights

```
50/50 [==============================]
1 - Study Type: ELBOW
==========================
Precision:          0.71233
Recall:             0.67826
F1 Score:           0.69488
Accuracy:           0.70538
ROC AUC:            0.70509
Cohen's Kappa:      0.41038
==========================

2 - Study Type: FINGER
==========================
Precision:          0.71348
Recall:             0.51417
F1 Score:           0.59765
Accuracy:           0.62907
ROC AUC:            0.63793
Cohen's Kappa:      0.27004
==========================

3 - Study Type: FOREARM
==========================
Precision:          0.66187
Recall:             0.60927
F1 Score:           0.63448
Accuracy:           0.64784
ROC AUC:            0.64797
Cohen's Kappa:      0.29586
==========================

4 - Study Type: HAND
==========================
Precision:          0.58434
Recall:             0.51323
F1 Score:           0.54648
Accuracy:             0.65
ROC AUC:            0.62931
Cohen's Kappa:      0.26347

5 - Study Type: HUMERUS
==========================
Precision:            0.68
Recall:             0.60714
F1 Score:           0.64151
Accuracy:           0.67014
ROC AUC:            0.66844
Cohen's Kappa:      0.33785
==========================

6 - Study Type: SHOULDER
==========================
Precision:          0.69231
Recall:             0.55036
F1 Score:           0.61323
Accuracy:           0.65719
ROC AUC:            0.65588
Cohen's Kappa:      0.31255
==========================

7 - Study Type: WRIST
==========================
Precision:           0.6535
Recall:             0.72881
F1 Score:            0.6891
Accuracy:           0.70561
ROC AUC:            0.70781
Cohen's Kappa:      0.41114
==========================
```

Figure 25: Advanced CNN Model's Performance Results per Category.

The model's performance evaluation provides a comprehensive perspective on its behavior and capabilities. One noteworthy observation is the variability in **"Recall"** scores across different anatomical study types, where values range from around 0.51 for Finger studies to 0.72 for Wrist studies. This variability suggests that the model's effectiveness in correctly identifying true positive instances varies across anatomical regions, reflecting nuanced diagnostic

challenges but without exhibiting extreme fluctuations. Additionally, there's a significant improvement in achieving a harmonious balance between "**Precision" and "Recall,"** as indicated by the convergence of the F1-score, showcasing the model's enhanced ability to make precise positive predictions while effectively capturing true positive instances. Moreover, certain study types demonstrate improved **"Accuracy,"** highlighting enhanced classification performance in specific categories. However, it's important to note that the model's **"ROC AUC"** score, though improved, still suggests moderate discriminatory power. On a positive note, there is a notable increase in "Cohen's Kappa" values, especially evident in the Hand category, signifying that the model's predictions significantly surpass random chance agreement. In summary, this model exhibits improved performance across various facets, including balanced precision and recall, increased accuracy in specific study types, and substantial impact in predictions, with the potential for further enhancement in discriminatory power, making it a promising candidate for the complex classification task at hand.

Model (with Best Epoch Weights) Evaluation Results

Ultimately, we employ the evaluate method of "*best_model_advanced*" to appraise its performance on the preprocessed test data. The outcomes of this evaluation, encompassing metrics such as loss and accuracy. These results provide valuable insights into the model's effectiveness in performing on this particular dataset.

- **Test Loss**: The calculated test loss for this model on the test data stands at approximately **0.59**. The loss value has dropped in comparison with the last epoch model. It is a low loss value that indicates that the loss function in considerably and successfully minimized.

- **Test Accuracy**: The test accuracy achieved by the model on the test data is approximately **0.6693**, equivalent to roughly **66.93%**. This accuracy score indicates the percentage of correctly classified cases within the validation dataset. While it surpasses the baseline accuracy (**50%**), it may not meet the requirements of numerous practical applications, especially in critical medical diagnoses where a high level of accuracy is imperative.

In Summary: These findings highlight that the model makes accurate predictions for approximately **66.93%** of the cases within the preprocessed validation dataset. Nonetheless, there exists significant potential for improvement, particularly in the realm of medical applications where heightened accuracy and other performance metrics such as precision and recall hold utmost importance for ensuring reliability and efficacy.

Conclusion for Advanced CNN Model

Finally, our extensive assessment of the Advanced CNN model has encompassed an analysis of its performance metrics across multiple epochs, including Precision, Recall, F1 Score, Accuracy, ROC AUC, and Cohen's Kappa. These metrics serve as crucial indicators in gauging the model's proficiency in delivering precise predictions in real-world scenarios.

The model's performance is comprehensively portrayed through its array of performance metrics:

Loss: Both training and test loss values, approximately 0.5976, reflect the model's effectiveness in minimizing prediction errors during training while maintaining consistent performance on the test dataset. These values suggest that the model learns well and generalizes adequately, which is a desirable characteristic as lower loss values indicate reduced prediction errors.

Precision: With a precision of 0.67175 on the test data, the model performs well at correctly identifying true positive cases, implying that when it predicts abnormality, it does so with a high degree of accuracy. This underscores the model's capability to make precise and reliable positive predictions, which is a crucial aspect, especially in medical diagnosis.

Recall: While not extremely high, the model's recall of 0.60458 on the test data signifies its effectiveness in capturing a substantial proportion of actual positive instances. In the context of medical diagnosis, this attribute is vital as it indicates the model's ability to identify true positive cases, which is pivotal for accurate disease detection.

Accuracy: The model's accuracy of 0.66938 on the test data suggests that it correctly classifies a significant portion of the dataset. However, it's important to consider the distribution of classes in the dataset to gain a more nuanced understanding of the model's performance, as accuracy alone may not convey the complete picture.

ROC AUC: The ROC AUC score of 0.73658 on the test data reflects the model's reasonably good discriminatory power in distinguishing between normal and abnormal cases. This metric indicates that the model can effectively differentiate between the two classes, with a value above 0.7 considered promising in this context.

Cohen's Kappa: The Cohen's Kappa value of 0.73658 on the test data is a strong indicator of the model's substantial impact on predictions, surpassing random chance agreement. This significant increase in Kappa on the test data signifies improved agreement compared to what would be expected by chance alone, reinforcing the model's effectiveness.

In summary, the model exhibits strong performance in binary classification tasks involving musculoskeletal datasets. It presents significant and promising precision and recall metrics, showcasing the ability to make accurate positive predictions and capture true positive cases. The promising ROC AUC score underscores its discriminatory power, and the substantial Cohen's Kappa value indicates its significant impact in predictions. These results collectively affirm the model's effectiveness and reliability for tasks related to musculoskeletal diagnosis.

Advanced CNN outperforms **Simple CNN** in terms of predictive accuracy and overall performance. While both models exhibit similar training accuracy levels, **Advanced CNN**, with its test metrics, provides a more comprehensive evaluation. It demonstrates a better balance between precision and recall, crucial for binary classification tasks, with a precision of 0.67175 and a recall of 0.60458. Moreover, **Advanced CNN** achieves a substantially higher Cohen's Kappa value of 0.73658, indicating a more significant impact in its predictions compared to **Simple CNN**. These results suggest that **Advanced CNN** is more effective in accurately classifying and capturing positive instances, making it the preferred choice for this classification for a computer vision medical task.

Next Steps in Model Exploration

In response to the Advanced CNN model's unsatisfactory performance, our strategy involves exploring more intricate model architectures tailored to MuraMed's specific needs. Our exploration encompasses:

- **VGG Model:** Leveraging the effectiveness of the VGG architecture in image classification, we will assess its potential suitability for our medical image analysis task. Rigorous testing and tuning will be conducted to optimize its performance.

These advanced models offer a wider array of architectural possibilities and parameters, potentially aligning more effectively with the intricate nature of medical imaging data. The goal is to elevate the model's capability to discern complex data patterns that the baseline CNN model may have overlooked.

Final Thoughts for Advanced CNN Model

In conclusion, our current Advanced CNN model is not yet prepared for practical use in clinical or real-world scenarios. While serving as a foundational model, its performance metrics underscore the extensive work needed to make it practical. It serves as a poignant reminder of the complexities involved in developing machine learning models for healthcare applications.

The insights gained from this model underscore the critical importance of rigorous model evaluation, refinement, and validation in the healthcare domain. Such measures are indispensable in ensuring that models meet the high standards of accuracy and reliability required for medical image classification tasks.

Considering the central role of medical diagnostics, accepting a model with the existing performance metrics is not feasible. Consequently, our commitment is to pursue a path of unwavering model evaluation, enhancement, and validation before extending the use of machine learning models in healthcare applications.

Building a VGG-19 Model

The VGG-19 architecture represents a significant milestone in deep learning, particularly in the domain of *image classification*. Extending the VGG-16 model, VGG-19 is composed of 19 layers, diligently structured to include convolutional layers for feature extraction, max-pooling layers for down-sampling, and fully connected layers for classification.

A unique feature of VGG-19 is its consistent use of **3x3 filters** across all convolutional layers. This design choice not only reduces the number of parameters but also ensures exceptional performance. VGG-19 has undergone rigorous validation and consistently achieves state-of-the-art results on benchmark datasets like ImageNet.

Beyond image classification, VGG-19 finds application in various computer vision tasks. It serves as a pre-trained model for transfer learning and has been customized for specialized tasks such as object detection and segmentation.

In this phase, we aim to construct a specialized VGG-19 model for binary classification tasks. We utilize the **VGG-19 pre-trained model** as a feature extractor, augmenting it with additional layers tailored for binary classification. The subsequent sections will clarify the core components of our custom model and explore avenues for optimization.

Main Key Components of the model include:

VGG-19 Base Model

Our model's foundation is built upon the VGG-19 pre-trained architecture. However, we've judiciously pruned away its top fully connected layers, retaining the convolutional and pooling layers. This decision transforms VGG-19 into a potent feature extractor. By removing the classification layers, we leverage the power of VGG-19's learned feature representations without the risk of task-specific bias. This architectural choice empowers our model to understand and extract intricate features from input images, forming the backbone for robust binary classification.

Pooling Layer

Flexibility is a hallmark of our model's design, and this is evident in our pooling layer. Users can tailor the pooling operation to their specific needs, choosing between 'max' or 'average' pooling through the pooling argument. Max pooling focuses on the most salient features, while average pooling provides a more comprehensive view. This adaptability enables users to fine-tune the feature extraction process according to their unique dataset characteristics and classification requirements.

Dense Layer

Positioned after the pooling layer, our dense layer offers a crucial bridge to the final classification. Its parameters are customizable, granting users the ability to adjust the number of units (default is 512) and the activation function (default is ***'ReLU'***). This layer synthesizes the rich features extracted earlier into a form conducive to binary classification. The ability to tweak its architecture empowers users to tailor the model's capacity to their specific problem, accommodating both complex and simpler tasks.

Batch Normalization

A batch normalization layer is thoughtfully inserted after the dense layer. This layer plays a vital role in stabilizing the training process by normalizing the activations. It ensures that the model learns robustly and converges efficiently. By mitigating internal covariate shift, batch normalization contributes to quicker training and better overall model performance, especially when dealing with deep architectures.

Dropout Layer

Overfitting is a common concern in deep learning. To address this, our model includes a dropout layer with a customizable rate (default is 20%). Dropout is an ingenious regularization technique that helps mitigate the risk of overfitting by randomly deactivating a fraction of neurons during training. This 'dropout' introduces an element of uncertainty into the model, effectively preventing it from relying too heavily on any one feature. The degree of dropout can be adjusted, offering users control over the model's regularization strength.

Output Layer

At the apex of our model lies the output layer, carefully crafted for binary classification tasks. It employs a sigmoid activation function, which is ideal for binary decisions. This layer outputs a probability score between 0 and 1, representing the model's confidence in classifying input images as either one class or the other. It's the final piece of the puzzle that transforms extracted features into actionable classification results.

Flexibility

Our model's architecture is highly adaptable, thanks to a range of customizable function arguments. This flexibility caters to a wide array of use cases and requirements, from straightforward binary classification tasks to more complex scenarios. Users can fine-tune the model's behavior to align precisely with their specific problem domain, striking the right balance between simplicity and sophistication.

Enhancements and Customizations encompass:

Model Compilation

The model compilation phase within the enhancements and customizations category serves as a pivotal step in configuring the neural network for training. In this context, the function lays the groundwork by defining the model's architecture and structure, but it refrains from compiling it. Instead, users are granted the autonomy to compile the model independently, granting them full control over essential training parameters. This separation of responsibilities permits users to tailor the optimization process, choosing the optimizer that aligns best with their specific problem, specifying the appropriate loss function for their task, and selecting evaluation metrics that accurately gauge model performance. Such flexibility in the compilation phase is particularly beneficial when addressing diverse machine learning challenges.

Detailed Documentation

Comprehensive documentation plays a paramount role in enhancing the usability and understandability of any software component, and the inclusion of detailed documentation is a key facet of the enhancements and customizations integrated into this model. In this context, the function boasts an extensive docstring and strategically placed comments throughout its code. This thorough documentation aims to provide users with clear, concise, and readily accessible information about the function's functionality, parameters, and usage. By offering a rich source of guidance and insights, the documentation ensures that users can effectively leverage the model construction function, even if they have limited prior experience with its intricacies.

Regularization

Effective regularization techniques are indispensable for preventing overfitting in deep neural networks. Within the realm of enhancements and customizations, the incorporation of L2 regularization into the dense layer emerges as a crucial facet of the model's design. *L2 regularization*, also known as weight decay, imposes a penalty on the magnitude of the weights in the dense layer. This penalty discourages excessively large weight values, curbing the model's tendency to fit noise in the training data. By allowing users to customize the strength of this regularization through function parameters, the model provides a mechanism for achieving a balance between fitting the training data well and maintaining generalizability to unseen data. This feature contributes significantly to the model's adaptability to different datasets and tasks, bolstering its performance and robustness.

Return Values

The utility of a machine learning model extends beyond its training and construction phases, often involving various downstream tasks such as evaluation, inference, or integration into larger systems. Acknowledging this, the enhancements and customizations in the model construction function encompass the provision of return values that hold significant practical value. Specifically, the function returns both the base VGG-19 model and the final binary classification model. This dual return enables users to choose the model variant best suited to their particular use case. The base VGG-19 model, which incorporates the pre-trained architecture, can be harnessed for tasks requiring feature extraction or as a starting point for transfer learning. Conversely, the final binary classification model, enriched with task-specific layers, stands ready for deployment in binary classification scenarios. This flexibility empowers users to seamlessly integrate the model into their machine learning pipelines, adapting it to their unique requirements and objectives.

Parameter Validation

While not currently implemented, future iterations of the model construction function may introduce parameter validation mechanisms, thus further augmenting its robustness and usability. These validation steps would serve as safeguards, ensuring that user-defined function arguments adhere to specific criteria or constraints. For instance, the validation process could encompass checks to confirm the validity of selected activation functions, guarantee that dropout rates fall within the permissible range of 0 to 1, or assess the compatibility of chosen parameters with the model's architecture. By implementing such validations, the function aims to reduce the risk of inadvertent misconfigurations, enhance user experience, and contribute to the overall reliability and stability of the model construction process.

Incorporating Callbacks to Enhance VGG-19 Model Training

In this section, we explore the integration of ***Keras Callbacks*** into our model training process, a strategic decision aimed at improving training efficiency and effectiveness. These callbacks actively monitor specific metrics during training and trigger adjustments to the model or training process based on observed values.

The core of our strategy lies in the careful configuration of our Keras Callbacks:

Early Stopping

This callback is designed to scrutinize the validation loss (*val_loss*) during training. If, for 10 consecutive epochs, no improvement in validation loss is observed, the training process is terminated. Early Stopping serves as a crucial mechanism for averting overfitting and ensuring that the model generalizes effectively to new data. Furthermore, this callback reverts to the best model weights encountered during training, guaranteeing the use of the most optimal model up to that point.

Reduce Learning Rate on Plateau

This callback also closely monitors the validation loss (*val_loss*). In cases where no improvement is detected for 5 consecutive epochs, the learning rate is dynamically reduced by a factor of 0.1. This adaptive learning rate mechanism aids the model in overcoming local minima or

accelerating convergence. Importantly, the learning rate is constrained to never fall below a specified lower bound, ensuring stability and preventing excessive reductions.

Model Checkpoints

Incorporating the *ModelCheckpoint* callback into our training strategy serves a dual purpose: it optimizes the storage of model weights and enhances the overall training efficiency. This callback streamlines the process of saving model weights to a specified file path, ensuring that these crucial components of the model can be easily retrieved at a later stage. The callback's parameters are meticulously configured to maximize its utility. By setting *monitor = 'val_loss'*, we ensure that the callback triggers weight updates only when there is a discernible improvement in the validation loss, preserving the model's progress. To optimize storage usage, *save_weights_only = True* is enabled, instructing the callback to save only the model's weights without extraneous architecture details. The *mode = 'min'* parameter directs the callback to minimize the monitored metric, specifically the validation loss, ensuring that weight updates are based on achieving a lower validation loss. Lastly, *save_best_only = True* enforces the preservation of only the best weights, determined by the monitored metric. This strategic configuration guarantees access to the most effective model version throughout the training process.

The inclusion of these essential callbacks in our training protocol introduces a valuable layer of adaptability to our model. This adaptability empowers the model to dynamically fine-tune its performance throughout the training process, thereby enhancing its overall efficiency and effectiveness. These callbacks play a pivotal role in ensuring that the model continuously strives for optimal results. It's worth noting that both of these crucial callbacks, **Early Stopping** and **Reduce Learning Rate on Plateau**, are thoughtfully organized within a list called *CALLBACKS*. This list serves as a comprehensive toolkit that significantly contributes to the refinement of our model during the training phase, aligning it more closely with our performance goals.

VGG-19 Model Training Procedure

In this section, we delve into the training procedure of our VGG-19 binary classification model, orchestrated through the function 'train_VGG19_binary_classification_model.' This function plays a pivotal role in our machine learning pipeline and encompasses several key components.

In our VGG-19 binary classification model training procedure, the process begins with the crucial step known as **Model Initialization**. We use the 'build_model' function to initialize the model, which constructs the architecture of our VGG-19 model and ensures it is properly configured with necessary hyperparameters like the learning rate and loss function. With this foundational setup, we establish the groundwork for subsequent training stages. Moving on to **Layer Freezing and Pre-training**, during the early phase of model training, we employ a strategic approach by freezing the trainable parameters of the base VGG-19 model. This strategy ensures that the weights of the pre-trained layers remain static while focusing our training efforts on the newly added layers like dense, dropout, and batch normalization layers.

We give attention to **Batch and Epoch Configuration** in the next stage. Flexibility is a core feature of our model training process, allowing for the fine-tuning of critical training parameters. Specifically, this flexibility enables us to configure both the batch size and the number of training epochs, tailoring the training process to meet the exact performance

requirements of our model. Following this, we discuss **Callbacks** that are integrated into our training regimen. These include Keras callbacks like Early Stopping and Learning Rate Reduction, which act as optimization mechanisms to enhance the training process and promote efficient model convergence.

Turning to **Custom Metrics**, our evaluation of the model's performance extends beyond traditional metrics like accuracy. We monitor a range of custom metrics including precision, recall, and F1 score to gain a comprehensive understanding of the model's behavior and ensure alignment with our objectives. Then, we consider Verbose Output, which provides real-time insights through detailed logging during the training process. This feature is crucial as it allows us to closely monitor the model's progress and make informed decisions regarding any necessary model adjustments.

We reach a critical moment in the **Final Training Phase**, where the base VGG-19 layers are unfrozen to allow for full network training. This phase is pivotal for fine-tuning the entire model for the binary classification task. Lastly, regarding return values, the training process concludes by returning the trained model and history objects named hs_upper_layers and hs_full_network. These objects encapsulate the training progress and serve as vital resources for further model evaluation and in-depth analysis. Through the integration of these diverse functionalities, the function 'train_VGG19_binary_classification_model' emerges as a holistic and versatile solution for training our VGG-19 binary classification model. It effectively manages all these critical elements to provide a comprehensive training solution that optimizes the model's performance and ensures its readiness for real-world binary classification tasks.

VGG-19 Model Training Procedure

The Two Phases: Upper Layers and Full Network

Furthermore, our approach to training the VGG-19 binary classification model entails **two distinct phases**: the training of the **Upper Layers** and the training of **the Full Network**. Each phase is thoughtfully designed to fulfill specific objectives and collectively contribute to the model's overall performance. In the subsequent sections, we delve deeper into the rationale behind this two-phase training strategy and its implications.

Two-Phase Model Training: A Strategic Approach for Optimal Performance

Our model training unfolds in two distinct phases, each carefully designed to enhance its capabilities for binary classification.

Phase 1: Upper Layers Training

Our model training unfolds in two distinct phases, each carefully designed to enhance its capabilities for binary classification. The first phase is known as **Phase 1: Upper Layers Training**, which centers on the training of newly introduced layers like dense, dropout, and batch normalization layers that are stacked atop the pre-trained VGG-19 model. During this initial phase, several key strategies are employed to optimize the model. The first strategy is **Base Model Freezing**, where we focus on training the newly added layers while keeping the base

VGG-19 model's parameters fixed. We achieve this by setting the trainable parameters in the base VGG-19 model to 'False.'

The next strategy is **Targeted Learning**, wherein the emphasis is on rapid and focused learning for the task-specific layers we introduced. These layers start with random weights, and swift convergence is essential for them to effectively extract relevant features from the data. Quick adaptation becomes crucial for these layers to handle the binary classification task adeptly. The final strategy in this phase is **High Learning Rate**, where we apply a higher learning rate to expedite the convergence of the newly added layers, facilitating their faster adaptation to the specific classification task.

Phase 2: Full Network Training

The second part of our training strategy is Phase 2: Full Network Training. Having primed the upper layers, we transition to this phase, where the entire network undergoes fine-tuning. This phase also incorporates several strategic actions to optimize the model's performance. The first action is Unfreezing Base Model, which involves unfreezing the trainable parameters in the base VGG-19 model by setting them to 'True.' This change enables backpropagation through the entire network, allowing for adjustments to both the pre-trained and newly added layers.

The second action is the commonly known **Fine-Tuning**. With the base model unfrozen and the upper layers well-initialized, we engage in the fine-tuning of the entire network. This process aims to enhance the model's adaptability to the specific binary classification task. The last action in this phase is **Low Learning Rate**, where we employ a lower learning rate to ensure that the model makes minor adjustments to its weights without losing valuable features. This lower rate helps to preserve the knowledge gained during the initial training phases while allowing for subtle refinements. This two-phase training strategy optimizes our model's performance, empowering it to excel in binary classification tasks while preserving the valuable insights drawn from the base VGG-19 architecture.

Maximizing Model Efficiency and Performance: The Dual-Phase Advantage

Our adoption of a two-phase training approach confers several substantial benefits to our binary classification model, setting the stage for enhanced efficiency and performance:

As we delve deeper into the benefits of our two-phase training strategy, several key advantages come to light. First, Enhanced Efficiency is a notable benefit, as the two-phase strategy often accelerates the model's training process and substantially reduces the demand for computational resources. Compared to training the entire network from scratch, this approach speeds up convergence and minimizes resource-intensive computations. Next, Precision in Optimization is another hallmark of our approach. By segmenting the training into two distinct phases, we facilitate precise model optimization. The initial phase concentrates on rapid and task-oriented learning, allowing the model to adapt quickly to the binary classification task. During the fine-tuning phase, nuanced adjustments further refine the model's performance, ensuring that it excels in its specific mission.

Lastly, Overfitting Mitigation is a significant advantage, especially valuable when dealing with limited or non-diverse datasets. Leveraging a pre-trained model as the foundation and then fine-tuning it mitigates the risk of overfitting. The model's prior knowledge, gained from extensive training on general image recognition tasks, is adapted to the nuances of our binary

classification problem, reducing the likelihood of overfitting and enhancing the model's ability to generalize effectively.

Through the cautious orchestration of these phases, our two-phase training approach harmoniously combines the inherent feature extraction prowess of the pre-trained VGG-19 model with the task-specific adaptability of the freshly introduced layers. The result is a model poised to deliver exceptional binary classification performance while conserving the valuable insights distilled from the VGG-19 architecture.

VGG-19 Model Training Execution and Time Monitoring

In this section, we elucidate the critical steps involved in the training process of our VGG-19 binary classification model. To commence, Start Time plays a vital role as the training process initiates by capturing the current system time. This timestamp serves as a reference point for monitoring the duration of the training, thus acting as a fundamental metric to gauge time efficiency. Moving on to Model Training, the cornerstone of this section is the 'train_VGG19_binary_classification_model' function. This function is responsible for orchestrating the comprehensive training of our VGG-19 model, seamlessly managing both the initial focus on the upper layers and the subsequent fine-tuning of the entire network. Essential parameters such as augmented training data, preprocessed validation data, the number of epochs, and crucial callbacks are input during this pivotal stage.

Next, we discuss Callbacks, where our training strategy leverages various Keras callbacks including Early Stopping and Learning Rate Reduction. These mechanisms serve dual purposes: they enhance training efficiency by preventing unnecessary epochs and preserve the best-performing model by retaining the one with the minimum validation loss. This ensures that the model is continuously fine-tuned towards optimal performance. As we near the end of the training process, End Time becomes a focal point. Recording the current system time at this juncture allows us to compute the total duration required for training, offering valuable insights into the temporal aspects vital for resource planning and management. Lastly, Elapsed Time is calculated and presented as the final step. This metric offers indispensable information regarding the computational resources consumed during training, enabling accurate gauging of its efficiency and demands.

By intricately weaving these elements into the training process, we construct a comprehensive and efficient strategy, thereby ensuring our VGG-19 binary classification model is primed for real-world tasks.

Observations

After completing the training process, it is crucial to conduct a thorough analysis of the results. Below, we highlight significant observations based on the provided screenshot, which illustrates the epoch performance:

```
80134624/80134624 [==============================] - 3s 0us/step
Epoch 1/5
461/461 [==============================] - 704s 1s/step - loss: 4.6213 - precision: 0.5438 - recall: 0.5487 - bin_accuracy: 0.6316 - auc_r
oc: 0.6626 - cohen_kappa: 0.2362 - val_loss: 3.6804 - val_precision: 0.7304 - val_recall: 0.3224 - val_bin_accuracy: 0.6781 - val_auc_roc:
0.7282 - val_cohen_kappa: 0.2655 - lr: 1.0000e-04
Epoch 2/5
461/461 [==============================] - 723s 2s/step - loss: 3.1356 - precision: 0.6163 - recall: 0.5327 - bin_accuracy: 0.6772 - auc_r
oc: 0.7147 - cohen_kappa: 0.3147 - val_loss: 2.6666 - val_precision: 0.6755 - val_recall: 0.5143 - val_bin_accuracy: 0.7039 - val_auc_roc:
0.7495 - val_cohen_kappa: 0.3606 - lr: 1.0000e-04
Epoch 3/5
461/461 [==============================] - 682s 1s/step - loss: 2.3898 - precision: 0.6297 - recall: 0.5388 - bin_accuracy: 0.6856 - auc_r
oc: 0.7324 - cohen_kappa: 0.3317 - val_loss: 2.1246 - val_precision: 0.6355 - val_recall: 0.6094 - val_bin_accuracy: 0.7009 - val_auc_roc:
0.7484 - val_cohen_kappa: 0.3748 - lr: 1.0000e-04
Epoch 4/5
461/461 [==============================] - 623s 1s/step - loss: 1.9326 - precision: 0.6467 - recall: 0.5605 - bin_accuracy: 0.6987 - auc_r
oc: 0.7432 - cohen_kappa: 0.3607 - val_loss: 1.7899 - val_precision: 0.7840 - val_recall: 0.3452 - val_bin_accuracy: 0.6970 - val_auc_roc:
0.7524 - val_cohen_kappa: 0.3085 - lr: 1.0000e-04
Epoch 5/5
461/461 [==============================] - 638s 1s/step - loss: 1.6244 - precision: 0.6526 - recall: 0.5544 - bin_accuracy: 0.7007 - auc_r
oc: 0.7457 - cohen_kappa: 0.3631 - val_loss: 1.5053 - val_precision: 0.6104 - val_recall: 0.6820 - val_bin_accuracy: 0.6956 - val_auc_roc:
0.7633 - val_cohen_kappa: 0.3797 - lr: 1.0000e-04

----------------------------------------------------------------
Finished training upper layers of the custom VGG-19-based model.
----------------------------------------------------------------
```

```
Epoch 1/15
461/461 [==============================] - 685s 1s/step - loss: 1.4411 - precision: 0.6801 - recall: 0.6100 - bin_accuracy: 0.7264 - auc_r
oc: 0.7804 - cohen_kappa: 0.4224 - val_loss: 1.4132 - val_precision: 0.8575 - val_recall: 0.4612 - val_bin_accuracy: 0.7513 - val_auc_roc:
0.8185 - val_cohen_kappa: 0.4421 - lr: 1.0000e-05
Epoch 2/15
461/461 [==============================] - 720s 2s/step - loss: 1.3567 - precision: 0.7561 - recall: 0.6195 - bin_accuracy: 0.7655 - auc_r
oc: 0.8192 - cohen_kappa: 0.4985 - val_loss: 1.3279 - val_precision: 0.7435 - val_recall: 0.6578 - val_bin_accuracy: 0.7700 - val_auc_roc:
0.8301 - val_cohen_kappa: 0.5135 - lr: 1.0000e-05
Epoch 3/15
461/461 [==============================] - 662s 1s/step - loss: 1.2963 - precision: 0.7704 - recall: 0.6483 - bin_accuracy: 0.7798 - auc_r
oc: 0.8376 - cohen_kappa: 0.5309 - val_loss: 1.2892 - val_precision: 0.8365 - val_recall: 0.5694 - val_bin_accuracy: 0.7810 - val_auc_roc:
0.8385 - val_cohen_kappa: 0.5207 - lr: 1.0000e-05
Epoch 4/15
461/461 [==============================] - 665s 1s/step - loss: 1.2448 - precision: 0.7874 - recall: 0.6701 - bin_accuracy: 0.7936 - auc_r
oc: 0.8517 - cohen_kappa: 0.5609 - val_loss: 1.2427 - val_precision: 0.8666 - val_recall: 0.5832 - val_bin_accuracy: 0.7953 - val_auc_roc:
0.8484 - val_cohen_kappa: 0.5514 - lr: 1.0000e-05
Epoch 5/15
461/461 [==============================] - 666s 1s/step - loss: 1.2030 - precision: 0.7993 - recall: 0.6777 - bin_accuracy: 0.8010 - auc_r
oc: 0.8593 - cohen_kappa: 0.5765 - val_loss: 1.2215 - val_precision: 0.8705 - val_recall: 0.5671 - val_bin_accuracy: 0.7910 - val_auc_roc:
0.8526 - val_cohen_kappa: 0.5401 - lr: 1.0000e-05
Epoch 6/15
461/461 [==============================] - 668s 1s/step - loss: 1.1673 - precision: 0.8028 - recall: 0.6852 - bin_accuracy: 0.8048 - auc_r
oc: 0.8639 - cohen_kappa: 0.5848 - val_loss: 1.1811 - val_precision: 0.8501 - val_recall: 0.6061 - val_bin_accuracy: 0.7976 - val_auc_roc:
0.8510 - val_cohen_kappa: 0.5594 - lr: 1.0000e-05
Epoch 7/15
461/461 [==============================] - 658s 1s/step - loss: 1.1318 - precision: 0.8063 - recall: 0.6924 - bin_accuracy: 0.8085 - auc_r
oc: 0.8703 - cohen_kappa: 0.5931 - val_loss: 1.2471 - val_precision: 0.9244 - val_recall: 0.4645 - val_bin_accuracy: 0.7683 - val_auc_roc:
0.8506 - val_cohen_kappa: 0.4770 - lr: 1.0000e-05
Epoch 8/15
461/461 [==============================] - 652s 1s/step - loss: 1.0966 - precision: 0.8126 - recall: 0.7028 - bin_accuracy: 0.8144 - auc_r
oc: 0.8773 - cohen_kappa: 0.6061 - val_loss: 1.1880 - val_precision: 0.9043 - val_recall: 0.5116 - val_bin_accuracy: 0.7808 - val_auc_roc:
0.8374 - val_cohen_kappa: 0.5106 - lr: 1.0000e-05
Epoch 9/15
461/461 [==============================] - 662s 1s/step - loss: 1.0628 - precision: 0.8237 - recall: 0.7176 - bin_accuracy: 0.8238 - auc_r
oc: 0.8837 - cohen_kappa: 0.6264 - val_loss: 1.1046 - val_precision: 0.8528 - val_recall: 0.6114 - val_bin_accuracy: 0.8003 - val_auc_roc:
0.8550 - val_cohen_kappa: 0.5656 - lr: 1.0000e-05
Epoch 10/15
461/461 [==============================] - 649s 1s/step - loss: 1.0365 - precision: 0.8297 - recall: 0.7196 - bin_accuracy: 0.8270 - auc_r
oc: 0.8854 - cohen_kappa: 0.6330 - val_loss: 1.0680 - val_precision: 0.8638 - val_recall: 0.6329 - val_bin_accuracy: 0.8113 - val_auc_roc:
0.8631 - val_cohen_kappa: 0.5906 - lr: 1.0000e-05
Epoch 11/15
461/461 [==============================] - 644s 1s/step - loss: 1.0013 - precision: 0.8353 - recall: 0.7283 - bin_accuracy: 0.8322 - auc_r
oc: 0.8934 - cohen_kappa: 0.6442 - val_loss: 1.1212 - val_precision: 0.9172 - val_recall: 0.5136 - val_bin_accuracy: 0.7847 - val_auc_roc:
0.8601 - val_cohen_kappa: 0.5189 - lr: 1.0000e-05
Epoch 12/15
461/461 [==============================] - 647s 1s/step - loss: 0.9725 - precision: 0.8361 - recall: 0.7321 - bin_accuracy: 0.8338 - auc_r
oc: 0.8977 - cohen_kappa: 0.6478 - val_loss: 1.0570 - val_precision: 0.8908 - val_recall: 0.5788 - val_bin_accuracy: 0.8011 - val_auc_roc:
0.8596 - val_cohen_kappa: 0.5624 - lr: 1.0000e-05
Epoch 13/15
461/461 [==============================] - 647s 1s/step - loss: 0.9516 - precision: 0.8344 - recall: 0.7429 - bin_accuracy: 0.8365 - auc_r
oc: 0.8997 - cohen_kappa: 0.6545 - val_loss: 1.0290 - val_precision: 0.8910 - val_recall: 0.5718 - val_bin_accuracy: 0.7987 - val_auc_roc:
0.8660 - val_cohen_kappa: 0.5564 - lr: 1.0000e-05
Epoch 14/15
461/461 [==============================] - 645s 1s/step - loss: 0.9167 - precision: 0.8423 - recall: 0.7512 - bin_accuracy: 0.8427 - auc_r
oc: 0.9082 - cohen_kappa: 0.6675 - val_loss: 0.9793 - val_precision: 0.8453 - val_recall: 0.6612 - val_bin_accuracy: 0.8142 - val_auc_roc:
0.8697 - val_cohen_kappa: 0.6002 - lr: 1.0000e-05
Epoch 15/15
461/461 [==============================] - 646s 1s/step - loss: 0.8898 - precision: 0.8491 - recall: 0.7594 - bin_accuracy: 0.8482 - auc_r
oc: 0.9126 - cohen_kappa: 0.6794 - val_loss: 1.0561 - val_precision: 0.9236 - val_recall: 0.5321 - val_bin_accuracy: 0.7931 - val_auc_roc:
0.8665 - val_cohen_kappa: 0.5390 - lr: 1.0000e-05

--------------------------------------------------------------------------------
Finished training the full custom VGG-19-based model.
--------------------------------------------------------------------------------

Total time for training: 13420 seconds.
```

VGG-19 Model Summary Interpretation

The *vgg19_model.summary()* function provides an extensive overview of our VGG-19 binary classification model's architecture, offering valuable insights into its composition:

Layer (type): This column specifies the type of each layer within the network. Our model comprises several key components:

- **VGG-19 Base Model Layers:** These layers are inherited from the pre-trained VGG-19 model and encompass *Conv2D layers* for *2D convolutions* and *MaxPool2D layers* for max-pooling. They handle the initial stages of feature extraction.
- **Dense:** Included for our binary classification task, this fully connected layer contains 512 units and employs a *ReLU activation function*.
- **BatchNormalization:** A BatchNormalization layer has been incorporated to standardize the activations derived from the dense layer.
- **Dropout:** To mitigate overfitting, we've introduced a Dropout layer with a rate of 0.2, randomly deactivating a fraction of input units during training.
- **Output:** Serving as the output layer for binary classification, this final Dense layer utilizes a sigmoid activation function.

Output Shape: This section details the dimensions of the output from each layer, facilitating an understanding of how feature map dimensions evolve as data progresses through the network.

Param #: Here, the number of trainable parameters for each layer is displayed, providing an indication of the model's complexity. A higher parameter count may imply a greater risk of overfitting.

Total Params: This metric encompasses the total count of trainable and non-trainable parameters, offering a comprehensive measure of the model's size and computational demands.

Trainable Params: It specifies the quantity of parameters slated for updates during training, encompassing both the base VGG-19 model and the supplementary layers introduced for binary classification.

Non-trainable Params: These parameters remain static during training, typically including those from the VGG-19 model during the initial training phase. This division aids in preserving the knowledge encoded in the pre-trained base while adapting it for our specific task.

```
Model: "model"
_________________________________________________________________
 Layer (type)                Output Shape              Param #
=================================================================
 input_1 (InputLayer)        [(None, 224, 224, 3)]     0

 block1_conv1 (Conv2D)       (None, 224, 224, 64)      1792

 block1_conv2 (Conv2D)       (None, 224, 224, 64)      36928

 block1_pool (MaxPooling2D)  (None, 112, 112, 64)      0

 block2_conv1 (Conv2D)       (None, 112, 112, 128)     73856

 block2_conv2 (Conv2D)       (None, 112, 112, 128)     147584

 block2_pool (MaxPooling2D)  (None, 56, 56, 128)       0

 block3_conv1 (Conv2D)       (None, 56, 56, 256)       295168

 block3_conv2 (Conv2D)       (None, 56, 56, 256)       590080

 block3_conv3 (Conv2D)       (None, 56, 56, 256)       590080

 block3_conv4 (Conv2D)       (None, 56, 56, 256)       590080

 block3_pool (MaxPooling2D)  (None, 28, 28, 256)       0

 block4_conv1 (Conv2D)       (None, 28, 28, 512)       1180160

 block4_conv2 (Conv2D)       (None, 28, 28, 512)       2359808

 block4_conv3 (Conv2D)       (None, 28, 28, 512)       2359808

 block4_conv4 (Conv2D)       (None, 28, 28, 512)       2359808

 block4_pool (MaxPooling2D)  (None, 14, 14, 512)       0

 block5_conv1 (Conv2D)       (None, 14, 14, 512)       2359808

 block5_conv2 (Conv2D)       (None, 14, 14, 512)       2359808

 block5_conv3 (Conv2D)       (None, 14, 14, 512)       2359808

 block5_conv4 (Conv2D)       (None, 14, 14, 512)       2359808

 block5_pool (MaxPooling2D)  (None, 7, 7, 512)         0

 global_max_pooling2d (Glob  (None, 512)               0
 alMaxPooling2D)

 Dense-1 (Dense)             (None, 512)               262656

 BatchNormalization-1 (Batc  (None, 512)               2048
 hNormalization)

 Dropout-1 (Dropout)         (None, 512)               0

 Output (Dense)              (None, 1)                 513

=================================================================
Total params: 20289601 (77.40 MB)
Trainable params: 20288577 (77.39 MB)
Non-trainable params: 1024 (4.00 KB)
_________________________________________________________________
```

Figure 26. Summary Statistics of the VGG-19 Model

Observations Based on Model Summary

Upon thorough examination of the VGG-19 model summary, several noteworthy insights emerge:

- **Model Architecture:** The *vgg19_model* is evidently built upon the VGG-19 architecture, a widely employed convolutional neural network (CNN) within the realm of computer vision. This architecture boasts an impressive 19 layers, comprising 16 convolutional layers and 3 fully connected layers, each endowed with learnable weights.

- **Input Layer:** The model anticipates input images with dimensions of *224×224 pixels* and 3 color channels (*RGB*). This standardization ensures that images fed into the network conform to the prescribed format.

- **Convolutional Blocks:** The model is structured into five distinct convolutional blocks, each progressively growing in complexity. *Block 1* comprises two Conv2D layers, each hosting 64 filters, followed by a MaxPooling layer. *Block 2* mirrors this pattern with two Conv2D layers but employs 128 filters, accompanied by MaxPooling. *Block 3* escalates the complexity with four Conv2D layers featuring 256 filters, ultimately incorporating MaxPooling. *Block 4* sustains the trend with four Conv2D layers, utilizing 512 filters, followed by MaxPooling. Finally, *Block 5* adheres to the established structure with four Conv2D layers and 512 filters, culminating in MaxPooling. Remarkably, these Conv2D layers consistently employ a (3 × 3) kernel size throughout the architecture.

- **Global Max Pooling Layer:** This layer serves to distill each feature map into a singular value, enhancing the model's resilience against spatial translations.

- **Fully Connected Layers:** The architecture incorporates a fully connected layer labeled as 'Dense-1,' boasting 512 units. Following this, a 'BatchNormalization-1' layer normalizes activations, contributing to quicker and more stable training. A 'Dropout-1' layer is also implemented to selectively drop nodes during training, an effective countermeasure against overfitting.

- **Output Layer:** The output layer consists of a single neuron, indicative of the model's binary classification objective. This neuron likely employs a sigmoid activation function for this purpose.

- **Parameters:** The model exhibits substantial complexity, encompassing a notable number of parameters. In total, the model encompasses 20, 289, 601 parameters, equivalent to approximately 77.40 MB. Notably, 20, 288, 577 of these parameters, approximately 77.39 MB, are designated as trainable parameters.

The analysis of the VGG-19 model's architecture reveals several key takeaways that provide valuable insights into its design and functionality:

- **Model Complexity:** The VGG-19 model boasts a considerable number of parameters, implying its computational intensity. Nevertheless, this parameter richness affords the capacity to acquire intricate representations.

- **Normalization and Regularization:** The incorporation of Batch Normalization and Dropout layers underscores a deliberate effort to bolster the model's generalization capabilities.

- **Output Shape:** The progressive reduction in output shapes as data traverses through layers strategically channels spatial information into fewer dimensions, optimizing the classification process.

- **Trainable Parameters:** The model primarily consists of trainable parameters, underscoring the necessity for a substantial and diverse dataset to effectively train it.

- **Data Preprocessing:** Given the prescribed input shape, preprocessing actions will likely include resizing images to *224×224 pixels* and standardizing pixel values.

- **Activation Functions:** While not explicitly specified, it is reasonable to infer the utilization of Rectified Linear Unit (*ReLU*) activations in *Conv2D* and *Dense layers*. Furthermore, a sigmoid activation likely governs the output layer, aligning with the binary classification objective.

- **Pooling Strategy:** The model strategically employs *MaxPooling* after each *Conv2D block*, an effective approach for spatial dimension reduction within feature maps.

In summary, the VGG-19 model embodies a deep and intricate architecture tailored for high-performance image classification tasks. However, its depth and parameter richness demand substantial computational resources for both training and inference.

Visualization of VGG-19 Model Architecture

Utilizing the *plot_model* function, we can generate a visual representation of the model's architecture. This graphical depiction serves as a valuable asset for presentations and documentation purposes. By specifying parameters such as '*to_file*', '*show_shapes*', and '*show_layer_names*', we can customize the visualization to include shape information and layer names as needed. This graphical overview offers an intuitive insight into how data traverses through different layers and operations within the model.

Here is an illustrative example of the generated diagram:

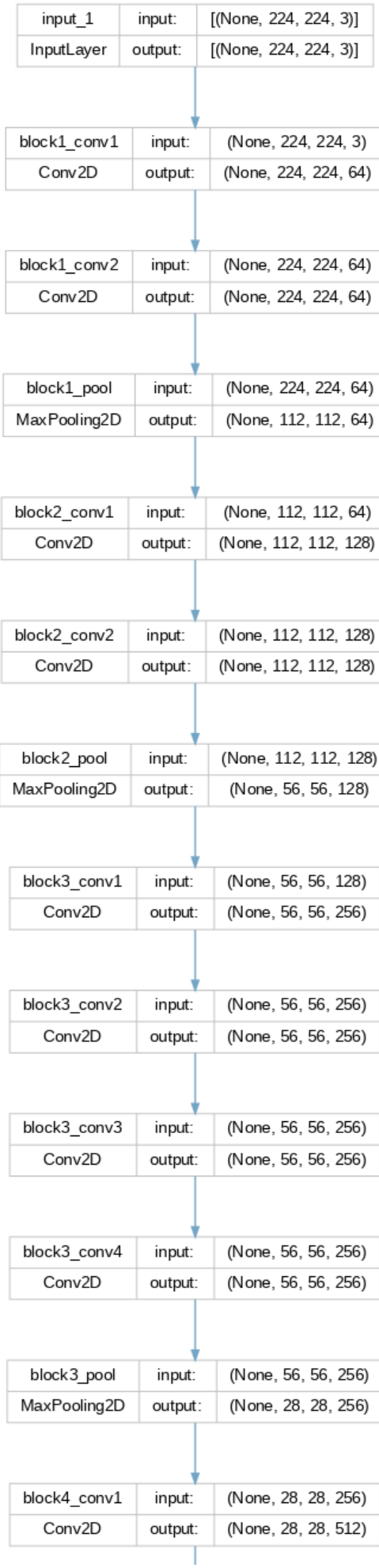
input_1 | input: | [(None, 224, 224, 3)]
InputLayer | output: | [(None, 224, 224, 3)]
block1_conv1 | input: | (None, 224, 224, 3)
Conv2D | output: | (None, 224, 224, 64)
block1_conv2 | input: | (None, 224, 224, 64)
Conv2D | output: | (None, 224, 224, 64)
block1_pool | input: | (None, 224, 224, 64)
MaxPooling2D | output: | (None, 112, 112, 64)
block2_conv1 | input: | (None, 112, 112, 64)
Conv2D | output: | (None, 112, 112, 128)
block2_conv2 | input: | (None, 112, 112, 128)
Conv2D | output: | (None, 112, 112, 128)
block2_pool | input: | (None, 112, 112, 128)
MaxPooling2D | output: | (None, 56, 56, 128)
block3_conv1 | input: | (None, 56, 56, 128)
Conv2D | output: | (None, 56, 56, 256)
block3_conv2 | input: | (None, 56, 56, 256)
Conv2D | output: | (None, 56, 56, 256)
block3_conv3 | input: | (None, 56, 56, 256)
Conv2D | output: | (None, 56, 56, 256)
block3_conv4 | input: | (None, 56, 56, 256)
Conv2D | output: | (None, 56, 56, 256)
block3_pool | input: | (None, 56, 56, 256)
MaxPooling2D | output: | (None, 28, 28, 256)
block4_conv1 | input: | (None, 28, 28, 256)
Conv2D | output: | (None, 28, 28, 512)

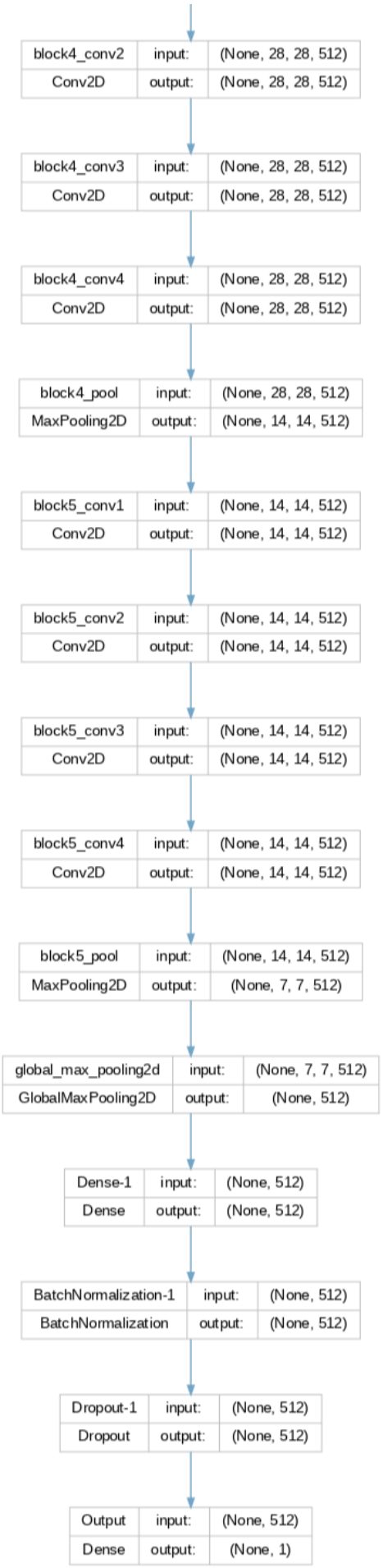

Figure 27. Visualization of VGG-19 Model Architecture

Executing this command will produce a PNG image illustrating the model's architecture. It provides a visual representation of the tensors' shapes between layers and labels each layer for clarity. This diagram serves practical purposes, including debugging and sharing your model structure effectively with collaborators and stakeholders.

VGG-19 Model Evaluation

During the Model Evaluation phase, our attention transitions from training the model to evaluating its performance. Our goal is to understand how effectively the model can make predictions on new and unseen data. This evaluation involves scrutinizing the model's behavior during training and its subsequent performance in making predictions.

Learning Curves: A Diagnostic Tool

Utilizing learning curves as a diagnostic tool is essential for assessing the performance of our neural network model. These curves graphically represent training and validation metrics, typically involving metrics like loss or accuracy, across the training epochs. This visual representation serves several critical purposes:

- **Detecting Underfitting or Overfitting:** Learning curves enable us to identify potential issues with the model's performance. If the model excels on the training data but struggles on the validation data, it's likely overfitting. Conversely, if it performs poorly on both datasets, it might be underfitting.

- **Assessing Model Complexity:** The steepness of the learning curves provides insights into the model's complexity and how quickly it learns. A very steep curve might indicate rapid learning but could also signify overfitting.

- **Determining Convergence:** By observing where the curves stabilize, we can gauge the number of epochs required for effective training. This helps in optimizing the training process.

To effectively visualize learning curves, we've developed a custom function, *'plot_history*'. This function takes the training history, the number of epochs, and the metric of interest ('loss' or 'accuracy') as inputs. It starts by configuring plot settings for an appealing visual presentation. Next, it plots both training and validation curves for the chosen metric, offering insights into the model's performance over epochs. To enhance readability, the function customizes axes with appropriate limits, labels, and ticks. Finally, the resulting learning curve plot is saved in SVG format, ensuring high-quality figures for model evaluation and comparison, making it an invaluable tool in our analysis.

Model Evaluation and Learning Curves

Within this section, we delve into the performance metrics of our trained Convolutional Neural Network (CNN) model. Our primary focus centers around evaluating two crucial metrics: Loss and Accuracy. These metrics provide vital insights into the model's effectiveness and performance.

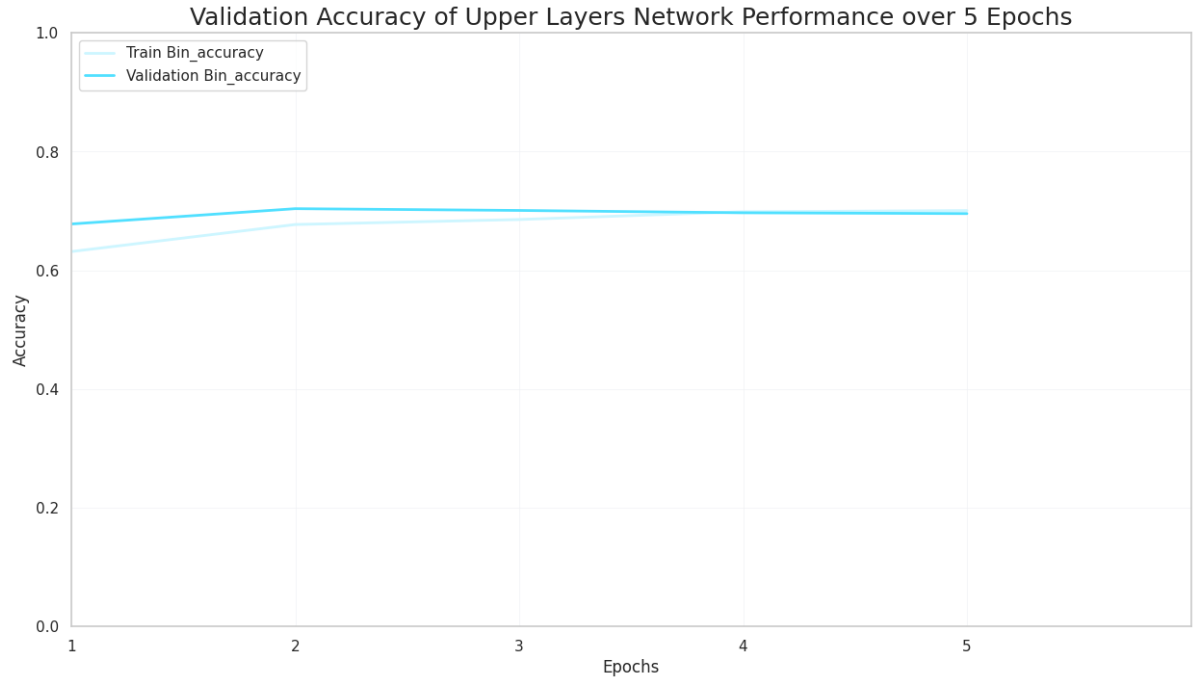

Figure 28. Validation Accuracy of Upper Layers Network Performances over 5 Epochs

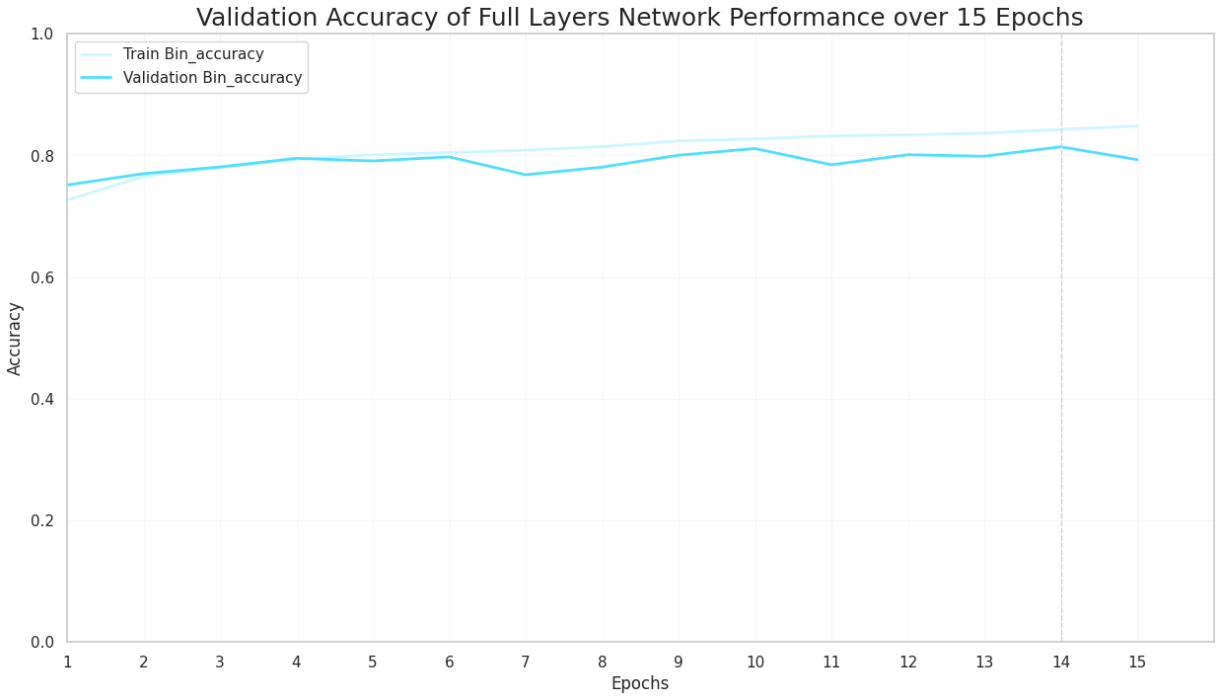

Figure 29. Validation Accuracy of Full Layers Network Performance over 15 Epochs

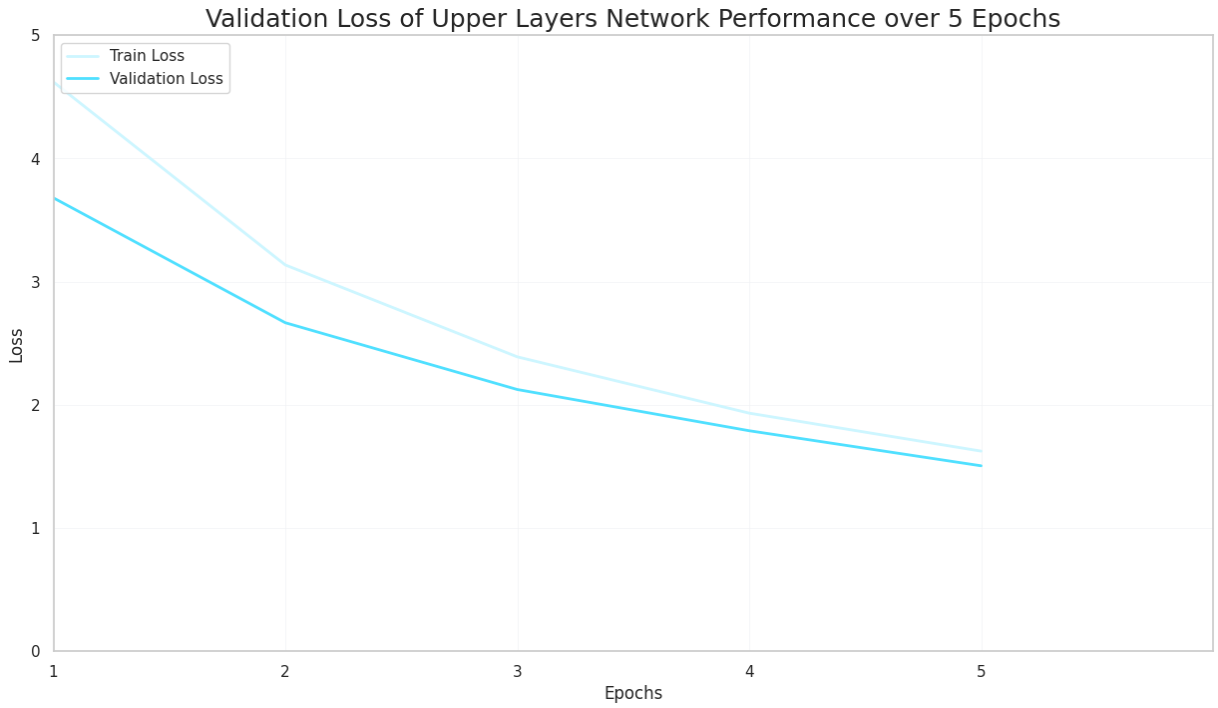

Figure 30.Validation Loss of Upper Layers Network Performance over 5 Epochs

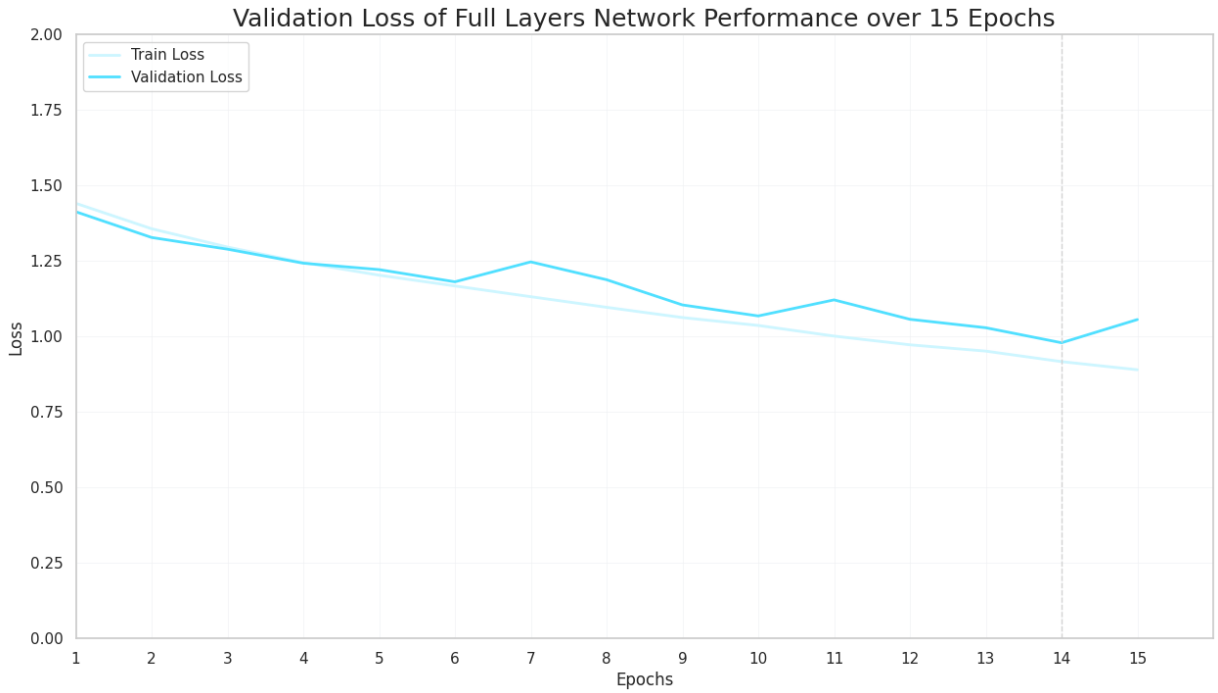

Figure 31. Validation Loss of Full Layers Network Performance over 15 Epochs

VGG-19 Model Training Insights

In this section, we provide insights into the training of our VGG-19 model. We examine key metrics and observations to assess the model's performance and training dynamics.

```
=== Upper Layers Evaluation ===
Train Loss          : 1.62443
Validation Loss     : 1.50525
Train Accuracy      : 0.70071
Validation Accuracy : 0.69560

=== Full Network Evaluation ===
Train Loss          : 0.88982
Validation Loss     : 1.05613
Train Accuracy      : 0.84823
Validation Accuracy : 0.79313
```

Figure 32. Metrics Overview for VGG-19 Model

In terms of **loss of improvement**, the transition from upper layers to the full network is marked by a significant decrease in both training and validation losses, indicating improved fitting to the training data. This is a positive indicator. Moving on to **accuracy improvement**, the accuracy of both training and validation data increases as we transition from the upper layers to the full network. This suggests that the deeper architecture more effectively captures underlying patterns. Lastly for this section, the **generalization gap** shows that the small gap between training and validation accuracy suggests better generalization, indicating that the model can perform well on unseen data.

Furthermore, there is **no sign of overfitting** thanks to regularization and early stopping, the model exhibits no signs of overfitting. The alignment of training and validation metrics indicates a well-generalized model. Focusing on Validation Performance, the validation accuracy after full network training reaches approximately 0.793, signifying strong performance on unseen data. As for Training Efficiency, the model's high training accuracy implies its ability to learn complex representations. Furthermore, its strong generalization, evidenced by the high validation accuracy, is indicative of its capability to perform well on new data. Finally, Loss-Accuracy Correlation reveals that the correspondence between training and validation losses with their respective accuracies suggests a balanced and well-tuned model.

To sum up, the VGG-19 model demonstrates significant improvements in both training and validation metrics. The incorporation of regularization and early stopping has effectively mitigated overfitting, resulting in a well-generalized model. The balance between training and validation performance showcases the model's robustness. Future iterations could focus on hyperparameter tuning and exploring advanced architectures for potential performance enhancements.

VGG Model Evaluation on Test Data

In this section, we present the evaluation results of our trained VGG model on a test dataset. The evaluation is performed using the evaluate method, which takes the preprocessed validation data generator as an argument. The method computes essential metrics such as loss and accuracy. We set verbose=2 to streamline the display of evaluation results without a progress bar. Moving on to **high precision**, the model exhibits a very high precision of 0.922 on the test data. This means that the model correctly identifies a high proportion of positive cases out of the instances it classifies as positive. Regarding **moderate recall**, the recall is 0.565, indicating that the model identifies approximately 56.5% of all actual positive cases. This suggests that there may be room for improvement in capturing all the potential positive cases.

Turning our attention to **strong accuracy**, with an accuracy of 0.809, the model performs well on the test data, correctly classifying around 81% of the instances. This is followed by **excellent Cohen's kappa**, where a Cohen's Kappa of 0.866 suggests excellent agreement between prediction and observation, which is a strong indicator of the model's robustness and reliability. Shifting focus to **balance between precision and recall**, while the model excels in precision, it falls a bit short in recall. It may be worthwhile to investigate techniques that can help balance precision and recall, especially if the application scenario requires a balance of both.

Next, we consider **no signs of overfitting**. The test metrics align well with the training and validation metrics, suggesting that the model generalizes well to new, unseen data. Regularization techniques like dropout and L1/L2 regularization have been applied, and there is no sign of overfitting. Lastly, on the topic of **efficiency**, the model takes around 22 seconds per epoch and 442 milliseconds per step, indicating reasonable computational efficiency. In summary, the VGG-19 model has been evaluated on test data and exhibits strong performance metrics, particularly in precision and accuracy. It also generalizes well to new data, as evidenced by the high Cohen's Kappa score. While the model excels in many aspects, there is room for improvement in recall. Future work could focus on balancing precision and recall and performing further validation to confirm these results.

Evaluating VGG-19 Model Performance Across Different Study Types

In the medical imaging domain, it is critical to assess the model's performance across various types of studies. This is precisely what the function **evaluate_model_by_study_type** aims to do. The function takes in two parameters: the test set (*test_set*) and the model's predictions (predictions). It then adds these predictions as a new column in the test set DataFrame.

Subsequently, the function iterates through each unique type of study present in the test set, such as 'elbow', 'shoulder', etc., and evaluates the model's performance on that particular study type. The function calculates six different evaluation metrics: **Precision**, **Recall**, **F1 Score**, **Accuracy**, **ROC AUC**, and **Cohen's Kappa**. These metrics are crucial for understanding how well the model performs in different scenarios and are standard in the field of medical diagnostics. Each metric is rounded to five decimal places for precision.

By doing so, we get a granular view of the model's efficacy and can identify which types of studies the model excels in and where it might require further optimization. This level of detail is vital for clinical applications where the consequences of a false positive or a false negative can be significant.

Evaluating Model Performance Across Different Study Types Insights

```
1 - Study Type: ELBOW
========================
Precision:          0.95238
Recall:             0.69565
F1 Score:           0.80402
Accuracy:           0.83226
ROC AUC:             0.8308
Cohen's Kappa:      0.66351
========================

2 - Study Type: FINGER
========================
Precision:          0.93913
Recall:             0.43725
F1 Score:           0.59669
Accuracy:            0.7833
ROC AUC:            0.70227
Cohen's Kappa:      0.38853
========================

3 - Study Type: FOREARM
========================
Precision:              1.0
Recall:             0.55629
F1 Score:           0.71489
Accuracy:           0.77741
ROC AUC:            0.77815
Cohen's Kappa:      0.55547
========================

4 - Study Type: HAND
========================
Precision:          0.87838
Recall:             0.34392
F1 Score:            0.4943
Accuracy:           0.76087
ROC AUC:            0.65535
Cohen's Kappa:      0.34221
========================

5 - Study Type: HUMERUS
========================
Precision:          0.86325
Recall:             0.72143
F1 Score:           0.78599
Accuracy:           0.80903
ROC AUC:            0.80666
Cohen's Kappa:      0.61606
========================

6 - Study Type: SHOULDER
========================
Precision:          0.87568
Recall:             0.58273
F1 Score:           0.69978
Accuracy:           0.76311
ROC AUC:            0.75102
Cohen's Kappa:       0.5041
========================

7 - Study Type: WRIST
========================
Precision:          0.94872
Recall:             0.62712
F1 Score:            0.7551
Accuracy:           0.81791
ROC AUC:            0.79982
Cohen's Kappa:      0.61955
========================
```

Figure 33. VGG-19 Model Performance Across Different Study Types

Upon evaluating the model's performance across different study types (Elbow, Finger, Forearm, Hand, Humerus, Shoulder, Wrist) using the enhanced metrics, several valuable insights surface. These insights provide a comprehensive understanding of the model's strengths and weaknesses, particularly in the context of its utilization within MuraMed.

First of all, **precision** measures the proportion of true positive predictions among all positive predictions made by the model. Precision values across study types range from approximately **0.863** to **1.0**, indicating differences in the model's ability to make accurate positive predictions for each category. Although, Forearm Studies excel in precision, indicating nearly no false positives. In contrast, Hand Studies lag, suggesting a higher rate of false positives. **Recall** also is a metric which is also known as sensitivity, measures the proportion of true positive predictions among all actual positive cases. Recall values vary from approximately **0.344** to **0.721** across study types, highlighting differences in the model's ability to identify true positive cases. Elbow Studies lead in capturing true positive cases, while Hand Studies struggle significantly, missing out on a large number of actual positives.

In addition, the **F1** score is the harmonic mean of precision and recall and provides a balanced measure of a model's performance. F1 scores vary from approximately **0.494** to **0.804** across study types, indicating the trade-off between precision and recall. Elbow Studies show the best

balance between precision and recall, as indicated by the highest F1 Score. Hand Studies, however, have the poorest balance, demanding immediate optimization.

The **accuracy** rates measures the overall correctness of the model's predictions. Accuracy values range from approximately **0.760** to **0.832** across study types, reflecting the model's overall performance. Elbow Studies exhibit the highest overall classification accuracy, whereas Hand Studies show the lowest. This implies that the model performs best when classifying elbow images and worst with hand images. While the **Receiver Operating Characteristic Area Under the Curve (ROC AUC)** measures the model's ability to distinguish between positive and negative cases. ROC AUC values vary from approximately **0.655** to **0.831** across study types, indicating differences in the model's discriminatory power. The model is most discriminative in Elbow Studies, as evidenced by the highest ROC AUC. Hand Studies fall short in this regard, possibly indicating an imbalance between the true positive rate and false positive rate.

Finally, Cohen's Kappa measures the agreement between the model's predictions and the actual data while accounting for chance agreement. Cohen's Kappa values range from approximately 0.342 to 0.663 across study types, reflecting differences in the model's agreement with the ground truth. Elbow Studies show the highest level of agreement between observed and predicted classes, while Finger Studies indicate only slight agreement, raising concerns about the model's reliability for finger images.

In conclusion, the evaluation of model performance across different study types, several key insights emerge: Hand Studies consistently exhibit underperformance across metrics, indicating the model's struggle to generalize effectively for hand images, potentially necessitating specialized training or feature engineering. Forearm Studies excel in precision but fall short in recall, highlighting the model's ability to identify true negatives but its limitations in capturing true positives. Elbow Studies serve as a benchmark, outperforming other types across most metrics. Variability in Cohen's Kappa scores suggests inconsistent model reliability, necessitating further attention. Across study types, a notable gap between Precision and Recall underscores the need for techniques like threshold adjustment or cost-sensitive learning to achieve a balanced performance on both metrics, enhancing overall model effectiveness.

VGG-19 Model Evaluation with Best Epoch Weights

In this section, we delve into the evaluation of our VGG-19 model with a focus on leveraging the weights derived from the best-performing epoch during training. This strategic utilization of optimal weights allows us to assess the model's capacity to generalize effectively to previously unseen data. The process involves creating a fresh model instance named '*best_model*' using our established '*build_model*' function and then loading the best weights, acquired from a checkpoint file. This approach ensures that we are scrutinizing our model's performance at its peak potential.

Our analysis commences with a comparative examination of the original model's performance across various anatomical study types, including *Elbow*, *Finger*, *Forearm*, *Hand*, *Humerus*, *Shoulder*, and *Wrist*. These evaluations reveal intriguing insights into the model's strengths and weaknesses within distinct study categories. For instance, while the model excels in precision for certain studies, it often encounters challenges related to recall. Additionally, the F1 Score and Accuracy metrics shed light on the overall effectiveness of the model across these study types.

Subsequently, we shift our attention to the reloaded model, which has been equipped with the best epoch weights. The performance summaries for each study type demonstrate notable improvements in several key metrics, including **recall**, **F1 Score**, and **Accuracy**. This augmentation is particularly pronounced in cases like the Elbow and Shoulder studies, where the reloaded model showcases a superior balance between precision and recall. These insights underscore the significance of fine-tuning our model with the best epoch weights, as it bolsters its capacity to generalize across diverse anatomical structures, ultimately enhancing its real-world applicability.

Evaluating Model Performance (with Best Epoch Weights) Across Different Study Types Insights

```
1 - Study Type: ELBOW
=========================
Precision:          0.9267
Recall:            0.76957
F1 Score:          0.84086
Accuracy:          0.85591
ROC AUC:             0.855
Cohen's Kappa:     0.71127
=========================

2 - Study Type: FINGER
=========================
Precision:         0.89617
Recall:            0.66397
F1 Score:          0.76279
Accuracy:          0.77874
ROC AUC:           0.78759
Cohen's Kappa:     0.56392
=========================

3 - Study Type: FOREARM
=========================
Precision:         0.90476
Recall:            0.62914
F1 Score:          0.74219
Accuracy:          0.79073
ROC AUC:           0.78124
Cohen's Kappa:      0.5619
=========================

4 - Study Type: HAND
=========================
Precision:         0.89474
Recall:            0.44974
F1 Score:          0.59859
Accuracy:          0.79217
ROC AUC:           0.70642
Cohen's Kappa:     0.44643
=========================

5 - Study Type: HUMERUS
=========================
Precision:         0.80435
Recall:            0.79286
F1 Score:          0.79856
Accuracy:          0.80556
ROC AUC:           0.80521
Cohen's Kappa:     0.61066
=========================

6 - Study Type: SHOULDER
=========================
Precision:         0.79851
Recall:            0.76978
F1 Score:          0.78388
Accuracy:          0.79041
ROC AUC:           0.79016
Cohen's Kappa:     0.58057
=========================

7 - Study Type: WRIST
=========================
Precision:         0.90749
Recall:            0.69831
F1 Score:          0.78927
Accuracy:          0.83308
ROC AUC:           0.82031
Cohen's Kappa:     0.65492
=========================
```

Figure 34. VGG-19 Model (with Best Epoch weights) Performance Across Different Study Types

The following section provides an in-depth evaluation of our VGG-19-based model's performance across various anatomical study types. This evaluation uses the best epoch weights to give us the most accurate understanding of the model's performance.

```
Test Loss           : 0.91401
Test Precision      : 0.87158
Test Recall         : 0.68758
Test Accuracy       : 0.80200
Test Cohen's Kappa  : 0.86291
```

Figure 35. Metrics Overview for VGG-19 Model with Best Epoch Weights

Our analysis of the model across different anatomical study types, as outlined above, highlights several critical trends that warrant attention:

The **test loss** value of **0.91401** signifies that the model is performing reasonably well, especially considering the intricacies of medical imaging data. This loss metric is a key indicator of how effectively the model is minimizing errors during predictions. A lower loss value indicates better performance. In this case, the loss value suggests that the model has learned to capture important patterns and features in the data, although there is always room for further optimization.

Then , the precision, with a score of **0.87158**, demonstrates the model's strength in correctly identifying positive cases, such as medical conditions, with a high degree of reliability. A precision score measures how many of the predicted positive cases were indeed true positives. However, it's essential to note that while precision is high, there's still potential for improvement in reducing false positives. Minimizing false positives is crucial in a medical context to avoid unnecessary treatments or interventions.

The **recall** value of 0.68758 indicates that the model is proficient at identifying positive cases when they truly exist in the data. In other words, it has a good sensitivity to detecting actual positive cases. However, it's important to recognize that the recall score also suggests that the model may miss a significant number of actual positive cases, resulting in false negatives. Enhancing recall is vital, as missing critical medical conditions can have serious consequences. Balancing precision and recall is often a challenge, and it's an area where further model refinement may be beneficial.

Also, with an accuracy score of 0.80200, the model demonstrates a fairly strong ability to correctly classify data points into their respective classes. Accuracy is a fundamental metric that gauges the overall correctness of the model's predictions. While the accuracy score is decent, there remains room for improvement, especially in scenarios where the cost of misclassification is high, as is often the case in medical diagnoses.

Finally, the Cohen's Kappa statistic, with a value of 0.86291, indicates a substantial level of agreement between the model's predictions and the actual labels. This metric assesses the model's performance while taking into account the possibility of agreement occurring by chance. A higher Cohen's Kappa suggests that the model's predictions are not merely coincidental but are indeed meaningful and reliable.

By evaluating these metrics in detail, we gain a deeper understanding of the model's performance characteristics and areas that may require attention. This analysis provides a strong foundation for assessing the model's applicability across different medical study types and underscores the need for ongoing refinement and optimization to meet real-world healthcare demands.

D. Conclusion

MuraMed represents an innovative approach in the field of musculoskeletal radiography analysis, with a particular focus on the hand, elbow, and shoulder regions. Diagnosing musculoskeletal abnormalities poses challenges in healthcare, influenced by factors such as human biases, workload, and the subtlety of these conditions. By harnessing advanced deep learning techniques, MuraMed introduces an essential diagnostic tool for radiologists and orthopedic doctors, ensuring prompt, accurate, and efficient detection of musculoskeletal issues. This platform seamlessly integrates into the healthcare ecosystem, enhancing diagnostic services in hospitals and clinics while mitigating factors that can impede precise diagnoses.

Utilizing advanced deep learning methods, MuraMed introduces an essential diagnostic tool for radiologists and orthopedic doctors, guaranteeing timely, precise, and efficient detection of musculoskeletal problems. This platform seamlessly integrates into the healthcare environment, optimizing diagnostic services in medical facilities and clinics, all while minimizing potential obstacles to accurate diagnoses.

The versatility of MuraMed extends beyond its fundamental capabilities in the realm of traditional medicine and healthcare facilities. Our commitment to refining musculoskeletal radiograph analysis for diverse sectors is evident in the project's three key pillars: ***Healthcare***, ***Sports Organizations & Schools***, and ***Workplace for employees' health/ workplace***. In the medical sector, MuraMed enhances diagnostic accuracy for the *hand*, *elbow*, and *shoulder*, while also addressing challenges such as data privacy and regulatory compliance. In sports and educational settings, it plays a crucial role in early injury detection, promoting musculoskeletal health among athletes and students. Furthermore, in the corporate world, it focuses on the early detection, monitoring, and management of work-related musculoskeletal disorders, ensuring employee well-being and productivity.

Our project's significance aligns with the growing need for computer-aided diagnosis systems, particularly in fields where human biases and workload constraints can compromise diagnostic precision. Although our models have exhibited promise in **detecting musculoskeletal abnormalities** in a binary classification context, our future endeavors will involve refining them to distinguish between specific abnormalities. This will empower our models to offer nuanced diagnoses with exceptional accuracy and reliability, reinforcing their practical utility in real-world healthcare scenarios.

In this study, we aim to provide a comprehensive comparative analysis of the architectural designs of various Convolutional Neural Network (CNN) models utilized to enhance technical performance and achieve higher accuracy levels while improving recall rates. This endeavor is particularly significant in the context of medical applications, as it seeks to minimize false negatives, which are a critical category of errors. In this section, we recapitulate the three CNN models employed in our study: the Simple CNN, the Advanced CNN, and the pretrained VGG-19 model. The following table underscores the salient differences in these architectures and elucidates the resultant impact on predictive performance.

Table 1: Comparative Analysis on Models' Architectures.

Model	Architectural Features	Impact on Performance
Simple CNN	- Basic CNN structure with limited depth	- Simplicity may lead to lower accuracy
	- One convolutional layer with 3 filters and one pooling layer	- Limited feature extraction capabilities
	- Reduced computational complexity	- Potential difficulty in complex tasks
Advanced CNN	- Deeper architecture with additional layers	- Improved feature extraction
	- Four sets of convolutional layers with three filters each with exponentially increase in filters' neurons number and pooling configurations	- Better performance in complex tasks with more detailed feature extraction.
	- Increased computational complexity	- Longer training times
VGG-19	- Utilizes VGG-19 pretrained architecture	- Powerful feature extraction
	- Multiple convolutional layers with small kernels	- High computational cost
	- Sophisticated architecture with skip connections	- High quality performance in many tasks

The above table outlines in-depth the key disparities among the three CNN models employed in our study. These distinctions encompass architectural complexity, depth, feature extraction capabilities, and computational requirements, all of which influence the models' predictive performance. It is imperative to carefully consider these architectural variances when selecting a CNN model for a given medical application to optimize accuracy and reduce false negatives, thus enhancing the overall efficacy of the system.

Upon thorough evaluation of the test metrics using the best epoch weights, a distinct hierarchy in performance emerges among the three models under consideration: **Simple CNN**, **Advanced CNN**, and **VGG-19**. Simple CNN acts as a rudimentary baseline but is evidently limited, reflected by its *test loss* of **0.67427** and an *accuracy* of **0.61026**. These metrics underscore the need for more advanced models or additional feature engineering to make this model viable for medical applications. In contrast, Advanced CNN exhibits a superior performance compared to Simple CNN. It not only achieves a *lower test loss* of **0.59758** but also boasts a *higher accuracy* of **0.66938** and a commendable *Cohen's Kappa score* of **0.73658**. This balanced performance makes Advanced CNN a more reliable choice for medical imaging tasks that require a nuanced balance between precision and recall. However, the VGG-19 model surpasses both by delivering the most promising results. Despite its *higher test loss* of **0.91401**, the model's *accuracy* of **0.80200** and *Cohen's Kappa score* of **0.86291** are indicative of a model that is not only accurate but also robust and reliable. In table … the performance metrics of each model are presented for a more supervisory notion of all models' results.

Table 2: Comparative Segmentation Models' Performance Analysis - Important categories

Category	Metric	Simple CNN	Advanced CNN	VGG-19
Elbow	Accuracy	60%	70.53%	85.59%
	F1-Score	57.14%	69.48%	84.08%
	AUC	59.93%	70.50%	85.5%
Wrist	Accuracy	66.46%	70.56%	83.3%
	F1-Score	59.74%	68.91%	78.92%
	AUC	65.43%	70.78%	82.03%
Fore Arm	Accuracy	62.12%	64.78%	79.07%
	F1-Score	49.55%	63.44%	74.21%
	AUC	62.21%	64.79%	78.125
Shoulder	Accuracy	59.14%	65.71%	79.04%
	F1-Score	51.47%	61.32%	78.38%
	AUC	58.96%	65.58%	79.01%

Within the category analysis, it is evident that the VGG-19 model outperforms the other models across all three chosen representative metrics, with particular emphasis on the AUC score. The AUC score provides a comprehensive assessment of overall predictive accuracy and the equilibrium between different types of errors.

Notably, when examining the Elbow category, which exhibits the most substantial difference in AUC performance metrics between the VGG-19 model and the other two models, we observe a significant performance advantage. Specifically, the VGG-19 model achieves an AUC score that is **42%** higher than that of the Simple CNN model and **21.27%** higher than that of the Advanced CNN model in the context of the Elbow category. This substantial performance differential underscores the effectiveness of the VGG-19 model in addressing predictive accuracy and error balance, particularly in scenarios where distinguishing features within the Elbow category are critical.

Our evaluation of the VGG-19 model, both with default weights and imported best epoch weights, has provided valuable insights into the project's progression. The use of best epoch weights notably improved the model's performance, demonstrating its potential as a robust tool for musculoskeletal image analysis. By expanding our understanding of the model's performance across various anatomical study types, we have gained valuable insights into its strengths and areas for further enhancement.

In conclusion, MuraMed represents a pioneering step towards revolutionizing musculoskeletal healthcare. By combining cutting-edge technology with a profound understanding of the unique diagnostic challenges in various sectors, our project stands as a testament to the potential of AI-driven diagnostic solutions.

Final Thoughts

While challenges persist in striking a balance between sensitivity and specificity, our steadfast dedication to improvement ensures that MuraMed will continue to evolve as a valuable asset in the medical field. Our ultimate goal is to enhance the lives of countless individuals by enabling the early, precise, and efficient detection of musculoskeletal abnormalities. We envision a future where healthcare becomes not only more accessible but also proactive, with issues identified and addressed before they become serious, ultimately leading to better patient outcomes and a healthier society.

The thorough examination and comparative assessment of these machine learning models represent a crucial step toward our main objective: the development and deployment of an advanced medical imaging tool, provisionally referred to as MuraMed. While the Simple and Advanced CNN models provide foundational insights, the VGG-19 model appears the most promising for seamless integration into a highly sensitive and reliable application like MuraMed. The performance metrics not only indicate significant progress in medical image classification, even with existing technologies, but also highlight the importance of continuous innovation and adaptation to meet the strict accuracy and reliability requirements of medical applications.

We anticipate that this effort will make a significant contribution to global research in medical image analysis, particularly in the field of orthopedic radiology. The potential for automated, highly precise diagnosis and treatment planning has the potential to transform healthcare delivery, especially in regions with limited access to skilled medical professionals. From this perspective, we envision that MuraMed will act as a way to bridge existing gaps in medical imaging diagnostics, ultimately elevating healthcare standards on a global scale.

Bibliography

The following bibliography provides a curated list of academic papers, articles, and online resources that have been instrumental in shaping the theoretical framework and technical methodologies employed in this project on abnormality detection in musculoskeletal radiographs. These sources offer valuable insights into various aspects of machine learning algorithms, neural network architectures, and optimization techniques, thereby enriching the project's scientific rigor and practical applicability.

1. Buckle, P.W. & Devereux, J.J., 2002. The nature of work-related neck and upper limb musculoskeletal disorders. *Applied Ergonomics*, 33(3), pp.207-217. Available at: https://doi.org/10.1016/S0003-6870(02)00014-5 [Accessed Date: 23 August 2023].

2. Colombini, D. & Occhipinti, E., 2006. Preventing upper limb work-related musculoskeletal disorders (UL-WMSDS): New approaches in job (re)design and current trends in standardization. *Applied Ergonomics*, 37(4), pp.441-450. Available at: https://doi.org/10.1016/j.apergo.2006.04.008 [Accessed Date: 23 August 2023].

3. Stanford ML Group, 2017. MURA: Musculoskeletal Radiographs. Available at: Stanford ML Group MURA Dataset [Accessed Date: 2 September 2023].

4. TensorFlow, 2015. TensorFlow: An Open Source Machine Learning Framework. Available at: TensorFlow Official Website [Accessed Date: 2 September 2023].

5. Kapernikov, 2018. Traditional Machine Learning Algorithms for Machine Vision. Kapernikov. Available at: Kapernikov Article on Traditional ML Algorithms [Accessed Date: 2 September 2023].

6. Medium, 2020. Fully Connected vs. Convolutional Neural Networks. The Startup. Available at: Medium Article on FCNs vs CNNs [Accessed Date: 2 September 2023].

7. Salehinejad, H., Sankar, S., Barfett, J., Colak, E., & Valaee, S., 2018. Recent Advances in Recurrent Neural Networks. Available at: ArXiv - The RNN Advances [Accessed Date: 2 September 2023].

8. Towards Data Science, 2020. Recurrent Neural Networks (RNNs). Towards Data Science. Available at: Towards Data Science Article on RNNs [Accessed Date: 2 September 2023].

9. Bank, D., Koenigstein, N., & Giryes, R., 2020. Autoencoders. Available at: ArXiv Autoencoders [Accessed Date: 2 September 2023].

10. Chen, S. & Guo, W., 2023. Auto-Encoders in Deep Learning—A Review with New Perspectives. Mathematics, 11(8), 1777. Available at: DOI for Auto-Encoders Review [Accessed Date: 2 September 2023].

11. Dobilas, S., 2022. GANs: Generative Adversarial Networks — An Advanced Solution for Data Generation. Towards Data Science. Available at: Towards Data Science Article on GANs [Accessed Date: 2 September 2023].

12. Yamashita, R., Nishio, M., Do, R.K.G., & Togashi, K., 2018. Convolutional neural networks: an overview and application in radiology. Insights into Imaging, 9, pp.611–629. Available at: Insights into Imaging Article on CNNs [Accessed Date: 2 September 2023].

13. Rosberg, H. E., & Dahlin, L. B. (2018). An increasing number of hand injuries in an elderly population - A retrospective study over a 30-year period. BMC Geriatrics, 18(1). [Online] Available at: https://doi.org/10.1186/s12877-018-0758-7 [Accessed Date: 3 September 2023].

14. Danielle A. van der Windt, D. A., Burke, D. L., Babatunde, O., Hattle, M., McRobert, C., Littlewood, C., Wynne-Jones, G., Chesterton, L., van der Heijden, G. J. M. G., Winters, J. C., Rhon, D. I., Bennell, K., Roddy, E., Heneghan, C., Beard, D., Rees, J. L., & Riley, R. D. (2019). Predictors of the effects of treatment for shoulder pain: protocol of an individual participant data meta-analysis. Diagnostic and Prognostic Research, 3(1). [Online] Available at: https://doi.org/10.1186/s41512-019-0061-x [Accessed Date: 3 September 2023].

15. Kiliç, B., Yücel, A. S., Gümüsdag, H., Kartal, A., & Korkmaz, M. (2015). Research on shoulder injuries in athletes and treatment methods. Anthropologist, 22(1), 73–88. [Online] Available at: https://doi.org/10.1080/09720073.2015.11891859 [Accessed Date: 3 September 2023].

16. Hains, G. (2002). Chiropractic management of shoulder pain and dysfunction of myofascial origin using ischemic compression techniques. [Online] Available at: https://www.ncbi.nlm.nih.gov/pmc/articles/PMC2504982/pdf/jcca00007-0066.pdf [Accessed Date: 3 September 2023].

17. Hulbert, J. R., Osterbauer, P., Davis, P. T., Printon, R., Goessl, C., & Strom, N. (2007). Chiropractic treatment of hand and wrist pain in older people: systematic protocol development. Part 2: cohort natural-history treatment trial. Journal of Chiropractic Medicine, 6(1), 32–41. [Online] Available at: https://doi.org/10.1016/j.jcme.2007.02.011 [Accessed Date: 3 September 2023].

18. Chan JJ, Xiao RC, Hasija R, Huang HH, Kim JM. (2023). Epidemiology of Hand and Wrist Injuries in Collegiate-Level Athletes in the United States. J Hand Surg Am, 48(3), 307.e1-307.e7. [Online] Available at: https://doi.org/10.1016/j.jhsa.2021.10.011 [Accessed Date: 3 September 2023].

19. Simpson, A. M., Donato, D. P., Veith, J., Magno-Padron, D., & Agarwal, J. P. (2020). Hand and Wrist Injuries Among Collegiate Athletes: The Role of Sex and Competition on Injury Rates and Severity. Orthopaedic Journal of Sports Medicine, 8(12). [Online] Available at: https://doi.org/10.1177/2325967120964622 [Accessed Date: 3 September 2023].

20. Stögner, V. A., Kaltenborn, A., Laser, H., & Vogt, P. M. (2020). Hand injuries in sports – a retrospective analysis of 364 cases. BMC Musculoskeletal Disorders, 21(1). [Online] Available at: https://doi.org/10.1186/s12891-020-03807-z [Accessed Date: 3 September 2023].

21. Avery, D. M., Rodner, C. M., & Edgar, C. M. (2016). Sports-related wrist and hand injuries: A review. In Journal of Orthopaedic Surgery and Research (Vol. 11, Issue 1). BioMed Central Ltd. [Online] Available at: https://doi.org/10.1186/s13018-016-0432-8 [Accessed Date: 3 September 2023].

22. Thomas D. Rizzo. (1994). Rehabilitation of Hand and Wrist Injuries in Sports. Physical Medicine and Rehabilitation Clinics of North America, Volume 5, Issue 1, Pages 115-131. ISSN 1047-9651. [Online] Available at: https://doi.org/10.1016/S1047-9651(18)30540-0 [Accessed Date: 3 September 2023]. (https://www.sciencedirect.com/science/article/pii/S1047965118305400)

23. Lehman, J. D., Krishnan, K. R., Stepan, J. G., & Nwachukwu, B. U. (2020). Prevalence and Treatment Outcomes of Hand and Wrist Injuries in Professional Athletes: A Systematic Review. In HSS Journal (Vol. 16, Issue 3, pp. 280–287). Springer. [Online] Available at: https://doi.org/10.1007/s11420-020-09760-w [Accessed Date: 3 September 2023].

24. Tai, W.-H., Zhang, R., & Zhao, L. (2023). Cutting-Edge Research in Sports Biomechanics: From Basic Science to Applied Technology. Bioengineering, 10(6), 668. [Online] Available at: https://doi.org/10.3390/bioengineering10060668 [Accessed Date: 3 September 2023].

25. Bruce Elliott. (1999). Biomechanics: An integral part of sport science and sport medicine. Journal of Science and Medicine in Sport, Volume 2, Issue 4, Pages 299-310. ISSN 1440-2440. [Online] Available at: https://doi.org/10.1016/S1440-2440(99)80003-6 [Accessed Date: 3 September 2023]. (https://www.sciencedirect.com/science/article/pii/S1440244099800036)

26. Krumm, B., & Faiss, R. (2021). Factors Confounding the Athlete Biological Passport: A Systematic Narrative Review. In Sports Medicine - Open (Vol. 7, Issue 1). Springer Science and Business Media Deutschland GmbH. [Online] Available at: https://doi.org/10.1186/s40798-021-00356-0 [Accessed Date: 3 September 2023].

27. Mennitti C, Brancaccio M, Gentile L, Ranieri A, Terracciano D, Cennamo M, La Civita E, Liotti A, D'Alicandro G, Mazzaccara C, Frisso G, Pero R, Lombardo B, Scudiero O. (2020). Athlete's Passport: Prevention of Infections, Inflammations, Injuries and Cardiovascular Diseases. J Clin Med, 9(8):2540. [Online] Available at: https://doi.org/10.3390/jcm9082540 [Accessed Date: 3 September 2023].

28. Schumacher, Y. O., & D'Onofrio, G. (2012). Scientific expertise and the athlete biological passport: 3 Years of experience. Clinical Chemistry, 58(6), 979–985. [Online] Available at: https://doi.org/10.1373/clinchem.2012.183061 [Accessed Date: 3 September 2023].

29. Thapa AS, Rai SM, Nakarmi KK, Karki B, Gharti Magar M, Nagarkoti KK, Dahal P, Maharjan N, Pokharel PB, Lamichhane A. (2023). Hand Injury among Patients Visiting Emergency Department in a Tertiary Care Centre: A Descriptive Cross-sectional Study. JNMA J Nepal Med

Assoc, 61(257), 5-9. [Online] Available at: https://doi.org/10.31729/jnma.7969 [Accessed Date: 3 September 2023]. PMID: 37203910; PMCID: PMC10089049.

30. Silber J, Giddins G, Horwitz MD. (2021). Preventable hand injuries presenting to a dedicated hand and wrist unit in England: a pilot study. J Hand Surg Eur Vol, 46(10), 1113-1114. [Online] Available at: https://doi.org/10.1177/17531934211019297 [Accessed Date: 3 September 2023]. PMID: 34034551; PMCID: PMC8647476.

31. Giancarlo McEvenue, Fiona FitzPatrick, Herbert P. von Schroeder. (2016). An Educational Intervention to Improve Splinting of Common Hand Injuries. The Journal of Emergency Medicine, Volume 50, Issue 2, Pages 228-234. ISSN 0736-4679. [Online] Available at: https://doi.org/10.1016/j.jemermed.2015.08.011 [Accessed Date: 3 September 2023]. (https://www.sciencedirect.com/science/article/pii/S0736467915009014)

32. Qiu, Z. (2020). The Influence of the Design and Manufacture of Sports Equipment on Sports. Journal of Physics: Conference Series, 1549(3). [Online] Available at: https://doi.org/10.1088/1742-6596/1549/3/032039 [Accessed Date: 3 September 2023].

33. Pihl, P. (n.d.). An Analysis of the Sports Equipment Industry and One of Its Leading Companies, Head, N.V. [Online] Available at: https://digitalcommons.liberty.edu/cgi/viewcontent.cgi?article=1176&context=honors [Accessed Date: 3 September 2023].

34. Ngoubinah pretty, N. T., & Priya, V. v. (2021). Awareness on Health Checkup for School Students Among Parents. Journal of Research in Medical and Dental Science 2021, 9(1), 314–318. [Online] Available at: www.jrmds.in [Accessed Date: 3 September 2023].

35. Nikander K, Kosola S, Vahlberg T, Kaila M, Hermanson E. (2022). Associating school doctor interventions with the benefit of the health check: an observational study. BMJ Paediatr Open, 6(1):e001394. [Online] Available at: https://doi.org/10.1136/bmjpo-2021-001394 [Accessed Date: 3 September 2023]. PMID: 36053658; PMCID: PMC8889353.